Dissertation

submitted to the

Combined Faculties for the Natural Sciences and for Mathematics

of the Ruperto-Carola University of Heidelberg, Germany

for the degree of

Doctor of Natural Sciences

Studies on evolution of drug resistance in *P. falciparum* malaria *in vivo* and *in vitro*

Presented by
Judith Straimer
Diploma-Biologist
Born in Heidelberg

Dissertation

submitted to the

Combined Faculties for the Natural Sciences and for Mathematics

of the Ruperto-Carola University of Heidelberg, Germany

for the degree of

Doctor of Natural Sciences

Presented by
Judith Straimer
Diploma-Biologist
Born in Heidelberg

Oral-examination: .....

Studies on evolution of drug resistance in *P. falciparum* malaria *in vivo* and *in vitro*

Referees: Prof. Dr. Michael Lanzer

Prof. Dr. Steve Ward

Part of this work contributed to the following publication:

Sasi P, Abdulrahaman A, Mwai L, Muriithi S, Straimer J, Schieck E, Rippert A, Bashraheil M, Salim A, Peshu J, Awuondo K, Lowe B, Pirmohamed M, Winstanley P, Ward S, Nzila A, Borrmann S (2009) In vivo and in vitro efficacy of amodiaquine against Plasmodium falciparum in an area of continued use of 4-aminoquinolines in East Africa. *J Infect Dis* **199:** 1575-1582

Ich erkläre hiermit, dass ich die vorgelegte Dissertation selbst verfasst und mich keiner anderen als der von mir ausdrücklich bezeichneten Quellen und Hilfen bedient habe.

....

Datum Judith Straimer

Acknowledgements

First of all, I want to thank Prof. Dr. Michael Lanzer for accepting the role of first referee and Prof. Dr. Steve Ward for accepting the role of second referee.

Bei Steffen Borrmann möchte ich mich für seine uneingeschränkt Unterstützung, sein Vertrauen und seine großzügige Förderung während der letzten 4 Jahre ganz besonders bedanken. Durch die vielen interessanten Gespräche mit dir habe ich besonders die mir zuvor gänzlich unbekannte Epidemiologie kennen und schätzen gelernt.

Ein ganz großer Dank geht an die Kinder und ihre Mütter in Pingilikani, die sich bereit erklärt haben an unseren Studien teil zu nehmen. Ohne die tapferen kleinen Patienten wäre diese Arbeit nicht möglich gewesen. Ebenso gilt mein Dank dem gesamten klinischen Personal in Pingilikani und allen Mitarbeitern von KEMRI in Kilifi.

Bei Elise möchte ich mich für die Zeit bedanken, die sie mir geopfert hat, wenn ich mal wieder ratlos auf dem Stuhl in ihrem Büro saß. Du hast dich immer so ausdauernd mit meinen Rätseln befasst und meistens auch noch eine schlaue Idee dazu gehabt. Danke schön.

Anja ist es zu verdanken, dass meine Bestellungswünsche auch in letzter Sekunde noch zuverlässig und flink erledigt wurden und dass ich dringend benötigten Reagenzien stets zur Verfügung hatte. Dafür und für die grundsätzliche organisatorische Leistung und Unterstützung im Labor und in der Zellkultur möchte ich mich wirklich ganz herzlich bei dir bedanken.

Katharina, ein ganz großes Dankeschön geht auch an dich. Deine Hilfe im Frühling 2009 war unersetzbar und du hast das wirklich großartig gemacht.

Andris danke ich für seine nervigen Diskussionen über die Gesellschaft, die Welt, seine Klischees und für das Teilen von Leid und Frust in manch einem Moment.

Ifey danke ich für ihre afrikanische Gemütlichkeit und die vielen Gummibärchen. Johannes für seine Adam Green Stimme, Yvonne für die vielen Muffins und Dirk fürs Messen manch einer Platte.

Auch bei meiner lieben Eltern, meinem Bruder, meinen lustigen, fröhlichen Freunden

fern ab des Labors, und bei meinen Basketball Mädels möchte ich mich ganz herzlich für ihre Unterstützung bedanken. Wenn sich mein Blick zu sehr in die Enge verirrt hatte, wurde mir durch sie alle immer wieder klar, dass Arbeit nicht alles ist.

Abbreviations

ACT	Artemisinin combination therapies
AM	Artemether
amp	ampicillin
AT	Annealing temperature
ATP	Adenosine triphosphate
bp	Base pairs
BSA	Bovine Serum Albumine
cDNA	complementary DNA
CQ	Chloroquine
DHA	Dihydroartemisinin
DHFR	Dihydrofolate-reductase
DHFS	Dihydrofolate synthase/folylpolyglutamate synthase
DHPS	Dihydropteroate synthetase
DMSO	Dimethylsulphoxide
DNA	Deoxyribonucleic acid
dsDNA	Double stranded DNA
e.g.	Exempli gratia (for example)
EDTA	Ethylendiaminotetraacetic acid
gDNA	Genomic DNA
GTP	Guanosine triphosphate
GCH	GTP cyclohydrolase
h(rs)	hour(s)
HIV	Human Immunodeficiency Virus
IC_{50}	50 % growth inhibitory concentration
i.e.	id est (that is)
Kb	Kilobase pairs
LB	Luria-Bertani
LM	Lumefantrine
M	molar
mM	millimolar (1×10^{-3} molar)
mmol	millimol (1×10^{-3} mol)
nM	nanomolar (1×10^{-9} mol)
nmol	nanomol (1×10^{-9} mol)
o.n.	Overnight

Oligo-dT	Tyrosine oligo
P.	*Plasmodium*
PBS	Phosphate buffered saline
PCR	Polymerase chain reaction
poly A	Polyadenosine
PPQ	Piperaquine
PTPS	6-pyruvoyltetrahydropterin synthase
Pyr	pyrimethamine
RNA	Ribonucleic acid
Rpm	revolution per minute
RPMI	Rosewell Park Memorial Institute
rRNA	Ribosomal RNA
RT	Room temperature
RT-PCR	real time polymerase chain reaction
SD	Standard deviation
SDS	Sodiumdodecylsulphate
SP	sulfadoxine-pyrimethamine
SSC	saline sodium-citrate
TAE	Tris/Acetic acid/EDTA
TBE	Tris/Boric acid/EDTA
TE	Tris/EDTA
U	units
UV	ultraviolet
V	Volt
(w/v)	Weight volume percent
µ	micro (1×10^{-6})

Summary

The global burden of Malaria remains high with a 2.2 billion people estimated to live in endemic areas (Snow et al, 2005). Prompt and efficacious chemotherapy remains an important cornerstone in the fight against malaria. Development of resistance is the parasite's mechanisms to respond to massive drug pressure.

In this study I analysed drug-parasites interactions *in vivo* and *in vitro* using discreet experimental approaches. I started by studying parasite survival *in vivo*, 7 days after treatment intervention. In the following, I analysed parasites isolates *in vitro* that had been exposed to various drugs over the last years in the community. In the final part of the project, I attempted to gain insight in the evolution of drug resistance *in vitro*. For this work, I set up induction of resistance experiments *in vitro* and analysed in a time course mechanisms of resistance. Of particular interest was here the relationship between gene amplification and the emergence of single nucleotide polymorphisms.

The results presented in this work show that 7 days after start of treatment (artemisinin combination therapy or amodiaquine) subpatent parasite populations were detected in 64/156 patients (41%) with high sensitivity. However, persistence of parasites was not associated with recrudescent infection at the individual level but showed instead correlation with initial parasite density in potentially less immune patients.

Analysis of field isolates revealed high prevalence of anti-folate resistance due to triple and double mutant *Pfdhfr*. In theses parasites, no gene copy number variations were detected for genes involved in the folate pathway.

However, induction of pyrimethamine resistance *in vitro*, lead to *Pfdhfr* amplification in two laboratory strains 3D7 (31 fold) and FCR3 (9 fold) associated with high cross-resistance to cycloguanil and trimethoprim but not to chloroquine. Further, I was able to identify gene amplification as a mechanism for acquisition of S108N in *Pfdhfr*.

My findings of persistent subpatent parasitaemia after treatment underline the need of understanding clearance rate, persistence and elimination of parasites after anti-malarial treatment, particularly in regard to recent reports of emerging artemisinin resistance in western Cambodia (Dondorp et al, 2009), My results also suggest that resistant phenotypes may persist in parasite populations, once introduced. And finally, my data suggest gene amplification as an intermediate step in the acquisition of resistance conferring point mutations in *P. falciparum.*

Zusammenfassung

Die globale Bedrohung für die menschliche Gesundheit durch Malaria bleibt weiterhin bestehen. Geschätzte 2.2 Millionen Menschen leben in endemischen Gebieten (Snow et al, 2005). Schnelle und effektive Behandlung sind entscheidend bei der Malariabekämpfung. Auf den Selektionsdruck durch Wirkstoffe reagiert der Parasit, *Plasmodium falciparum*, durch die Bildung von Resistenzen.

In dieser Studie habe ich die Wechselwirkungen zwischen Wirkstoff und Parasit durch umsichtig geplante experimentelle Ansätze *in vivo* und *in vitro* untersucht. Zu Beginn wurden die Überlebenschancen des Parasiten *in vivo*, 7 Tage nach einer Behandlung analysiert. Anschließend wurden Isolate von Parasiten, die während der letzten Jahre unterschiedlichen Wirkstoffen in der Gemeinde von Pingilikani ausgesetzt waren, *in vitro* charakterisiert. Im letzten Teil der Arbeit habe ich versucht Einblicke in die Entstehung von Resistenzen *in vitro* zu erlangen. Resistenz wurde *in vitro* induziert um Resistenzmechanismen über einen Zeitraum von mehreren Monaten hin analysieren zu können. Besonders interessant war hier der Zusammenhang zwischen Vervielfältigung von Genen und das Auftreten von Punktmutationen.

Die vorliegenden Ergebnisse zeigen, dass durch eine hoch sensitive Methode 7 Tage nach Behandlungsbeginn (Artemisinin Kombinationspräparate oder Amodiaquin) in 64 von 156 Fällen (41%), noch Parasiten in a-symptomatischen Patienten nachgewiesen werden konnten. Die persistierende Parasitämie war jedoch nicht mit einem Risiko von wieder auftretenden Symptomen verbunden. Ein Zusammenhang mit der Parasitendichte zu Begin der Behandlung konnte jedoch in weniger immunen Patienten festgestellt werden.
Die Analyse von Parasiten Isolaten wies auf eine starke Verbreitung von Anti-Folat Resistenz hin, hervorgerufen durch Mutationen in *Pfdhfr*. Gen Vervielfältigung wurde in den Genen des Folat Stoffwechsels nicht gefunden. Im Gegensatz dazu führten die Resistenz-Induktions-Experimente durch Pyrimethamin *in vitro* zu einer deutlichen Vervielfältigung von *Pfdhfr* in 3D7 (31-fach) und FCR3 (9-fach), die mit ausgeprägter Cross-Resistenz (Cycloguanil und Trimethoprim) verbunden war. Außerdem ist es mir gelungen, Vervielfältigung von Genen als mechanistische Grundlage für die Entstehung von Punktmutationen in *P. falciparum* zu beschreiben.

Meine Daten zu persistierenden Parasiten nach Behandlung erlangen besondere Bedeutung, gerade im Hinblick auf kürzlich veröffentlichte Berichte über das

Auftreten von Artemisin Resistenz im westlichen Kambodscha (Dondorp et al, 2009). Meine Ergebnisse weisen auch darauf hin, dass einmal in einer Population etablierte resistente Phänotypen bestehen bleiben.

1. Introduction

1.1 Malaria's past and present epidemiology

Malaria is a human disease caused by a protozoan pathogen. Four species infecting humans are identified: *Plasmodium falciparum*, *Plasmodium vivax, Plasmodium malariae and Plasmodium ovale*. Recently, *Plasmodium knowlesi*, a primate malaria parasite, was identified as the fifth human *Plasmodium* species (Singh et al, 2004).

Evidence suggests its evolution from a free-living, chloroplast-containing protozoan, which first became adapted to aquatic invertebrates (Wilson & Williamson, 1997), before evolving into a human intracellular parasite in vertebrate hosts. The closest relative to *P. falciparum* is the malaria parasite of chimpanzees, *P. reichenowi* (Escalante & Ayala, 1994). Molecular evidence confirm that the clad formed by these two species is only remotely related to other *Plasmodium* species and diverged around 130 million years ago (Escalante & Ayala, 1995). It is estimates that five million years ago, when the human line and the African great apes diverged, *P. falciparum* and *P. reichenowi* were also separated (Carter & Mendis, 2002).

The agrarian revolution in Africa resulted in intensified parasite transmission vie the *Anopheles* vector. Human populations increased in numbers and lived in agglomerations close to water sources or containers. For mosquitoes, a constant supply of blood and abundant breeding sites were created (Carter & Mendis, 2002).

The first appearance of malaria in historical references dates back to the Chinese Canon of Medicine (Nei Ching), 4700 year ago, which mentions symptoms, typical for malaria, as the periodicity of fever for example. Later, Hippocrates (460 to 377 B.C.) described the different recurring forms of fever and left no doubt about the presence of malaria in Greece. Only in the second century B.C., malaria reached the mainland of Italy. However during the prosperity of the Roman Empire, swamps surrounding Rome were drained and malaria was not a major thread. Only with the decline of the empire (400 A.C.) malaria established around the shores of the Mediterranean, from where it spread probably during the Dark or Middle age to northern Europe. After malaria had reached its widest geographical expansion in the 19th century, during which half of the world's population lived at significant risk of infection, it was eliminated from North America and Northern and Western Europe after World War II (Carter & Mendis, 2002).

Today, the global burden of malaria remains high. In 2002 2.2 billion people are estimated to live in endemic areas (Figure 1) in the year 2002 (Snow et al, 2005). In the same year an estimated 515 million clinical events (range 300 – 660) were

caused by *Plasmodium falciparum* of which 70% were occurring in African regions (Snow et al, 2005), mostly in children under the age of 5 years. Not only the prevalence is highest but also severe life threatening manifestations of malaria were tenfold higher in Africa than in similar malaria endemic areas (Snow et al, 2005).

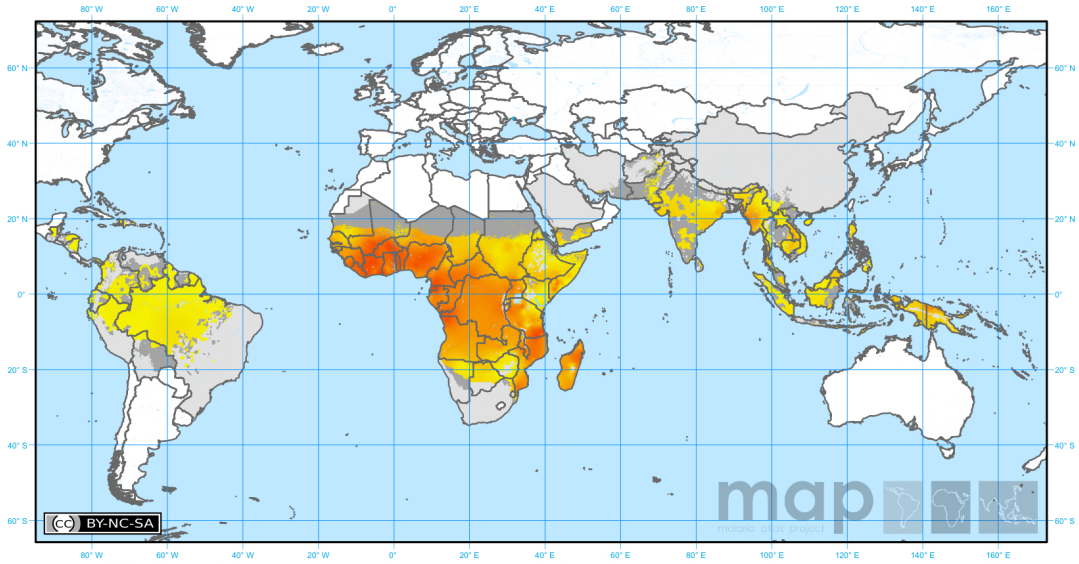

Figure 1 *Plasmodium falciparum* endemicity map 2007 (Hay et al, 2009)

Very recent observations have shown a decline in malaria transmission and burden in Zanzibar (Bhattarai et al, 2007) and The Gambia (Ceesay et al, 2008). These reductions occurred after the introduction of artemisinin combination therapies (ACT) between 2002 and 2003. With the decline in transmission, fewer cases of severe malaria and associated morbidity were also reported for Kilifi District Hospital, Kenya (O'Meara et al, 2008). Furthermore the proportion of patients presenting with positives slides decreased significantly (indicator of parasite prevalence in the population). In accordance to the hypothesis of a direct correlation of immunity and parasite prevalence, a significant increase in the mean age of slide positive patients was observed (O'Meara et al, 2008).

The samples for this work were collected at the Pingilikani study site (Figure 1-1). This study site has been established as part of a Heidelberg University-initiated collaboration with the Kenya Medical Research Institute (KEMRI), Centre for Geographic Medicine Research-Coast (CGMR-C). The site is located 20 km south of the town of Kilifi, on the Kenyan cost. The study area is characterised by perennial transmission of *P. falciparum* with bi-annual peaks after the long (April-June) and short (November-December) rainy seasons. Before the recent reductions in

transmission intensity, the risk of infection was estimated at 22 to 53 infective bites per person per year (Mbogo et al, 2003).

Figure 1-1 (left) Map of Kilifi district, Kenya. (right) Pingilikani dispensary.

1.2 Life cycle

Plasmodium falciparum, a unicellular haploid eukaryote of the Phyllum *Apicomplexa* has co-evolved with its human and mosquito hosts over millions of years. Its complex life cycle (Figure 1-2) encompasses three stages of two distinct proliferation forms with massive mandatory intracellular asexual multiplication, sporogony (mosquito midgut) and schizogony (liver and blood).

During a blood meal, an infected *Anopheles* mosquito injects with its saliva sporozoites into the skin of the human host. Sporozoites, a banana shaped motile stage, migrate through the skin around the bite site until they reach a blood vessel, which they actively invade. With the blood stream, they are then passively transported to the sinusoid endothelium of the liver. Here they enter the liver tissue through Kupffer cells (Frevert et al, 2005) and migrate through a number of liver cells until they invade a hepatocyte and establish themselves in a parasitophorous vacuole. From a single sporozoites up to 50 000 merozoites are formed by clinically silent schizogony. Merosomes are membranous structures that contain large numbers of merozoites (Sturm et al, 2006). They bud from the hepatocyte into the blood stream, accumulate in the lung (shown in *P. berghei*) (Baer et al, 2007) where they burst and release the merozoites, which then ultimately invade erythrocytes (Sturm et al, 2006) and thereby, establish pathogenic blood stage infection. Within

the erythrocytes, early ring stages develop to trophozoites, the metabolically most active form of the blood stages with massive replication of DNA. Trophozoites develop into schizonts, carrying 24 merozoites. Merozoites are released by active egress into the blood and initiate the next cycle of erythrocyte infection. The replication cycle in the blood stream takes approximately 48 hours but unlike other *Plasmodia*, *Plasmodium falciparum* replication cycles are not synchronised across a massive population of up to 10^{12} parasites per infection. Symptoms, associated with *P. falciparum* infections, are therefore not subjected to a clear periodicity (Baer et al, 2007).

Due to yet poorly characterised external stimuli a proportion of ring form parasites eventually commit within 10 to 14 days to gametocytogenesis. With the ingested blood meal, female and male gametocytes reach the gut of the female *Anopheles* mosquito, where they mate and form a zygote, the only diploid stage of the *Plasmodium falciparum* life cycle. The zygote transforms into a motile ookinete, which traverses the midgut epithelium and forms an oocyste between the epithelial lining and the basal lamina. Within its boundaries thousands of sporozoites are produced by mitotic replication. Midgut sporozoites egress actively from the oocyste (Aly & Matuschewski, 2005), reach the salivary gland through the haemolymph and invade the salivary gland to be injected with the next blood meal back into the human host. The development within the mosquito is temperature-dependant and takes between 10 and 14 days.

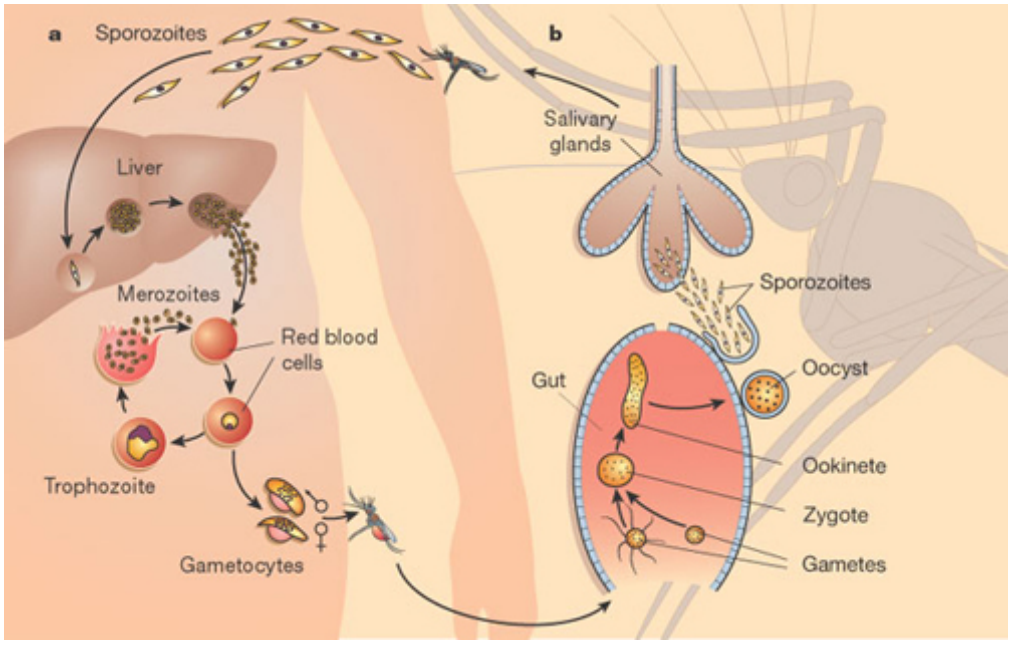

Figure 1-2 Plasmodium falciparum life cycle (Menard, 2005).

1.3 Clinical manifestations in endemic areas and definition

The clinical manifestations of *Plasmodium* differ not only among species but also between different endemic areas. For the purpose of this work, I will focus on the characteristic symptoms for *P. falciparum* malaria in endemic areas.

The case definition of malaria is compounded by (i) gradual acquisition of immunity as a function of repeated exposure and (ii) lack of specificity of clinical symptoms, mainly fever. Residents of areas with high transmission of *P. falciparum* acquire a partial immunity ("semi-immunity"), which develops progressively upon repeated exposure to the parasites. Protection against severe malaria is acquired relatively early, whereas defence against uncomplicated malaria and the parasite itself builds up very slowly, throughout life (Langhorne et al, 2008). Because of variable degrees of stage-specific immunity, a simple correlation of parasite density to severity of disease is not applicable. Also, in areas of high transmission where the prevalence of parasites in the population reaches up to 80% in children ≤ 10 years old (Smith et al, 1993) nonspecific symptoms (fever) do not necessarily imply that clinical malaria is present. Regarding the evaluation of new interventions, a precise definition of clinical cases though is important. It has been proposed to use the parasite density cut off of 2,500 parasites / µl of blood in association with fever ≥ 37.5 °C in children between 1 and 15 years to define a clinical case of malaria in endemic areas (Mwangi et al, 2005). For young infants (≤ 1 year) and for adults from the age of 15 onwards, the simple presence of parasites in association with fever is sufficient to define a clinical case of malaria (Mwangi et al, 2005).

Severe malaria, which includes cerebral malaria, can mainly be defined by coma or impaired consciousness and respiratory distress. Mortality is highest when these three symptoms overlap (Marsh et al, 1995). Poor outcome is further accompanied by hypoglycaemia, whereas severe anaemia and jaundice are signs of severe disease but do not show a significant correlation with mortality (Marsh et al, 1995). Co-morbidity can be an additional risk factor or a consequence of severe malaria. To improve specificity of the severe malaria definition, children with meningitis, lower respiratory tract infection, bacteraemia and gastroenteritis with severe dehydration, should be excluded. In contrast the exclusion of children with HIV or malnutrition did not improve case definition (Bejon et al, 2007). If additionally a parasite threshold of ≤ 2500 parasite / µl of blood was applied, the malaria-attributable fraction of children presenting with severe disease increased up to 95 % with a sensitivity of 85% (Bejon et al, 2007).

1.4 Malaria control strategies and the emergence of drug-resistance in *Plasmodium falciparum*

In the absence of a highly protective anti-malarial vaccine in the foreseeable future, malaria control continues to rely mainly on prompt and effective treatment of uncomplicated disease episodes. Efficient public health care facilities, use of insecticide treated bed nets (ITNs), and vector and larval control will also remain part of a comprehensive control strategy. An overview of the various control measurements is given in the following paragraph as well as an estimation of their potential impact.

Like for any infectious disease, prevention is the most efficient strategy for reducing disease burden. Vector and larval control is one arm of this policy. Especially vector control using massive spraying of DDT (Dichlorodiphenyldichloroethylene) has contributed to dramatically reduced malaria incidences and even elimination of malaria from parts of the world in the 1960s. After the publication of “Silent Spring” by Rachel Carson in 1962, in which the devastating effects on the environment were depicted, DDT was banned and WHO abandoned malaria elimination as a policy goal, shifting its focus on “control”. The history of DDT usage has been reviewed in detail (Eskenazi et al, 2009). The re-emergence of malaria after the stop of massive vector control efforts showed the consequences of over-reliance on a single intervention. Larval control in tropical geographic settings is a very ambitious task as potential breeding sites are numerous, often covered by vegetation, small and thus difficult to detect, to survey and to control.

Beside vector and larval control as preventive measurements, insecticide treated bed nets (ITNs) also reduce transmission, morbidity and both malaria-specific as well as all-cause mortality. Coverage has been very patchy but combined efforts and free distribution has led to an almost complete coverage of ITNs in some regions and countries. But as long as the prevalence of parasites in the population is high and mosquitoes are not significantly reduced in population size, the chance of getting infected especially at dawn is still considerable. It is unrealistic to assume that from early dawn on, which in sub Sub-Saharan Africa occurs between 17h30 and 18h30, all people at risk would place themselves under bed nets.

A more recent prevention strategy is based on intermittent preventive treatment in pregnancy (IPTp) and infants (IPTi). Pregnant woman and infants are the highest risk groups due to a lack of antibody-mediated recognition of parasite-encoded variant erythrocyte surface molecules conferring cytoadherence to endothelial cells or placental syncytiotrophoblasts in the placenta, respectively, expressed during

infections in immunologically naïve individuals (Bull & Marsh, 2002). Chemoprophylaxis is one instrument to protect this vulnerable group but as the name implies, relies on efficacious preventive treatment.

The improvement of public health care facilities is part of the major effort to reduce the incidence of severe malaria. Early access to treatment needs to be ensured by facilitating access to affordable and freely available drugs.

Overview of antimalarial drugs

The traditional Chinese medicine knew about the anti-fever qualities of "Qinghao" (Chinese for *Artemesia annua*) and used the plants extract for more than 2000 years. Similarly in South America, Incan herbalists used the bitter bark from the Cinchona tree (*Cinchona succirubra*) to treat the fever. Quinine the active component of the Cinchona bark was only discovered and isolated in 1820 and artemisinin combination therapies (ACT) were developed for scalable industrial production only in the 21st century. Until today a substantial effort is invested in the discovery of new therapeutic principles from the study of traditional herbal medicine.

The production of synthetic compounds in the beginning of the 20th century and random screening of large chemical compound libraries led to the discovery of 4-aminoquinolines. Chloroquine, the most prominent derivative, was massively used over 40 years because of its excellent safety, low cost, rapid action and advantageous pharmacokinetic profile. However, parasite resistance spread globally, including to Africa.

Parallel research led to the discovery of anti-folates as potent anti-cancers and anti bacterial drugs. Subsequently their activity against *Plasmodium* could also be shown. Sulfadoxine-pyrimethamine (SP; Fansidar®) is the most prominent anti-folate combination. SP was introduced as first line treatment soon after chloroquine had failed and was distributed until its own failure a few years later. Today multi-drug resistance is wide spread. Following WHO recommendations artemisinin based combinations (ACTs) are now used as first-line treatment in all endemic countries. Given the importance of ACTs and the absence of variable therapeutic alternatives, the recent reports of declining efficacy (Alker et al, 2007; Denis et al, 2006a; Denis et al, 2006b; Noedl et al, 2008) and artemisinin-resistant malaria (Dondorp et al, 2009) in western Cambodia are rising the prospects of a renewed public health crisis: untreatable malaria.

History proves that the malaria parasite can develop resistance to all classes of inhibitors. Various mechanisms of resistance are known. Mechanistically and from an evolutionary perspective, phenotypic alterations have to be differentiated from

heritable genetic changes. A classical phenotypic, non-heritable change is the over-expression of drug targets or drug transporters.

Genetic alterations that translate into the selectable phenotypic changes include single nucleotide polymorphisms (SNPs) and gene amplifications. Genetic changes can lead to altered drug-binding sites in target or transporter proteins and/or stable over-expression of such proteins.

1.5 Gene duplication and amplification

Gene amplification is a common adaptive mechanism with various biological functions. In the following paragraph an overview of gene amplification and its implication in development and differentiation, in evolution and in drug resistance is given. At the end the molecular basis for the emergence of duplication and further amplification are summarized.

Gene amplification in development

The need of high amounts of a particular gene product during development, proliferation or cell differentiation has favoured gene amplification as an adaptive strategy in various organisms. For instance, in amphibians, the gene encoding for ribosomal RNA is selectively amplified during oogenesis (Gall, 1968) and in oocytes (Brown & Dawid, 1968) and thus ensures synthesis of high amounts of proteins, which are essential for development of the embryo. Some Dipteran flies *Rhynchosciara americana* (Glover et al, 1982; Santelli et al, 2004), *Bradysia hygida* (Laicine et al, 1984) and Sciara coprophila (Wu et al, 1993) use gene amplification in their salivary glands to produces high amounts of structural proteins. Gene amplification in *Drosophila melanogaster* has also been described. Two cluster of chorion (eggshell) are amplified in follicle cells (Spradling, 1981; Spradling et al, 1980) and two additional amplicons were recently identified in a genomic hybridization array (Claycomb et al, 2004).

Gene amplification in evolution

In the 1970 book “Evolution by Gene Amplification” by Ohno’s described the occurrence and the necessity of extensive gene amplification events during the evolution of vertebrates. The expansion of whole genomes was only possible by previous amplification of large chromosomal regions and subsequent divergence. In contrast smaller-scale copy number variations (CNV) between closely related species are an indicator for more recent and ongoing evolution. Recently, a genome-wide study of five hominoid species, including humans was performed. The majority of gene amplifications were found to have occurred over the last 15 million years, i.e.

during the evolution of great apes and humans (Fortna et al, 2004). Within single species, the presence of gene families is a convincing example for the importance of amplification in evolution. Often gene families cluster in the genome and share a common ancestor. In summary, gene amplification can give rise to new genes with similar or divergent functions. The exact mechanisms of selection and its driving force, however, are still debated.

The evolutionary trajectory of an amplification event depends on whether its result is selectively neutral (=no change in phenotype) or provides an immediate fitness benefit (=phenotypic adaptation). According to the neutral hypothesis (Kimura, 1968), genetic diversity is maintained by a balance between random mutations or amplifications and genetic drift, which occurs due to chance in the distribution of allele frequencies from generation to generation. Once a selectively neutral gene duplication has accidently occurred, the probability of fixation or loss in a population is determined by random genetic drift (Bergthorsson et al, 2007). This is a direct function of population size: the larger the population, the less likely is fixation as outcome (Lynch et al, 2001). With regard to the additional genomic copy, Ohno predicted that only selectively neutral amplicons could diverge and gain new functions. (I) The subsequent fate of the additional copy can be depicted in three scenarios. (1) Mutations can render the additional copy non-functional by the introduction of a STOP codon or by point mutation in key structures of the protein (non-functionalization); or (2) the copy gains a beneficial function (neo-functionalization) or (3) sub-functionalization occurs and the two newly arisen copies partition the task of the ancestral gene (Force et al, 1999; Lynch & Force, 2000). With sub-functionalization, two new genes with distinct functions are created.

(II) Alternatively one minor activity of the protein could suddenly gain increasing importance in variable ecological conditions (Bergthorsson et al, 2007). Or important for this work, if the initial amplification results in a phenotypic change, the allele can be under positive selection pressure. Both mechanisms would assure the maintenance of the additional copy without the above-described functionalization.

The role of gene amplification in drug resistance

Gene amplification is a common mechanism in drug resistance of bacteria, protozoan and mammals. In bacteria plasmid borne gene amplification is distinguished from amplification occurring on chromosomes. *Proteus mirabilis* was the first organism, grown in the presence of antibiotics, which was found to display an increase in plasmid size conferring resistance (Rownd et al, 1971; Rownd & Mickel, 1971). A few years later a chromosomal gene amplification with up to 30 additional copies was

found in *Escherichia coli* conferring high levels of ampicillin resistance (Normark et al, 1977). For both mechanisms various examples followed the initial discovery. In protozoa gene amplification was also shown to play a specific role in the emergence of resistance. In *Leishmania* species, antimony-resistant strains were found to have increased copy numbers of various genes implicated in resistance (Leprohon et al, 2009; Lin et al, 2008). The most prominent example for gene amplification in *Plasmodium falciparum* is probably *mdr*, which encodes for Pgh1, a homologue to the human P glycoprotein 1. The trans-membranous protein is located at the parasite's food vacuole (Cowman et al, 1991) and confers resistance to several anti-malaria drugs (Reed et al, 2000). Recently amplification of the GTP cyclohydrolase was discovered first in laboratory *P. falciparum* strains (Kidgell et al, 2006) and later in *P. falciparum* field strains from south East Asia (Nair et al, 2008). GTP cyclohydrolase is the first enzyme of the folate pathway. The biological relevance of its amplification is not yet understood but thought to be associated with anti-folate resistance.

In mammalian cancer cells resistance to methotrexate was associated by amplification of the *dhfr* gene in murine cells (Kaufman et al, 1978; Schimke et al, 1978a; Schimke et al, 1978b) in hamster ovary (Kaufman & Schimke, 1981) and finally in leukaemia patients treated with methotrexate (Horns et al, 1984).

Molecular mechanism

The known molecular mechanisms for gene amplification are as diverse as their roles in cellular processes. In principle four major mechanisms can be distinguished: NAHR (non allelic homologous recombination), NHEJ (non homologous end joining), FoSTeS (Fork Stalling and template switching) and retrotransposition. In the following the four mechanisms are briefly described and explained.

NAHR (non allelic homologous recombination)

NAHR is a mechanism of chromosomal DNA rearrangement, which is facilitated by low copy repeats (LCR) (Shaw & Lupski, 2004; Stankiewicz & Lupski, 2002), by *Alu* repeat elements (Babcock et al, 2003; Han et al, 2008) and by pseudogenes (Kim et al, 2008; Stankiewicz & Lupski, 2002). The rearrangement can occur during meiosis and mitosis. The minimal sequence homology required in both cell division cycles is different. Whereas chromosomal rearrangement during mitosis occurs already at sequences, which share high homologies over only 200 to 300 bp (Waldman & Liskay, 1988), is the minimal requirement for rearrangement during meiotic cell division more stringent (sequence homology over 300 to 500 bp) (Reiter et al, 1998).

NHAR can result in deletion, duplications or inversion of genomic DNA sequences depending on which parts of chromosomes are involved. Important for the understanding of NAHR is the formation of a crossing over junction, which during the subsequent dissociation process can create a loss on one DNA strand and a gain on the other strand (rearrangement). The replication machinery is not involved. An interchromosomal NAHR is the formation of a crossing over junction between two homologous chromosomes at a non-allelic sequence site and can be direct, inverted or complex. NAHR is also occurring between chromatids (interchromatid) and within one chromatid (intrachromatid) (Figure 1-3) (Lupski, 1998; Stankiewicz & Lupski, 2002). Following cell division, the chromosomes with either lost or gained DNA sequences are distributed randomly to the daughter cell. The outcomes of NAHR are therefore only apparent after S1 phase has occurred.

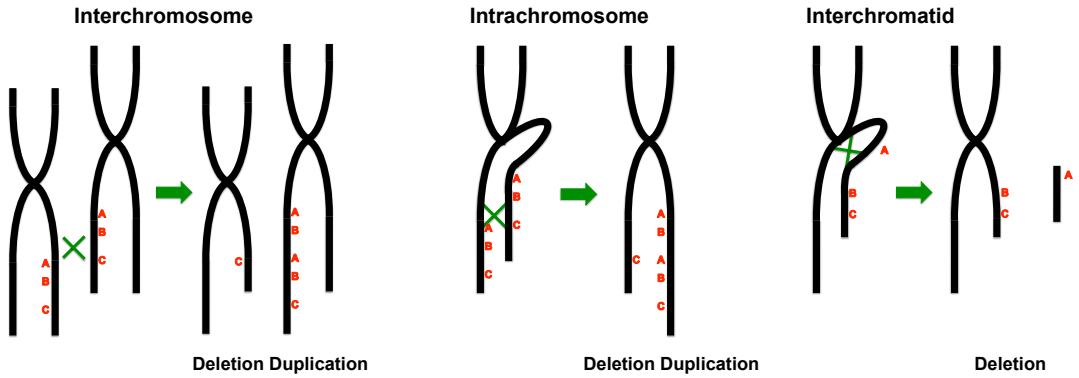

Figure 1-3 Non allelic homologous recombination (NAHR) adapted from (Stankiewicz & Lupski, 2002). An example of each of the three principal recombination events is shown. A,B and C indicate three genes located on the chromatids. The green cross represents a crossing over event. Deletion, duplication and inversions are the results of NAHR, which can occur interchromosomal, intrachromosomal and interchromatidal. The deletion in the intechromatid NAHR event can also result in a translocation or inversion, if the fragment is reintegrated.

NHEJ (non homologous end joining)

Non-homologous end joining (NHEJ) is a mechanism used by eukaryotic cells to repair a double strand break. Double strand breaks can be introduced by reactive oxygen species, by ionising radiation and by DNA replication over a nick in one DNA stand (Lieber et al, 2003). In contrast to NAHR, NHEJ occurs independent of repeat units, but structural features of genomic regions might facilitate a double strand break. In and around breakpoints, where NHEJ had occurred, short sequence homologies, 2 – 4 base pair repeats, palindromic sequences and sequences able to

form a intrastrand hairpin (TTTAAA) were discovered (Toffolatti et al, 2002). After a double strand break (DSB), exonucleases create on both loose ends of the break single stranded DNA (Figure 1-4). In the case of DSB repair without recombination, the two loose ends invade a homologous chromosome and copy the missing sequence. The resulting holiday junction is resolved without recombination. But if DSB repair leads to recombination, two possible mechanisms are distinguished. (1) A second DSB generates two additional loose ends and random joining of the ends leads to recombination of large DNA sequences. (2) The strand of one end invades either a non homologous, foreign or an upstream region of the same strand and by replication using the invaded strand as template an additional copy of that genomic region is created. Strand invasion often results in tandem orientation of the duplicated region, a so-called head to tail arrangement (Lee et al, 2006). But it can also result in translocation, inversion or loss, if a second DSB separates, during the process of strand invasion and replication, the newly synthesised DNA fragment from the template and from its own strand (Lee et al, 2006). Important for the understanding of NHEJ is that this process can result in duplication when a template is present from where the additional DNA can be read and copied from. This is a fundamental difference to NAHR, by which only rearrangements of chromosomal regions occur.

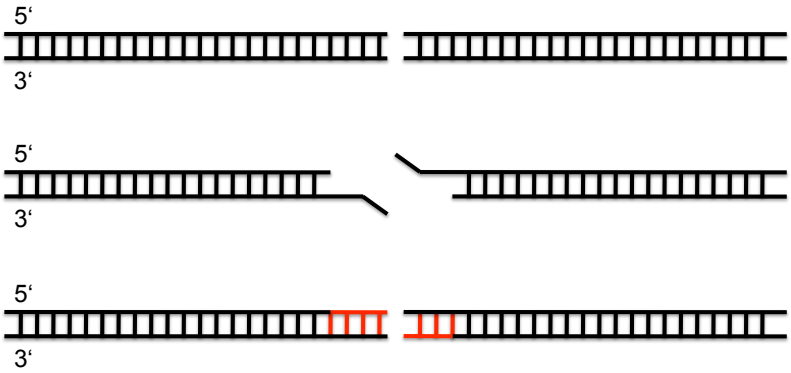

Figure 1-4 Non homologous end joining (NHEJ) adapted from (Gu et al, 2008). A double strand break (DSB) is repaired by creating first a single stranded end on both sides of the break, induced by exonuclease activity. The loose ends can invade a homologous strand to copy the missing sequence to fill the gap and the two ends are rejoined. Often some nucleotides are missing at the junction site. Recombination occurs if the single strand invades a foreign double helix or if two unrelated ends are joined.

DNA amplification during replication

Another common mechanism of gene amplification is through the process of DNA replication. As mentioned above, *Dipteran* flies use gene amplification during their development to produce high amount of structural proteins. The mechanism by which they achieve amplification is repeated firing of a replication initiation zones and bidirectional replication fork movement (Delidakis & Kafatos, 1989; Heck & Spradling, 1990; Liang & Gerbi, 1994; Liang et al, 1993; Osheim et al, 1988; Yokosawa et al, 1999). With one firing after the other and the movement of the replication fork in both directions two bubbles are created within the previous one. The model has been fittingly dubbed 'onionskin' (Figure 1-5) (Liang et al, 1993). Characteristic for this model is the gradual decline of amplification the further apart a sequence is located from the initiation zone. The target of amplification has to be in close proximity to the initiation zone. Surrounding genes are often only partially amplified and not functional by having lost parts of theirs open reading frame or promoter regions.

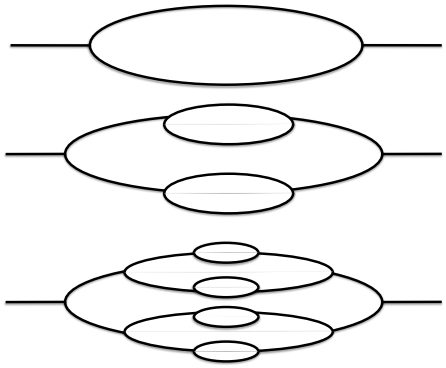

Figure 1-5 Onionskin model adapted from (Claycomb & Orr-Weaver, 2005). Repeated firing of an initiation site created bidirectional replication forks within each other.

Fork Stalling and Template switching (FoSTeS)

Another process in which DNA replication is involved and gene amplification is created is the Fork Stalling and Template switching (FoSTeS) mechanism (Figure 1-6). The model is based on stalling of the replication fork during which the lagging strand disengages from its template and invades another replication fork in proximity (Lee et al, 2007). Depending on whether the new replication fork is situated downstream or upstream of the original one, gene duplication or deletion are the consequences. The orientation of the newly synthesised gene depends on which strand of the new replication fork is used as template. If the invading strand places itself on the leading strand a tandem repeat of the genes is created, if the strand places itself on the lagging strand an inverse orientation of the two duplicated genes is generated. This process of fork pausing and template switching can occur several times in a row and thus creates complex sequence duplication, triplication in both possible orientations and deletions (Lee et al, 2007). The requirements for strand switching during replication were proposed to consist of small homology regions, such as small direct or inverted repeats (Lee et al, 2007).

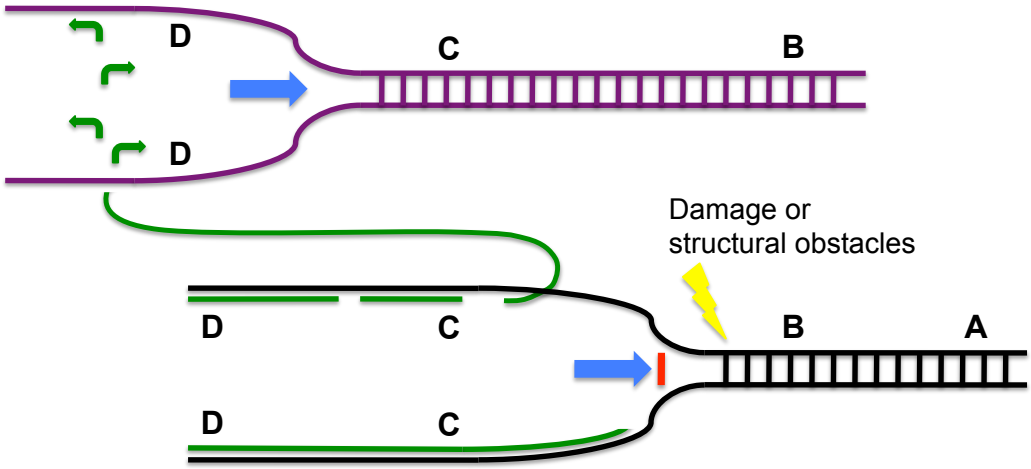

Figure 1-6 Fork Stalling and Template Switching (FoSTeS) adapted from (Gu et al, 2008). The replication fork pauses at damages or at structural obstacle in the DNA and the lagging strand disengages from its template and invades a neighbouring replication fork. Here an example is shown in which the neighbouring replication fork is still behind the original and gene D and C are copied again. Depending on which strand is used as template and in which direction the synthesis starts, are tandem and inverse orientation of the new gene possible. This process can occur multiple times before the strand finds back on its original template, creating very complex new structures and amplifications. Important is the fact that the real situation is three-dimensional, which shortens the possible distances between the forks significantly.

Transposable elements

Two majors classes or transposable elements have to be distinguished: DNA transposons, which jump by a cut and paste mechanism and RNA retrotransposons, which move by a copy and paste mechanism. DNA transposons jump as DNA from place to place within chromosomes and RNA transposons move via an RNA intermediate. In the first step they are transcribed into RNA and then reverse transcribed back into DNA by a self-encoded enzyme. Various degradations and inactive forms, as well as a few active forms are found in all eukaryotic genomes. During the movement of a transposable element, surrounding sequences or exons (exon shuffling) or genes are accidently co-transported to a different location. In human cells the only still active autonomous transposon is the long interspersed element-1 (L1), which covers about 15% to 18 % (Goodier & Kazazian, 2008; Kazazian & Moran, 1998) of the human genome.

Frequency of copy number variation

The frequency by which point mutations occur in mammals is estimated around 10^{-9} per generation (Drake et al, 1998). The spontaneous appearance of copy number

variations (CNVs) is up to 5 orders of magnitude higher, 10^{-4} per generation (Inoue & Lupski, 2002).

In a recent publication on mutation rates in *Plasmodium falciparum*, it was estimated that a single point mutation at position 108 in the *Pfdhfr* gene occurred between 3 x 10^{-11} and 2,5 x 10^{-9} per generation (Paget-McNicol & Saul, 2001). Mutation rates may vary from organism to organism and the actual rate is extensively dependent on the DNA repair machinery, but it is unquestionable that in eukaryotes CNVs occur several magnitudes more frequently than spontaneous single point mutations.

The stability and the maintenance of newly acquired amplifications is dependant on their beneficial or detrimental effects and can vary significantly.

1.6 Folate pathway

The de novo folate synthesis pathway in *Plasmodium falciparum* has been identified and characterized extensively (Figure 1-7). The only remaining unidentified missing link, the PTPS (PFF1360w), which catalyzes the step between the first enzyme and the third enzyme of the pathway, was also recently described (Dittrich et al, 2008; Pribat et al, 2009). The first enzyme of the folate pathway was identified in 1985. The GTP cyclohydrolase (PFL1155w) catalyzes the conversion from GTP to 7,8-dihydroneopterin3'-triphosphate (DHN-PPP) (Krungkrai et al, 1985). The apparent absence of a dihydroneopterin aldolase (DHNA) activity in *Plasmodium falciparum* cell extracts could only recently be solved by the identification of 6-pyruvoyltetrahydropterin synthase (PTPS) (Dittrich et al, 2008). PTPS is conventionally involved in the tetrahybiopterin (BH_4) (Thony et al, 2000) pathway but the presence of a glutamic acid instead of a cysteine residue in the active site possibly explains the gain of a different or additional function in *Plasmodium falciparum*, i.e. converting DHN-PPP into 6-hydroxymethyl-7,8-dihydropterin (Dittrich et al, 2008). The catalytic activity of PPPK and DHPS, which catalyse the two following steps in the folate pathway, were found to be encoded by a single gene in *Plasmodium falciparum*, named *Pfdhps* (Triglia & Cowman, 1994). First the pyrophosphokinase (PPPK) adds a pyrophosphate (PP_i) through hydrolysis of ATP to AMP and thereby generates 6-hydroxymethyl-7,8-dihydropterin pyrophosphate (DHPP). In the second catalytic step para-aminobenzoic acid is added by DHPS to form 7,8-dihydropteroate (DHP) (Brooks et al, 1994; Triglia & Cowman, 1994), the substrate of DHFS. The following poly-glutamylation is an essential step in prokaryotes and eukaryotes. Four to seven glutamyl residues are added resulting in altered transport properties of the co-factor in the cell and changed enzyme kinetics (Schirch & Strong, 1989). Conventionally, two different enzymes catalyze addition of

the first and subsequent addition of glutamates. In *Plasmodium falciparum* the bifunctional enzyme DHFS, encoded by *Pfdhfs,* fulfils both activities and thus generates 7,8-dihydrofolate (H_2Folate) (Lee et al, 2001; Salcedo et al, 2001). DHFR, which catalyzes the NADPH-dependant reduction of H_2Folate to tetrafolate (H_4Folate) was identified in *Plasmodium falciparum* already in the late nineties (Bzik et al, 1987). Tetrafolate contributes to the one-carbon pool and functions as co-enzyme in the cell.

Of note, the gene *Pfdhfr* encodes also for a bifunctional enzyme. After the addition of a methyl group on H_4Folate by the serinehydroxymethyltransferase (SHMT), the second function of DHFR-TS is the transfer of this methyl group on a dUMP molecule to generate dTMP, essential for DNA replication. The enzyme is called thymidylate synthase (TS).

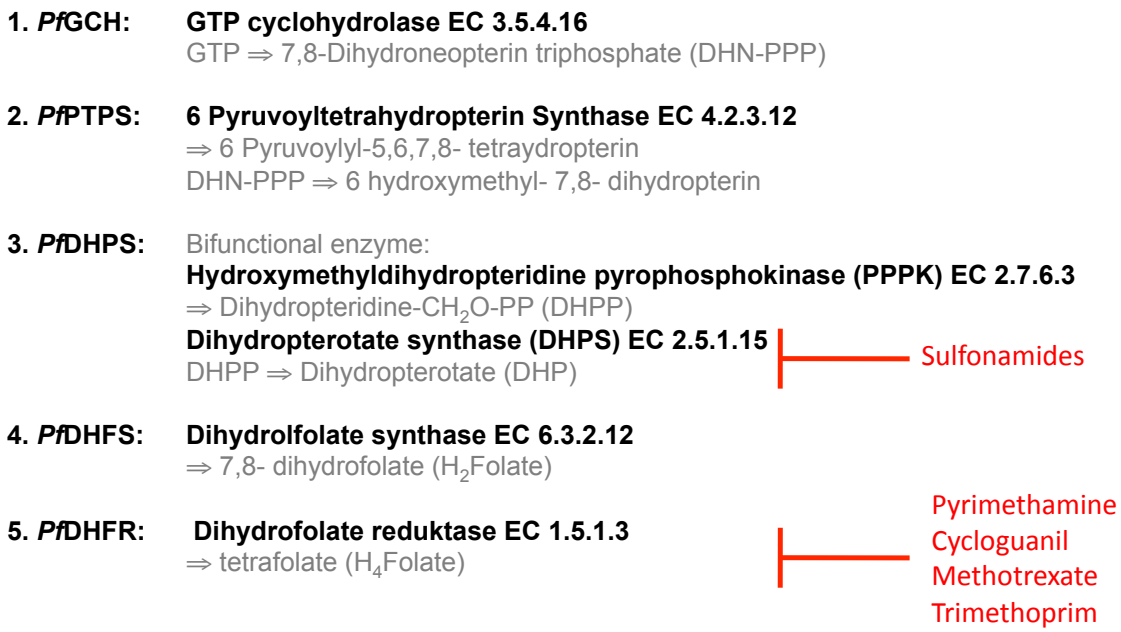

Figure 1-7 Folate biosynthesis pathway in *Plasmodium falciparum.* (black) enzyme names, (grey) substrates and products, (=>) catalysed reaction. The enzymes of the folate pathway are listed in order of their sequential activity. The biosynthesis starts with GTP, which is converted to DHN-PPP. The following enzymes generate through the intermediates of DHPP and DHP, H_2 Folate and H_4 Folate. Two enzymes in this pathway are known drug targets for inhibitors (in red).

Folate derivatives are essential co-factors in cellular processes. The synthesis of nucleotides and the metabolism of several amino acids depend on it. Especially heavily dividing cells rely on the synthesis of folate for DNA replication. In fact, even before the discovery of the involved genes and the characterisation of their enzymatic activities, the folate pathway has been targeted in malaria parasites, in

cancer and in bacterial infections. In the 1930s the search for synthetic antimalarials led to the discovery of pyrimethamine and proguanil, a prodrug that is rapidly converted *in vivo* to its active metabolite cycloguanil (McGready et al, 2003). In the 1940 sulfanilamide was found to inhibit growth of monkey malarian parasites (Coggeshall, 1940). A few years later in the 1960s trimethoprim was introduced for clinical use in the treatment against bacterial infections in Western Europe, but soon after its introduction first cases of resistance were reported, as reviewed by (Skold, 2001).

Sulfonamides target the DHPS, whereas pyrimethamine, cycloguanil and trimethoprim are DHFR inhibitors. Soon after their introduction to treat malaria, first clinical failures were reported, even after single exposures (Martin & Arnold, 1968) and resistance to these drugs was found to be conferred by mutations in both genes encoding for the respective enzymes. Resistance against sulfadoxine, a sulfonamide used in fixed-dose combination with pyrimethamine (SP) in the treatment against malaria, was directly associated to point mutations in *dhps*, which decrease the inhibition efficiency of both drugs (Triglia et al, 1997). In East Africa, mutations at codons A437G and K540E of *DHPS*, together with the triple mutations of *dhfr* were shown to be significant predictors of SP treatment failure in Kenya, Malawi and Uganda (Kublin et al, 2002; Omar et al, 2001; Staedke et al, 2004).

The three mentioned DHFR inhibitors selected for various mutations in *dhfr*. Pyrimethamine was the most widely used drug and various groups soon reported particular SNPs or SNP combinations (haplotypes) as underlying mechanism of resistance (Cowman et al, 1988; Peterson et al, 1988). The most prominent and most relevant point mutations of *dhfr* are at the amino acid positions 108, 51, 59, 16 and 164. Although cross-resistance to anti-folates is commonly found, particular point mutation confer differential resistance patterns. The amino acid substitution at position 16 (A16V) was always found to be associated with S108T and results in high cycloguanil resistance (up to 1,000 fold) (Sirawaraporn et al, 1997), without altering pyrimethamine sensitivity (Foote et al, 1990; Peterson et al, 1990). The laboratory strain FCR3 is a representative for this group of parasites. In the field, very few parasites are reported with this particular combination of point mutations (Biswas et al, 2000). The low catalytic activity of the enzyme carrying A16V alone or in combination with S108T (Sirawaraporn et al, 1997) is, together with extensive use of pyrimethamine, most likely the reason for its rareness. Sirawaraporn et al. have investigated *dhfr* mutations in isolation or as haplotypes and assessed their catalytic efficiency and the degree to which they confer resistance against pyrimethamine and cycloguanil. The findings are summarized in the following paragraph. The mutation

S108N alone shows the best balance between establishment of pyrimethamine resistance and conserving highest catalytic activity. All other three mutations at position N51I, C59R and I164L only marginally decrease sensitivity to pyrimethamine and moderately alter cycloguanil sensitivity. All three SNPs show significantly reduced enzyme activity, when present alone. In combination, however parasites carrying double mutant N51I/S108N displays an ideal balance of high resistance and high enzyme efficiency, which is even greater than S108N alone. The triple mutant N51I/C59R/S108N displays again a significant loss of enzyme efficiency (20 fold) but gains at least 10 fold pyrimethamine and cycloguanil resistance. Triple mutant DHFR enzyme will thus only confer a survival benefit to parasites in a population under high continuous pyrimethamine drug pressure. The quadruple mutant N51I/C59R/S108N/I164L restores part of its enzyme efficiency and shows highest attainable resistance pattern for both, pyrimethamine and cycloguanil (Sirawaraporn et al, 1997).

In contrast to this detailed analysis of mutated enzyme activities compared to wild type is a recently published work. In a comparative study on the catalytic activity of wild type and mutated DHFR enzyme the authors could show the opposite effect. An even higher catalytic activity of the mutated enzyme compared to wild type DHFR was measured (Sandefur et al, 2007). The authors concluded that their findings would explain the persistence of mutated dhfr in Africa even after removal of SP.

Trimethoprim-sulfamethoxazole was found to reduce morbidity and mortality in HIV infected patients in sub-Saharan Africa, when given as chemoprophylaxis against opportunistic infections (Anglaret et al, 1999; Mermin et al, 2006; Wiktor et al, 1999) and was therefore recommended by UNAIDS. The overlapping use of two anti-folates targeting DHFR in a single population is of great concern. It was demonstrated that parasites carrying one to three mutations in DHFR were less susceptible to trimethoprim (Iyer et al, 2001) and resistance of trimethoprim was found to be highly correlated to pyrimethamine (Khalil et al, 2003).

In addition to the mentioned amino acid substitution in response to anti-folate drug pressure, gene amplification of *dhfr* was described in cancer (Carman et al, 1984; Horns et al, 1984; Trent et al, 1984) and in rodent malaria (Cowman & Lew, 1989). In *Plasmodium falciparum*, two studies suggested *dhfr* gene duplication following selection for pyrimethamine resistance *in vitro* as a potential resistance mechanism (Inselburg et al, 1987; Thaithong et al, 2001). Intriguingly, *dhfr* gene duplication or amplification, however, has never been reported in *P. falciparum* field isolates.

1.7 Detection of drug resistance *in vivo*

In general two major methods are used to determine drug sensitivity and resistance; the *in vitro* test and the *in vivo* test. Specificity and sensitivity are increased when theses two complementary tests are used side by side.

The activity of an anti-malarial drug against reference laboratory-adapted strains of parasite isolates obtained from patients can be performed *in vitro* by determining the drug concentration required to inhibit 50% of maximal growth in unexposed control cultures (IC_{50}). A patent isolate can consist of several clones with different genetic background and evolutionary histories. The *in vitro* method can be calibrated against reference strains with known sensitivities and it generates reproducible phenotypes under optimal artificial conditions. Drug parasite interactions are directly measured due to the absence of *in vivo* confounding factors, e.g. pharmacokinetics, innate and adaptive immunity and initial parasite load, just to give a few examples. Therefore a direct correlation of IC_{50} values and treatment failure at the individual level is often not observed (Sasi et al, 2009).

In the *in vivo* test the rate of treatment failure is determined by monitoring parasite persistence or reappearance for up to 8 weeks through microscopic analysis of blood smears. The test addresses the clinically relevant questions of whether an antimalarial treatment can lead to complete elimination of blood stage infections (Borrmann et al, 2008), but the sensitivity of this method is limited to the detection limit of the microscope, i.e. ~ 20 parasites/µl corresponding to a total body biomass of $\leq 10^8$ parasites. Beside the sensitivity, the definition of treatment failure is also critical. In high transmission areas, reappearance of parasites in the blood requires PCR-based molecular techniques to distinguish recrudescent from re-infection. These techniques have limited resolution power even under hypothetical ideal assay conditions due to the finite allele diversity of local parasite populations. This leads to unreliable treatment outcome estimates. In summary, the *in vivo* test is clinically indispensable but its sensitivity, especially for determining complete parasite removal is too variable to serve as a phenotype for classifying drug-resistant infections (even when drug exposure is controlled for).

As emerging or spreading of parasite resistance to commonly used drugs is associated with failure of chemotherapeutic regimens to completely eliminate primary asexual blood stage infections, the importance of early detection and monitoring becomes obvious. An early and reliable detection of failing drugs is particularly important in regard to the recent reports of declining artemisinin efficacy in Thailand (Alker et al, 2007) and Cambodia (Denis et al, 2006a; Denis et al, 2006b; Noedl et al,

2008). In addition, the fact that incompletely eliminated infections are variably suppressed by acquired immune responses raises the intriguing question of whether even susceptible blood stage infections can survive maximal drug pressure during treatment at or below a hypothetical minimum infectious intra-host population size (~50,000 parasites; corresponding to the inoculum of liver stage merozoites into the circulation). This may be important since wild type parasites are predicted to outgrow resistant parasite due to fitness benefits. It would also influence the rate with which de novo resistance can be selected for during treatment, i.e. at peak plasma drug concentrations, as opposed to blood stage infections arising during convalescence when plasma concentrations of long-half life drugs have dropped below the minimal inhibitory concentration.

1.8 Aim of the study

The survival of the parasite depends on numerous factors, such as transmission efficiency, vector behaviour and control on the one hand and host genetics, innate immunity and the efficacy of human interventions (Figure 1-8).

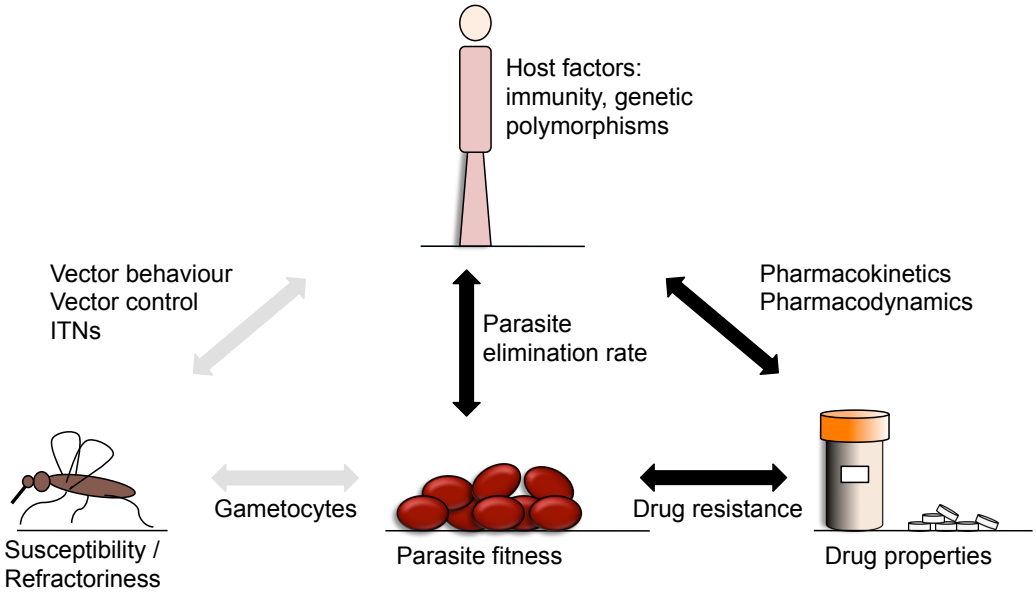

Figure 1-8 Parasites survival determined by vector, host and drug interactions.

Prompt and efficacious chemotherapy remains an important cornerstone in the fight against malaria. Drug-parasites interactions are the major determinant of outcome. The study aims at dissecting biological correlates of this interaction using discreet experimental approaches *in vitro* and *in vivo*.

I started by studying parasite survival *in vivo*. This was also important for designing subsequent experiments that are relevant and provide insight in the molecular events leading to emergence of parasite resistance in malaria endemic areas.

Closely related to this question, I then analysed parasites isolates that had been exposed to various drugs over the last years in the community for drug susceptibility *in vitro*. The genetic background of these parasites is expected to be shaped by balancing fitness costs and benefits under varying drug pressure (Figure 1-8). Here resistance has developed *in vivo* but the phenotype was assessed *in vitro*.

In the final part of the project, I attempted to gain insight in the evolution of drug resistance *in vitro*, i.e. in isolation. Cell culture conditions are controlled and so cause

and effect con be more clearly assigned. In particular, I focused on the molecular mechanisms with an evolutionary perspective. For this work, I set up induction of resistance experiments *in vitro* and analysed the time course and sequence of resistance mechanisms.

For the *in vivo* studies, I analysed data from patients who received amodiaquine in the beginning and later artemisinin combination therapies (ACTs) after implementation as first-line treatment in the study area in November 2006. The two combination therapies were artemether-lumefantrine (Coartem) and dihydroartemisinin-piperaquine (Eurartesim).
For the *in vitro* work, I used pyrimethamine, because SP (Fansidar®) was used in the previous years as first-line treatment and the parasite population under investigation was therefore massively exposed to the drug. Importantly, initial studies had shown that induction of resistance *in vitro* is feasible (Paget-McNicol & Saul, 2001; Thaithong et al, 2001). Of particular interest was the relationship between gene amplification and the emergence of single nucleotide polymorphisms.

2. Material and methods

2.1 Materials

2.1.1 Chemicals

Acetic acid	J.T. Baker, Deventer, NL
Agarose	Invitrogen GmbH, Karlsruhe, DE
Albumax II	Gibco Invitrogen, Karlsruhe, DE
Ampicillin	Sigma Aldrich, Taufkirchen, DE
Bacto™ Agar	BD, Heidelberg, DE
Bacto™ Pepton	BD, Heidelberg, DE
Chloroquine diphosphate salt	Sigma Aldrich, Taufkirchen, DE
D-(+) Glucose	Sigma Aldrich, Taufkirche, DE
D-Sorbitol	Fluka, Sigma Aldrich
Dimethylsulfoxide (DMSO)	Sigma Aldrich, Taufkirchen, DE
Dodecylsulfat-Na-salt (SDS)	Serva, Heidelberg, DE
Ethylendiamintetraacetic acid) EDTA	Acros
Ethanol absolute 100%	J.T. Baker, Denventer, NL
Ethanol 96%	JT Baker, Deventer, NL
Ethidiumbromide 1% (10mg/ml)	Carl Roth GmbH, Karlsruhe
Ethidiumbromide	Sigma Aldrich, Taufkirchen, DE
Gentamicin 50mg/ml	Gibco Invitrogen, Karlsruhe, DE
Giemsa Solution	Merck, Darmstadt, DE
Glycerol	Carl Roth GmbH, Karlsruhe, DE
HEPES	Carl Roth GmbH, Karlsruhe
Human AB Serum	Blood bank, Uniclinic Heidelberg
Hydrogenchloride	Merck, Darmstadt, DE
Hypoxanthine 10mM	ccpro, Oberdorla, DE
Potassiumacetat	VWR, Darmstadt, DE
Potassiumchloride	AppliChem GmbH, Darmstadt
Kaliumhydrogenphosphat-Trihydrat	Merck, Darmstadt, DE
Maleic acid	Carl Roth GmbH, Karlsruhe, DE
Methanol	J.T. Baker, Deventer, NL
Sodiumacetat	Grüssing, Filsum, DE
Sodiumchlorid	Riedel, Hannover, DE

Tri-sodiumcitrat-dihydrate	Carl Roth GmbH, Karlsruhe
Sodiumhydrogencarbonate	Grüssing, Filsum, DE
Sodiumhydroxid	Merck, Darmstadt, DE
Phosphate buffered saline	Sigma Aldrich, Taufkirchen, DE
Pyrimethamine	Sigma Aldrich, Taufkirchen, DE
RNA DNA Stabilization reagent for blood	Roche, Mannheim, DE
and bone marrow	Roche Mannheim, DE
RPMI with L Glutamine	Gibco, Invitrogen, Karlsruhe, DE
RPMI 1640 Medium without Glutamine	Sigma Aldrich, Taufkirchen, DE
Dodecylsulfat-Sodium salt SDS	Serva, Heidelberg, DE
Sybr Safe DNA Gel stain 10.000 x in DMSO	Invitrogen GmbH, Karlsruhe, DE
Hydrochlirid acid	Merck, Darmstadt, DE
Saponin	Sigma Aldrich, Taufkirchen, DE
Sybr Green I stock solution 10,000 x (DMSO)	Invitrogen GmbH, Karslruhe, DE
Trimethoprime	Sigma Aldrich, Taufkirchen, DE
Tris	Carl Roth GmbH, Karlsruhe, D
Trishydrochlorid	Carl Roth GmbH, Karlsruhe, D
Triton x 100	Carl Roth GmbH, Karlsruhe, D
Tween 20	Gerbu Biochemicals GmbH, Gaiberg, DE

2.1.2 Commercial Kits

DIG High Primer DNA Labeling	
and Detection starter Kit II	Roche, Mannheim, DE
Fast Sybr Master Mix	Applied bioystems (ABI)
mRNA Isolation Kit for blood	
and bone marrow	Roche, Mannheim, DE
QIAamp DNA-Blood Kit	QIAGEN, Hilden, DE
QIAgen PCR Purification Kit	QIAGEN, Hilden, DE
QIAquick Gel extraction Kit	QIAGEN, Hilden, DE
RETROscript	Ambion, Huntingdon, UK
RNeasy Mini Kit	QIAGEN, Hilden, DE
RNase-Free DNase Set	QIAGEN, Hilden, DE
SuperScript III one-step RT-PCR System	Invitrogen GmbH, Karlsruhe, DE
TOPO TA cloning® kit	Invitrogen GmbH, Karlsruhe, DE
Turbo DNA free Kit	Ambion, Huntingdon, UK

2.1.3 Consumables

ABgene PCR plates	Thermo Scientific, Waltham,USA
Amersham Hyperfilm™ ECL	GE Healthcare, Buckinghamshire
Cryotobes	Nunc, Langenselbold, DE
Cover for 96 well plate	Greiner Bio-one, Firckenhausen
FIA-Plate, black, 96 well plate	Greiner bio-one, Frickenhausen
Filter Tip 10E, 20, 100, 200, 1000	Greiner bio-one, Frickenhausen
Filter Cap cell culture flask, 25cm^2, 175cm^2	Greiner Bio-one, Firckenhausen
Kodak BioMax MR film	Sigma Aldrich, Taufkirchen, DE
Hybond N$^+$ - membrane	GE Healthcare, Buckinghamshire
Universal Tips, yellow, blue	Greiner bio-one, Frickenhausen
PP test tube, 15ml, 50ml	Cellstar, Greiner bio-one
Pipette, 1ml, 2ml, 5ml, 10ml, 25ml	Cellstar, Greiner bio-one
Safe lock tubes 1,5 ml	Eppendorf, Hamburg
RNase free Biopure 1,5 ml	Eppendorf, Hamburg
PCR softstrips 0,2ml, colour	Biozym Scientific GmbH, Oldendorf
epT.I.P.S. Reloads 2-200µl	Eppendorf, Hamburg
epT.I.P.S. Reloads 20-300µl	Eppendorf, Hamburg
96 well plate (black and clear	Greiner Bio-one, Firckenhausen

2.1.4 Equipment

AdventurerPro™ balance	Ohaus
Computer hardware	iMac
Computer software	
7500 System software	Applied biosystems
Bioedit	Ibis Therapeutics, Carlsbad
Endnote	Thomson Reuters
EnzymeX3.1	Mekentosj.cin
Microsoft office 2008	Microsoft,
Quantity one®	BIO-RAD
Primer Express	Applied biosystems
Prism 5	GrahpPad Software
Centrifuge	
Microcentrifuge GALAXY mini	vWR
Biofuge pico	Hereus, Kendro, Langensolbold

Fresco 21	Hereus Instruments, Hanau
Megafuge 1.0 R	Heraeus
Databases	
GeneDB	www.genedb.org
PlasmoDB	www.plasmobd.org
NCBI	www.ncbi.nlm.nih.gov/pubmed/
DNA Workstation (DNA/RNA UV cleaner)	G.Kisker, Steinfurt
Eclipse E 200 Microscope	Nikon
Electrophoresis System	BIO-RAD, Munich
Freezer	
-80°C	Heraeus GmbH, Hanau
Premium no frost (-20°C)	Liebherr, Biberach, DE
Premium (4°C)	Liebherr, Biberach, DE
Geldoc XR	Biorad, Munich, DE
Herasafe bench	Heraeus GmbH, Hanau, DE
Incubator Heracell 150	Heraeus / Thermo
Isotherm System 3880	Eppendorf, Hamburg
Microwave	LG
Mini PROTEAN 3	BIO-RAD, Munich
Mini Sub cell	BIO-RAD, Munich
Multipipette, 10µl, 100µl, 300µl	Eppendorf, Hamburg
Mastercycler epgradient	Eppendorf, Hamburg
Mini-PROTEAN® 3 CELL	BIO-RAD, Munich
Ph Meter	Schott
Pipette controller accu jet pro	Brand GmbH, Wertheim
Pipettes, 0,1-2,5µl, 2-20µl, 20µl-200µl, 100µl-1000µl	Eppendorf, Hamburg
PowerPac™ Bsic Power Supply	BIO-RAD, Munich
PowerPac™ HC Power Supply	BIO-RAD, Munich
Printer hpdeskjet 6122	Hewlett Packard, Heidelberg, DE
7500 Real time PCR system	Applied biosystems, Foster City
Sub-cell GT	BIO-RAD, Munich, DE
Sub-Cell® GT Agarose Gel	BIO-RAD, Munich, DE
Thermomixer compact	Eppendorf, Hamburg, DE
Thermostatt Waterbath	Mendingen
TransBlot Semi-Dry Transfer cell	BIO-RAD, Munich, DE
Vortex Mixter	neoLab

2.1.5 Buffer, ladder, medium and solutions

Buffer

Blocking solution	10 x blocking solution Diluted in maleic acid buffer
Denaturing solution	1,5M NaCl 0,5M NaOH
Detection buffer	0,1M Tris-HCL 0,1M NaCl pH 9,5
0,5 M EDTA (1 L)	186,1 g Na_2EDTA pH = 8 (NaOH)
Freezing solution (50 ml)	3 % sorbitol (1,5 g) 0,65 % NaCl (0,325 g) 28 % 14 glycerol (14 ml) Filtered
Maleic acid buffer	0,1M maleic acid 0,15M NaCl pH 7,5
MSF Lysis buffer	20mM Trise base pH 7,5 5mM EDTA 0,008 % (w/v) Saponin 0,08% (w/v) Triton X-100 Filter
Neutralising solution	1,5M NaCl 0,5M Tris-HCL
20 x SSC	3M NaCl 0,3M Sodiumcitrat 1mM EDTA
Step 1 washing solution	3 x SSC 0,5% SDS

Step 2 washing solution	2 x SSC 0,5 % SDS
50 x TAE buffer (1L)	2 M Tris base (242 g) 1 M glacial acetic acid (57,1 ml) 0,05 M EDTA, pH=8
10 x TBE buffer (1L)	890 mM Tris base (108 g) 890 mM boric acid (55 g) 20mM EDTA, pH=8
Thawing solution 1	12 % NaCl Filtered steril
Thawing solution 2	1,6 % NaCl Filtered steril
Thawing solution 3	0,9 % NaCl 0,2 % Glucose Filtered steril
Washing buffer	0,1M maleic acid 0,15M NaCl 0,3% Tween pH 7,5

DNA Ladder

Generuler^{TM} 1kb DNA Lader	Fermentas
100bp DNA Ladder	Invitrogen
DNA Molecular weight Marker III (Digoxigenin-labeled)	Roche, Mannheim

Medium

Complete cell culture medium (500 ml)	RPMI with L Glutamine (Gibco) 12 ml AB Serum (heat inactivated 56°C) 0,1 mM Hypoxanthine 250 µl Gentamicin (Stock 50mg/ml) 2,5 g Albumax (filtered sterile)

LB Medium for bacterial culture (1 L)	5 g Yeast extract
	5 g NaCl
	10 g Trypton
	(15 g Agar for plates)
	(Ampicillin 0,1 mg/ml for selection)

2.1.6 Plasmodium falciparum parasites strains

Laboratory strains

Table 2-1 lists the *P. falciparum* laboratory strains used in *in vitro* cultures in this work.

Table 2-1 *P.falciparum* strains, origins and donated from

P. falciparum lab strains	Country of origin	Donated from
Dd2	Indochina	Prof. Lanzer
D10	Papua New Guinea	Prof. Lanzer
3D7		Prof. Lanzer
Hb3	Honduras	Prof. Lanzer
FCR3	The Gambia	Prof. Lanzer

Plasmodium falciparum field isolates

Field isolates were collected in the course of a clinical audit of amodiaquine in Kilifi, Kenya (Sasi et al, 2009) (2.2.4.2) and from a comparative study on ACT (unpublished) (2.2.4.1). Blood samples were taken from patients suffering from mild malaria with a parasitaemia of 2000 to 200 000 parasites/µl on day 0 before treatment and on the day of parasite recurrence. The erythrocytes were isolated from the whole blood and the parasites were adapted to *in vitro* cultures for further experiments.

2.1.7 Enzymes

All restriction enzymes and corresponding buffers were purchased from New England Biolabs.

DNase was purchased from Ambion, Huntingdon, UK, Taq poylermase from Fermentas, St Leon Rot, DE.

2.1.8 Oligonucleotides and sequencing reaction

2.1.8.1 Oligonucleotides

Primers were purchased from Eurofins MWG operon or Invitrogen.

Table 2-2 Oligonucleotides If no accession numbers are available exact chromosomal locations are indicated. These primer pairs are all in proximity to the *dhfr* locus und therefore on chromosome 4.

Primer name (gene)	Sequence 5 ‘ to 3 ‘	Accession number
RESA A (for)	ATGAGACCTTTTCATGCATATAG	PFA0110w
RESA B (for)	CTATATATCATTTTAAATGGTAATCTTGG	PFA0110w
RESA C (rev)	CCAAGCGATTTGGTTCAACACAGTC	PFA0110w
RESA D (rev)	CTAAGTATACACCATCTTTTACGG	PFA0110w
Pfgch Southern for	CAATAATCAAAGTTACAGG	PFL1155w
Pfgch Southern rev	AGCATCGTGCTCTTTAACTCCCC	PFL1155w
Pfgch RT for	GGAGTTAAAGAGCACGATGCT	PFL1155w
Pfgch RT rev	ACTGTAGGATTCTCTTTTTCTGCTT	PFL1155w
PfgchSNP’s for	AACGAATGTGAGAAGGAAGACC	PFL1155w
Pfgch SNP’s rev	CCTGTAACTTTGATTATTG	PFL1155w
Pfgch compl Seq for1	ATTTTTCATTTAATGGACTGG	PFL1155w
Pfgch compl Seq rev1	CCTTCCTTATTTTCTTCTTTGG	PFL1155w
Pfgch compl Seq for2	CCAAAGAAGAAAATAAGGAAGG	PFL1155w
Pfgch compl Seq rev2	ATACATAAATGTTTAGCTAC	PFF1360w
Pfptps Seq for	TCCTATTGTTAATCTGACC	PFF1360w
Pfptps Seq rev	TAACCTATTTTTATATATACC	PFF1360w
Pfptps RT for	CCCAGAAAGAGATTGTATAAAACTTCCT	PFF1360w
Pfptps RT rev	ACATCCATTTCTTCTATTAGTTGGTTAAGA	PFF1360w
Pfdhps Seq for	TGAAATGATAAATGAAGGTGC	PF08_0095
Pfdhps Seq rev	GCTGTAGGAAGCAATTGCTAATCC	PF08_0095
Pfdhps RT for	ACAAATGATAGAAGAAACGCTGTGTT	PF08_0095
Pfdhps RT rev	AAGCCTTTCATACAAGTAGGAGCTATT	PF08_0095
Pfdhps Seq for	TTTGTTGAACCTAAACGTGC	PF08_0095

Primer name (gene)	Sequence 5 ‘ to 3 ‘	Accession number
Pfdhps Seq rev	AAAGTTGATCCTTGTCTTTCC	PF08_0095
Pfdhps Seq for neu	TTTGTTGAACCTAAACGTGC	PF08_0095
Pfdhps Seq rev neu	AAAGTTGATCCTTGTCTTTCC	PF08_0095
Pfdhfs Seq for	AGAGGTAGCACAATATTTACC	PF13_0140
Pfdhfs Seq rev	ATCTAAGCGCCCTCCAATCCC	PF13_0140
Pfdhfs RT for	ACAAAGCCGAGAAACTTGAGTGT	PF13_0140
Pfdhfs RT rev	TCCTTTAAGGTGTCGCCAAATT	PF13_0140
Pfdhfr Southern for	CAAAGTGATCGAACGGGAGTAGG	PFD0830w
Pfdhfr Southern rev	CAAGGAGGTAATGCCATTTGG	PFD0830w
Pfdhfr RT for	AAGATCATGTGATTTAGGGCTAGGA	PFD0830w
Pfdhfr RT rev	TGCGCAGGTTGCAAATTACA	PFD0830w
Pfdhfr 5UTR for	CCAACATTTTCAAGATTGATAC	PFD0830w
Pfdhfr SNP’s for	ATGATGGAACAAGTCTGC	PFD0830w
Pfdhfr SNP’s rev	GTTACTAGTATATACATCGC	PFD0830w
Pfdhfr Seq(Probe) for	TAAGGATATGGGAAGCTAATGG	PFD0830w
Pfdhfr Seq(Probe) rev	TAAGTGTTGGGAATGGATAGGG	PFD0830w
Pfdhfr Seq 5UTR for	CCAACATTTTCAAGATTGATAC	PFD0830w
Pfdhfr Seq mid for	GATCTAATAGTTTTACTTGGG	PFD0830w
Pfdhfr Seq mid rev	ACGTATTACCATTTGTTTCTCC	PFD0830w
Pfdhfr Seq 3UTR rev2	AAAAATTCTTAACCGTTCAGG	PFD0830w
Gln tRNA RT for	CTTCGGGTGGATCAGCTAGC	PFD0780w
Gln tRNA RT for	GCAGCAGGAGTTCTGATGGAA	PFD0780w
PFD0795w RT for	CTGCAGCAGTATTAATGCTCGTAAC	PFD0795w
PFD0795w RT for	CCTTTGGTCCATACGTTTAGGG	PFD0795w
PFD0840w RT A1	GAATCTCCTGAAGCAGAGGGAA	PFD0840w
smGTP bind RT for	ACACGTGCCTACCCTACACC	PFD0810w
smGTP bind RT rev	ATTTTACCCACAACCAATTCTTCC	PFD0810w
PFD0810w rev neu1	TTGTGATAATCCCTAAATGTGC	PFD0810w
PFD0810w rev neu2	ATATATAACAATTATGAGG	PFD0810w

Primer name (gene)	Sequence 5 ‘ to 3 ‘	Accession number
PFD0815 RT for	ATGGAAAAGTTCCATTAACTTCCG	PFD0815c
PFD0815 RT rev	CCTCCACGTATTTGGGAACG	PFD0815c
PFD0820w for	TGGTATGAAATGCCGACTCCT	PFD0820w
PFD0820w rev	TATGAGGGCCAACCTGTTTGTCTAC	PFD0820w
RNA binding-RTfor	AAAGAATATATGAAATAGGAAACGAGCA	PFD0825c
RNA binding-RTrev	GCTCATTCAATCTGTTAATTTGTTGC	PFD0825c
LETM RT for	GCAAAAGAGCAGCTAGCCAAA	PFD0835c
LETM RT rev	TTCCTTTTCTTCTATGAGCTGTTGTAAA	PFD0835c
BP FCR3 rechts rev1	AAAGGTACGTTTCACACACC	PFD0835c
BP FCR3 rechts rev1	AATGTTTTGACAAAACCGTAGG	PFD0835c
LETM-840 RT for	TGATAGTTCAGACGAGCAGATAACTTTT	762908-762935
LETM-840 RT rev	TGTTAACTGTTCGTTACACTTTTTCAAAA	762933-762961
PFD0840w RT A1	GAATCTCCTGAAGCAGAGGGAA	PFD0840w
PFD0840w RT A2	TTAGTAGGCAACTCACTTGTTAATACCTT	PFD0840w
PFD0840w RT A for	GTGGTGCGGCGATCATTATA	PFD0840w
PFD0840w RT A rev	AACAAAGTTATCCACCTTAAATTTGAAGT	PFD0840w
PFD0840w RT B1	AGGATTAAGGAGAACAGGAACGG	PFD0840w
PFD0840w RT B2	ATATGACCCCCTTCTTGCGA	PFD0840w
PFD840-RT-mid-for	CATAACGAAAACCCTAAGGATGTTC	776154-776178
PFD840-RT-mid-rev	TCAAAGGGTACGCTAAAAAAAATATTT	776245-776269
Cdc rKinase RT for	CAGAATTTCAGCACAGGAAGCA	PFD0865c
Cdc rKinase RT rev	GGGAATTCGTTAAAGTAAGGATGG	PFD0865c
PFD0840Z1for	CGAGAAACCAAACGAACTCGC	PFD0840w
PFD0840Z2for	GTTGATGGATTACGGTCAACTCG	PFD0840w
PFD0840Z3for	CCACGTGTATGTCGTACGAACC	PFD0840w
PFD0840Z4for	GTTATTCGGACGAAGCGCACG	PFD0840w
PFD0840Z5for	ATCCACGTGGGATTTCGTAAGC	PFD0840w
PFD0840Z6for	GTCGTGTTCTTGCGGTGTGC	PFD0840w
LETM-5-rev	AGAATATGACACAAATTAGTAGG	762744-762766

Primer name (gene)	Sequence 5 ‘ to 3 ‘	Accession number
3D7-3’for1	GATGACAAAATTACCTGAACG	756926-756946
3D7-3’for2	CGTCAGTTTTTTTATCTTCGGG	PFD0835c
3D7-5’rev1	TTACATTATTGAAATGCACC	739147-739166
3D7-5’rev2	CTGTAAAATAGCCAAAATTTGG	739311-739332
3D7-5’rev3	ACTCATTTGTATTATCTCTTCC	748949-748970
FCR3-3’for1	AAGGTACGTTTCACACACCC	760617-760636
FCR3-5’rev1	GATATTTCTACCCATAATTAAGC	732650-732670
FCR3-5’rev2	GTATTTATATGATTAGATTGTCC	735530-735552
Actin southern for	CAAGCTTTAGTTGTTGACAACG	PFL2215w
Actin southern rer	GGAGCTTCTGTTAATAACACTGG	PFL2215w
Tubulin RT for	TGATGTGCGCAAGTGATCC	PF10_0080
Tubulin RT rev	TCCTTTGTGGACATTCTTCCTC	PF10_0080

Table 2-3 Probes designed for real time PCR analysis

Name	Accession number	MAL	Label – Sequence – quencher
GCH	PFL1155w	MAL 12	FAM-ACTATAACGTATGCATCTTA-TAMRA
PTPS	PFF1360	MAL 6	FAM-TTCTACTGAAGAAATTGG-TAMRA
DHPS	PF08_0095	MAL 8	FAM-TTCTAGAAACTGCTCTGC-TAMRA
DHFS	PF13_0140	MAL 13	FAM-TTCCATCCGTTCATAGCT-TAMRA
DHFR	PFD0830w	MAL 4	FAM-TTTACTCATATGATTGCACAAGT-TAMRA
β tubulin	PF10_0080	MAL 10	JOE-TAGCACATGCCGTTAAA TATCTTCCATGTCT-TAMRA
gapdh	PF14_0598	MAL 14	JOE-AAGGAATCTTAGGATACA-TAMRA

2.1.8.2 Sequencing reaction

Sequencing was performed by GATC, Konstanz, Germany and is described in more detail in 2.2.1.11.

2.2 Methods

2.2.1 Molecular methods

2.2.1.1 *Plasmodium falciparum* gDNA isolation

Parasites were harvested from blood culture and the erythrocyte plasma membrane was ruptured as described in paragraph 2.2.3.3. The obtained parasite pellet was re-suspended in 200µl 1 x PBS and the parasite genomic DNA was isolated with the DNA QIAamp DNA Blood Kit. The instructions were followed as indicated in the protocol of the manufacturer. The DNA was eluted from the column in 80 – 120 µl elution buffer depending on the size of the parasite pellet obtained from the culture.

2.2.1.2 *Plasmodium falciparum* total RNA isolation

Parasites were harvested from blood culture and the erythrocyte plasma membrane was ruptured as described in paragraph 2.2.3.3. The parasite pellet was re-suspended in 200µl RLT buffer (Qiagen RNeasy Kit) and parasite total RNA was isolated with the Qiagen Rneasy Kit. The instructions were followed as indicated in the protocol of the manufacturer. The DNase digest was included in the protocol during the washing steps. Total RNA was eluted from the column in 30 – 50 µl of double distilled water.

2.2.1.3 *Plasmodium falciparum* mRNA isolation

mRNA was isolated with the mRNA Isolation Kit (Roche, Mannheim). 1ml of whole blood from each patient of the study was given into a 14ml falcon tube with 10ml of Roche mRNA stabilisation solution. The lysat was carefully mixed and stored at 4°C until transport from the satellite site in Pingilikani to KEMRI in Kilifi town, where the samples were stored at -80°C until purification. Blood sampling and transport to KEMRI generally occurred on the same day.

The isolation of the mRNA was then performed with the *mRNA Isolation Kit for blood and bone marrow (*Roche, Mannheim, DE). The instructions were followed as indicated in the protocol of the manufacturer.

2.2.1.4 Plasmid preparation from bacteria

A bacterial over night culture of 5ml supplemented with 0,1 mg/ml Ampicillin was centrifuged in two steps in a 2 ml Eppendorff tube. The bacterial pellet was re-suspended in the 250µl P1 buffer and the instructions were followed as indicated in the protocol of the manufacturer.

2.2.1.5 DNase treatment

The mRNA isolation protocol from Roche did not include a DNase digest during purification. The mRNA isolation is based on oligo dT magnetic beads and the manufacturer claims this sufficient to separate mRNA from genomic DNA. In *Plasmodium falciparum* though, runs of 30 adenines are common. Therefore an additional DNase digest was performed after purification to eliminate the possibility of genomic DNA contamination, which would falsify analysis and results.
DNase treatment was preformed with the *Turbo DNA free Kit* from Ambion and the instructions were followed as indicated in the protocol of the manufacturer.

2.2.1.6 Precipitation and purification of nucleic acid

Precipitation of DNA is a common method to concentrate and purify DNA. Through the addition of salt and ethanol the DNA looses its solubility and can be precipitated by centrifugation.
The standard protocol, which was used, is described in the following paragraph:

To 1 volume of DNA	1/10 volume of 3 M Sodium Acetate pH = 4,8 and
	2,5 volumes of 100% Ethanol

were added and well mixed. The samples was incubated for 2h at -80°C, centrifuged at 13 000 rpm in a table top centrifuge for 20 min at 4°C. The pellet was washed with 500µl of 70% Ethanol and centrifuge again at 13 000 rpm for 10 min at 4°C. The white DNA pellet was dried at 37°C for 5 to 10 min and re-suspended in the desired volume of double distilled water.
For purification of PCR products the *QIAgen PCR Purification Kit* was used and the instructions were followed as indicated in the protocol by the manufacturer.
If DNA was separated with gel electrophoresis, the desired fragment was excised of the agarose gel under UV light and purified with the *QIAquick Gel extraction Kit.* The instructions were followed as indicated in the protocol by the manufacturer.

2.2.1.7 Reverse Transcription (cDNA Synthesis)

Total RNA or mRNA was transcribed into cDNA with the RETROscript from Ambion. Oligo d'T primers were used to initiate cDNA synthesis and the instructions were followed as indicated in the protocol by the manufacturer.

2.2.1.8 One step reverse transcription PCR (Invitrogen)

For one step reverse transcription and amplification of a specific DNA fragment the *SuperScript III one-step RT-PCR System* from Invitrogen was used. In the first step

the mRNA is specifically transcribed into cDNA for 45 min at 42 °C and then directly amplified in a polymerase chain reaction (2.2.1.9).

2.2.1.9 Polymerase chain reaction (PCR)

Polymerase chain reaction was established to amplify a particular gene or sequence of interest with specifically designed oligonucleotides. Sequence information was downloaded from databases www.plasmodb.org and www.genedb.org. Due to the high AT content in the genome of *Plasmodium falciparum*, oligonucelotides were designed in regions with possibly high GC content. One universal PCR protocol was used for all reaction with minor changes, mentioned in the respective paragraphs. Genomic DNA, cDNA, Plasmid or bacterial colony served as template.

1 x Reaction buffer	Roche, Mannheim
200µM d'NTP's Mix	Fermentas
2mM $MgCl_2$	Roche, Mannheim
1µM Oligonucleotide each	MWG or Invitrogen
2,5u/50µl Taq Polymerase	Fermentas

Final volume of the reaction was 25µl or 50µl depending on the subsequent experiments.

An Eppendorff Thermocylcler was used and the cycling conditions are listed in the table bellow. 35 cylces (Step 2 – Step 4) for one reaction were the standard protocol. Extension time was adapted to template length (1kb/1min).

Table 2-4 Standard PCR cycling conditions.

Initial denaturation of the template DNA	3:00 min	94°C
Denaturation of the DNA (Step 2)	0:45 min	94°C
Annealing of the oligonucleotides (Step 3)	0:30 min	58°C
Extension of the fragments by the *Taq polymerase* (Step 4)	1:00 min	60°C
Final Extension to ensure complete amplification	10:00 min	60°C
Pause		4°C

PCR to reveal breakpoints of 3D7 and FCR3 amplicons

FCR3 and 3D7 were subjected to numerous PCR analyses to reveal breakpoint of amplicon, which are described in 3.3.1.5.

The primer used for 3D7 are listed in table Table 2-2 and are marked with the names 3D7 3' for and 3D7 5'rev. 3' and 5' indicate the possible breakpoints on either side of *dhfr*. In addition the group of primers marked with PFD0840Z1-6 for were combined with primers upstream of *dhfr*.
The analysis of the gap in 3D7 amplicon was performed with Pfdhfr primers labelled with forward, 3D7 3' for, LETM RT for/rev and LETM 5'rev (5' is here 5' of LETM).
The FCR3 breakpoint was analysed with FCR3 5'rev and FCR3 3'for and later with PFD0815c RT rev, PFD0815c new rev1/2 and BP FCR3 right rev1/2.

2.2.1.10 Agarose gel electrophoresis

Gel electrophoresis allows the distinct separation of DNA fragments of different sizes and their visualisation. Agarose dissolved by heating in a buffer forms a gel matrix with pores when it cools down. These pores are wide enough for DNA fragments to run through when a constant electric current is applied between the two poles of a suitable chamber.
In this work different percentages of Agarose were used depending on the size of the DNA fragments to be separated. Higher percentage for a denser matrix and smaller fragments and lower percentage for longer fragments and wider pores. The agarose (0,5 % - 2 %) was dissolved and heated in 1 x TAE buffer or 1 x TBE buffer. 0,01 % *Sybre safe* was added and the fluid gel was casted in a tray before it had cooled down. A comb was put on one end of the gel where it forms small pockets in which the DNA was loaded once the gel had solidified. A power supply produces between 80 V and 130 V between the poles and the gel was run between 45 min and 2h depending on the size of the fragments to be separated and the lengths of the gel.
A picture was taken with Gel Doc XR from Biorad.

2.2.1.11 Sequencing of PCR fragments

The five enzymes of the folate pathway were sequenced in the 20 field isolates from Kilifi, Kenya and in the parasites lines resulting from the drug pressure experiments.
Sequencing was performed with GATC biothech in Konstanz, Germany (www.gatc-biothech.com). PCR fragments were purified, solved in water and send with the oligonucleotide for sequencing in the following concentrations and volumes.

PCR product	10 – 50 ng/µl (in 30µl)
Plasmid DNA	30 – 100 ng/µl (in 30µl)
Oligonucleotide	10 pmol/µl (in 30µl)

Sequences were analyses and aligned with Bioedit. The 3D7 genome from Plasmodb served as reference genome.

Pfgch (PFL1155w), *Pfptps* (PFF1360w) and *Pfdhfr* (PFD0830w) were fully sequenced, *Pfdhps* (PF08_0095) and *Pfdhfs* (PF13_0140) only partially with primer covering at least all annotated SNPs in the open reading frames. The sequence of *Pfptps* was covered with one primer pair, so were the regions of annotated SNPs in *Pfdhps* and *Pfdhfs*. For *Pfgch* and *Pfdhfr* three overlapping PCR fragments were generated with the designed oligonucleotides listed in Table 2-2. Primer names are composed as follows: gene accession number, comp (complete), seq (sequencing)/SNP and for (forward)/rev (reverse).

2.2.1.12 Ligation of PCR fragments for bacterial cloning

The standard PCR reaction with the *Fermentas* Taq polymerase was used, through which an extra A at the 3' end of each PCR fragment is added. 50 µl of PCR product were purified and solved in water and the ligation of vector and PCR fragment was performed at RT for 1 to 5h and with the addition of a salt.

7 µl of PCR product
2 µl salt solution (provided)
1µl of TOPO vector (provided)

The ligation was then used in bacterial transformation or stored at -20°C.

2.2.1.13 Real time PCR

Real time PCR assays were used for gene copy number quantification, amplicon size determination and transcriptional analysis.
For the gene copy number quantification and the transcriptional analysis a Taqman Probe (ABI and MWG) was designed whereas for the determination of the amplicon size a sybr green based assay was established.
For analysis of the results the ΔΔct method was used. β-tubulin and *gapdh* served as endogenous controls and at least one reference genome (3D7, Dd2, D10 or FCR3) was run on every experiment on each 96 well plate.

Real time PCR with Taqman probe to analyse copy number and transcription

All primer and probes were designed with Primer Express 3.0 Software from ABI. Probes were labelled 5' with FAM (*Pfgch, Pfptps, Pfdhps, Pfdhfs and Pfdhfr*) or with JOE (β tubulin and *gapdh*) and the quencher TAMRA was attached 3'. Primer and probe were ordered from ABI, MWG and Invitrogen and are listed in detail in Table 2-2 and Table 2-3. Primer names are composed of gene accession numbers, RT (real time) and for (forward)/rev (reverse).

900nM of each primer and 300nM of each probe were used in the TaqMan universal PCR master mix (ABI).

To determine the copy number, genomic DNA was isolated (2.2.1.1) from the parasite culture and used for the reaction. To analyse the transcriptional profile total RNA (2.2.1.2) or mRNA (2.2.1.3) was isolated and transcribed into cDNA (2.2.1.7) and used in the assay. A negative control containing only water was run on each plate and in the expression experiments, mRNA or total RNA were also run on a plate to exclude gDNA contamination. The reaction was set up as follows in a total reaction volume of 25µl.

Taqman universal PCR master mix 2 x		12,5µl
DNA/mRNA		50ng
Endogenous control	Forward primer	900nM
	Reverse primer	900nM
	MGB Taqman Probe	300nM
Gene of interest	Forward primer	900nM
	Reverse primer	900nM
	MGB Taqman Probe	300nM

All measurements were performed in duplicates and the cycling conditions are shown in Table 2-5. Stage 3 was repeated 50 times. Data collection as performed in stage 3 step 2.

Table 2-5 Standard real time PCR cycling conditions (probe)

Stage	Repetitions	Temperature	Time
1	1	50.0 °C	02:00
2	1	95.0 °C	10:00
3 step 1	50	95.0 °C	00:15
3 step 2		60.0 °C	01:00

Real time assay to determine amplicon size

The size of the amplified DNA fragment containing the *dhfr* locus was determined with a sybr green based assay. The genomic context of *dhfr* was analysed on PlasmoDB (www.plasmodb.org) and the neighbouring genes were checked for

amplification. Primers were designed for genes at different distances upstream and downstream of the *dhfr* locus are listed in Table 2-2.

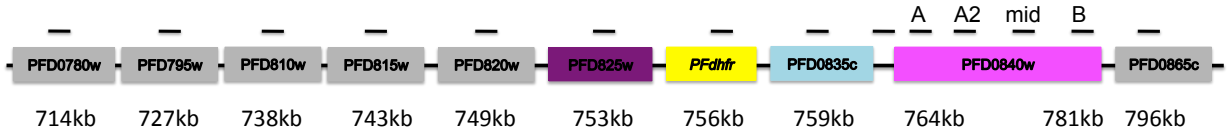

Figure 2-1 Genomic context of *Pfdhfr* (adapted from plasmoDB). Boxes indicate genes. (grey) PDF0780w - PDF0820w, (purple) PDF0825w, (yellow) *dhfr*, (blue light) PDF0835c, (magenta) PDF0840w, and (grey downstream) PDF0865c. Distances are shown below in kilo bases. Small black lines represent the primer pairs in each open reading frame.

The oligonucleotides (150nM) were designed with Primer Express 2.0 and are listed in detail in Table 2-2. Primer names are composed of gene accession numbers, RT (real time) and for (forward)/rev (reverse). A reaction mix was set up as follows:

Power SYBR green master mix (ABI) 2 x		12,5µl
DNA/mRNA		50ng
Gene of interest	Forward primer	900nM
	Reverse primer	900nM

With the usage of the sybr green master mix each gene is analysed in an individual well. The internal controls are not adjusting for pipeting errors and the quantification is less accurate compared to a Taqman probe. Nevertheless, it is clearly possible to determine amplification. The Power SYBR green master mix (ABI) was used with the following Cycling conditions.

Table 2-6 Standard real time PCR cycling conditions (sybr)

Stage	Repetitions	Temperature	Time
1	1	95.0 °C	00:15
2	40	95.0 °C	00:15
		58.0 °C	00:15
		60.0 °C	00:45
3 (Dissociation)	1	95.0 °C	00:15
		60.0 °C	01:00
		95.0 °C	00:15

Analysis of the results

The real time PCR analysis was performed with the ΔΔ ct (cycle threshold) method. The threshold was set at the exponential phase in the lower third of the curve and the cycle threshold (ct) was read in the analysis table for all the curves selected (ABI 7500 system software). As each reaction was performed at least in duplicates, the mean ct value was calculated. The delta ct (Δct) and the delta delta ct (ΔΔct) were then calculated as shown below.

$$\Delta ct = ct_{(internal\ control)} - ct_{(gene\ of\ interest)}$$

$$\Delta\Delta ct = \Delta ct_{(reference)} - \Delta ct_{(treated)}$$

Plasmodium falciparum β-tubulin (PF10_0086) or *gapdh* (PF14_0598) served in all experiments as endogenous control to standardize the amount of DNA in each reaction. The reference genome varied depending on the experimental set up and will be mentioned in the corresponding chapter of the results.

2.2.1.14 Restriction endonucleases digest

Restriction endonucleases recognise a specific sequence of mostly 4 to 6 bp in double stranded DNA and cleave at this site the phosphodiesterbond thus generating two or more DNA fragments.

Genomic DNA, PCR products and bacterial vectors were cut by restriction enzymes. The restriction digest of genomic DNA was preferably carried out in higher volumes (100 – 200 µl), for PCR fragments and bacterial vectors a total reaction volume of 10 – 20 µl was sufficient. The 10x reaction buffer was adjusted to the final volume as well as the units of the restriction enzyme. The restriction digest was carried out at 37°C and over night to ensure complete digestion of the DNA.

2.2.1.15 Southern blot

The southern blot was performed with a nonradioactive, digoxigenin (DIG) labelled probe, which is detected by a chemieluminescence reaction. The result can be visualized on a light sensitive film. The DIG High Primer DNA Labeling and Detection starter Kit II (Roche, Mannheim) was used in this experiment.

Labelling of the probe

The DNA for probe was obtained from a PCR reaction of two times 50µl reaction volume. The used oligonucleotides are listed in Table 2-2 and are ladled with Gene name and the addition “Southern”.

The reaction was purified and eluted in 20µl of double distilled water. The concentration of the DNA was measured in a nanodrop machine. Up to 2µg of DNA were used for the labelling reaction. The DNA was denatured at 99°C for 10 min, cooled on ice and 4 µl of the DIG-High Prime labelling enzyme were added. The reaction was incubated over night at 37°C. To stop the labelling reaction, the probe was incubated at 65°C for 10 min and then stored at 4°C.

gDNA preparation and restriction digest

Parasites were cultured until a parasitaemia of 10% was reached in the trophozoite stage. The parasites and the DNA were isolated as described in the corresponding chapters (2.2.3.3 and 2.2.1.1). Two µg of genomic DNA were digested with restriction enzymes in a total reaction volume of 100µl. To choose an appropriate set of restriction enzymes 30 kilo bases surrounding the *Pfdhfr* locus (PFD0830w) and the *Pfactin* (PFL2215w) locus were carefully analysed with the program EnzymeX 3.1. The sequence information was down loaded from www.plasmoddb.org. Three combinations of restriction enzymes were suitable for the analysis. The expected fragments are easily separable with a low percentage agarose gel electrophoresis.

Table 2-7 Restriction enzymes and buffers used for Southern blot analysis

Restriction enzyme	NEB buffer	*Pfactin* expected size	*Pfdhfr* expected size
EcoRV	Buffer 3	6891 bp	8018 bp
EcoRV + *NheI*	Buffer 2	6154 bp	4935 bp
EcoRV + *EcoRI*	*EcoRI* buffer	5494 bp	2461 bp

The reaction was performed at 37°C over night and an additional µl of each enzyme was added for one hour the next morning to ensure complete digestion of the genomic DNA. The DNA was precipitated (2.2.1.6) and re-suspended in 10µl of double distilled water.

Running condition for the agarose gel and its preparation for the blot

The DNA was loaded on a 0,7% agarose gel supplemented with 1 x SYBR® safe DNA gel stain and run over night at 20V in 0,5 x TBE buffer. A picture was taken with the Geldoc XR (Biorad) and the gel was bathed for 15 min in 0,25 M HCL to de-purinate the DNA to facilitate following transfer. The gel was shortly rinsed in double distilled water and incubated in denaturing buffer for 30 min under constant agitation on a platform shaker. Denaturing of the DNA prepares the strands for later hybridization. The denaturing buffer was poured off and the gel was again shortly

washed with double distilled water and then neutralized and equilibrated in 10 x SSC for 30min.

Southern blot

The membrane and two extra thick filter papers were cut to the exact size of the gel and the membrane was equilibrated for 10 min in 2 x SSC buffer. The transfer was conducted from top to bottom, which has the advantage that it also uses gravity as a driving force for the buffer and the DNA. The blot was built as shown in Figure 2-2. A stack of paper towel served as basis in a tray. On top one extra thick Whatman® paper soaked in 10 x SSC was placed followed by the membrane, the gel and another extra thick Whatman® paper also soaked in 10 x SSC. The connection with the two elevated container filled with 10 x SSC was established with two 2 mm Whatman® papers as shown in Figure 2-2. Air bubbles between the different layers were carefully avoided. Transfer was performed for a minimum of 5 h to ensure complete transfer of the DNA.

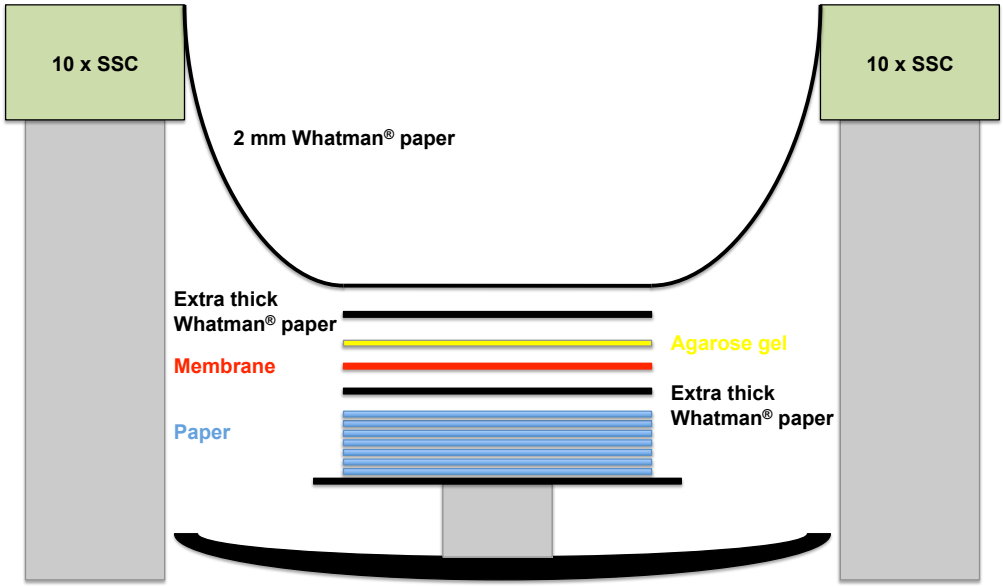

Figure 2-2 Southern blot. (Green boxes) containers filled with 10xSSC on elevation. (blue sheets) paper with high power ob absorption, (black thick line) extra thick Wahtman paper, (red line) positively charged. Blotting was performed minimum 5 h.

Cross-linking, prehybridization and hybridazation with the probe

Before processing the membrane after the transfer, the pockets of the gel were marked with a pencil on the membrane and the upper right corner was cut with clean scissors. The membrane was then laid with the DNA side facing up on a 2 mm

Whatman® paper soaked with 2 x SSC. The DNA was cross-linked with a UV stratagene cross linker and the program auto crosslink.
The membrane was then immediately rinsed in double distilled water and pre-hybridized for 30min in 25ml of DIG Easy Hyb granules at 37°C in a glass tube rotating in a hybridization oven. The pre-hybridization solution was poured off and 20ml of hybridization solution supplemented with 10µl of *Pfdhfr* and 10µl of *Pfactin* DIG labelled probe were added. Hybridization solution was incubated over night.

Washing, blocking and detection
All the following steps were carried out in the glass tube rotating in the oven at 37°C. The formulations of the buffers are listed in chapter 2.1.5. The membrane was washed 2 times for 5 min with *Step 1 washing solution* (3 x SSC, 0,5 % SDS) and 2 times for 15 min with *Step 2 washing solution* (2 x SSC, 0,5% SDS). The membrane was then briefly rinsed in *washing buffer* and blocked for 1h in 100ml of *1x blocking solution* (10 x blocking solution diluted in maleic acid). The blocking solution was discarded and 20 ml of fresh blocking solution supplemented with 1µl of Antibody solution (Anti-Digoxigenin AB) was added onto the membrane and incubated for 30 min. The membrane was then carefully washed twice with ample volumes of *washing buffer* for 15 min. With clean forceps the membrane was pulled out of the glass tube into a small dish with 20 ml *detection buffer* to equilibrate it for 5 min.
The membrane was then put with its DNA side facing up into a development folder in a plastic bag. On 100 cm^2 of membrane 1ml of ready-to-use CSPD was added and immediately evenly spread out on the membrane with the help of the closing plastic bag. Air bubbles were carefully avoided, as well as drying out of the membrane, which both causes uneven and high background. The cassette was incubated at 37°C for 10 min to enhance the luminescence reaction.
In the dark room an Amersham Hyperfilm™ ECL, a high performance chemiluminescence film was cut to the appropriate size and exposed onto the membrane for 5 to 15 min and developed. Additionally a Kodak BioMax MR film was exposed for 30 min to 90 depending on the strength of the signal.

2.2.2 Microbiological methods

2.2.2.1 Bacterial transformation

The bacterial system was used to clone and amplify single DNA molecules. Fragments were ligated with the TOPO vector (2.2.1.12), which contains a selection marker for ampicillin. Only cell containing the plasmid were then able to grow on LB_{amp} Agar plates.

Top 10 competent cells (Invitrogen) were used for bacterial transformation. Cells were stored at -80°C and thoroughly thawed on ice. 5 µl of the ligation (2.2.1.12) were given to 40µl of competent cells and kept on ice for 20 min. Cells were heat shocked at 42°C for 30sec and immediately put back on ice. 100µl of SOC medium were added and the transformed cells were incubated shaking at 37°C for 1h. After one hour cells were shortly pelleted, 80µl of medium was withdrawn and the rest re-suspended and plated on a LB_{amp} Agar plate and incubated at 37°C over night.

Colony screening

Colonies were first screened with PCR. Standard master mix with insert specific primer was aliquoted into PCR tubes. One colony at the time was picked with clean tips and kept for 1 to 3 minutes in a single PCR tube with the master mix. Tips were removed and the reaction was started. Results were *analysed* on an Agarose gel and positive colonies were confirmed with plasmid preparation (2.2.1.6) from a bacterial culture (2.2.2.2) of the indentified colony.

2.2.2.2 Bacterial culture of transformed colonies

One colony was picked with a clean tip and used to inoculate 5 ml of LB_{amp} medium supplemented with 100µg/ml in a sterile tube for bacterial culture. The culture was grown over night in a shaker at 37 °C and harvested by a stepwise centrifugation in a 2 ml Eppendorff tube. The plasmid preparation is described in chapter 2.2.1.4

2.2.3 Methods of *Plasmodium falciparum*

2.2.3.1 *Plasmodium falciparum* culture conditions

Plasmodium falciparum was cultured *in vitro* in T75 or T25 cell culture flasks from Greiner in the incubator Heracell 150 (Heraeus / Thermo) at 37°C. Complete cell culture medium (2.1.5) was prepared and the parasites were grown in the presence of O^+ or A^+ blood (5% haematocrit) and a gas mixture of 5% CO_2, 5% O_2 and 90% N_2. The parasite population was kept between 0,1 and 10% (parasites/erythrocytes) with regular change of medium and the addition of fresh blood.

Staining of P. falciparum culture with Giemsa (thin blood slide)

The growth of the parasite culture was controlled with regular thin blood smears. A drop of the sedimented erythrocytes was given onto the surface of a clean glass slide and spread evenly, air dried and fixed for 1 min in 100% methanol. The fixed cells were then stained in 5 – 10% Giemsa solution for 10 min. Slides were examined on a light microscope using a 100x objective under oil immersion.

Freezing of parasites

On a regular basis aliquots of parasite cultures were preserved and stored in liquid nitrogen.

A re-suspended culture was centrifuged for 3 min at 2100 rpm in a 50 ml falcon tube in a Megafuge 1.0 R (Heraeus). The supernatant was discarded and 1 volume of the *freezing solution* (2.1.5) was added to the erythrocyte pellet. The suspension was evenly divided into 1 to 3 cryo-tubes and frozen in liquid nitrogen.

Thawing of parasites

When parasites are thawed, the glycerol is replaced by a high salt concentration (12% NaCl). During the thawing procedure the salt concentration is slowly decreased to the culturing conditions. This change of osmotic pressure has to be carried out very carefully to allow the cells to adapt to each solution and avoid lyses.

One aliquot of frozen parasites was slowly warmed in a water bath (37°C) and 200 µl of the *thawing solution 1* (12% NaCl) (2.1.5) were slowly added. 9 ml of *thawing solution 2* (1,6 % Nacl) (2.1.5) were added at a rate of 1 drop per second to avoid lyses of erythrocytes. The suspension was centrifuged at 2100 rpm for 3 min in a Megafuge 1.0 R (Heraeus). Supernatant was discarded and *thawing solution 3* (0,9% Nacl + 0,2% Glucose) (2.1.5) was added in the same careful way. Again another centrifugation step followed and the erythrocyte pellet was washed with 10 ml of complete medium (2.1.5) before it was re-suspended in 14ml of complete medium

and given in a culture flask with 500 µl of fresh A^+ or O^+ erythrocytes. The newly awaked parasites were kept in the incubator for at least 48 h without interruption.

Synchronizing the parasite population

Plasmodium falciparum parasites grow in an asynchronous population in *in vitro* culture when untreated. For some experimental designs, synchronized parasite population were needed. Synchronization is performed when ring stages are seen in a blood smear culture. The culture was then centrifuged and the medium was replaced by 5 % sorbitol and incubated for 10 min at 37 °C. After the incubation the sorbitol was removed by centrifugation and replaced by complete medium. The culture was brought back to normal culturing conditions. This treatment depletes the culture of all mature blood stages, i.e. trophozoites and schizonts. Ring stages are not affected by the treatment. To obtain complete synchronisation the procedure was repeated in two to three consecutive cycles.

2.2.3.2 Cloning out single parasites from a population

The parasite population that had lived under constant and increasing drug pressure had become an inhomogeneous population due to mutational changes in the genome. One single parasite had to be isolated to obtain a clonal population, which was then analysed in further experiments. Therefore the parasitaemia of the culture was determined and with the help of a serial dilution a 20 ml culture with 500 µl of erythrocyte concentrate and 10 parasites in total was pipetted. These 20 ml were evenly spread on a 96 well plate with each well obtaining 200 µl. Change of medium was performed once a week. The parasite growth was controlled by small blood smears first after 2 weeks and then every second day until parasites were visible under the microscope. The positive cultures of single wells were then taken into a T 25 culture flask and grown in standard culture conditions as described in 2.2.3.1.

2.2.3.3 Plasmodium falciparum parasite isolation from culture

For DNA and RNA isolation from *Plasmodium falciparum*, 35 ml of parasite culture with parasitaemia of 10 % were centrifuge at 2100 rpm in a 50 ml falcon tube. The supernatant was discarded and the erythrocyte membrane was lysed with 2% Saponin in 1 x PBS. The parasites were separated with an additional centrifugation step at 3800rpm for 3min and washed with 1 x PBS. The purified parasites were re-suspended in 200 µl 1 x PBS for DNA purification or re-suspended in an appropriate volume (300µl or 600µl) of RLT buffer (Qiagen) for total RNA isolation.

2.2.3.4 *In vitro* drug sensitivity assay (IC_{50})

Drug sensitivity of the culture-adapted parasites was measured with an *in vitro* drug response rate assay. The four drugs chloroquine, pyrimethamine, trimethoprim and cycloguanil were analysed in one 96 well plate. Each assay was repeated at least 3 times on different days and means with standard deviations were calculated. One *mother plate* was generated on which 11 dilutions of each drug were arranged horizontally in duplicates. The accuracy of each new mother plate was verified with 3D7 in a control assay. Only if the measured values for 3D7 were in the range of the expected, the *mother plate* was used to determine the drug sensitivity of the field isolates. 15 assays were performed with one mother plate and it was kept for up to 4 weeks at 4°C. The 96-well plate in which the drug sensitivity assay was performed is called *daughter plate*.

Mother plate:

A stock solution of each test compound was diluted in culture medium to the desired starting concentration, which was determined based on the predicted drug sensitivity level within the population of the isolates.

A 96-well plate was used to prepare serial (3 fold) dilutions of the drugs. 200 µl medium were pipetted into each well. 100 µl of stock solution of each drug is added in the second column and leaving the first with only medium. The first drug in well 2A and 2B, the second drug into well 2C and 2D… The serial dilution is performed with a multipipett. 100µl are transferred from column 2 to column 3 and well mixed by pipetting. From column 2 again 100µl are transferred to the next column (4). This procedure is repeated until well 12. The mother plate was immediately used or stored for up to 4 weeks at 4°C.

Daughter plate for the assay:

The IC_{50} were measured at 1% ring stage parasite culture (2% haematocrite). 100µl of the culture was added into each well from column 2 to 12 and in wells 1A to 5A. 12,5µl of the mother plate was added into the corresponding wells (column 1 to column one…). The negative control consisted of erythrocytes (2% haematocrite) in 6A, 7A and 8A. The plates were incubated at standard culture conditions for 72h. After 72h 100µl lysis buffer (0,02% Sybr green) was added and incubated 1 h before measuring the fluorescence in a fluostarOPTIMA.

The IC_{50} values were calculated with the help of an Excel sheet, in which means of the duplicates are calculated as well as means of positive and negative controls. The curve and the slope for each drug were calculated and the IC_{50} was read in ng/ml.

2.2.3.5 Induction of resistance

Resistance was induced by culturing *plasmodium falciparum* 3D7 and FCR3 under increasing pyrimethamine pressure. Starting concentration of the drug pressure experiment was determined by measuring the respective IC_{50} (2.2.3.4) value of pyrimethamine for both strains. The IC_{50} of 3D7 was 20nM and 60nM for FCR3 (Table 3-2). I therefore decided to start the experiment with a pyrimethamine concentration of 20nM. The drug concentration was increased in 20nM steps up to 200nM, then directly to 300nM and subsequently up to 400nM, to 800nM and finally to 1,6 µM pyrimethamine. At each concentration parasites were cultured until they regained their usual replication rate. Generally the parasites adapted within two weeks (7 cycles) to the new concentration. A parasite pellet was collected at every concentration to isolate DNA and RNA. Both strains were kept in parallel in 35ml of complete medium in a T75 culture flask. Regularly parasite aliquots were frozen in liquid nitrogen.

A genetic and phenotypic analysis of the drug-adapted parasites was performed. All results were analysed relative to baseline parasites.

Phenotypic changes were assessed in an *in vitro* drug sensitivity assay (2.2.3.4). Relative transcriptional changes of the five enzyme of the folate pathway were determined with a real time PCR assay (2.2.1.13) using cDNA (2.2.1.2 and 2.2.1.7) as template.

Gene copy numbers variances (CNV) of the five enzymes of the folate pathway were analysed during the experiment. Relative CNVs were also determined with a real time PCR assay (2.2.1.13) using genomic DNA as a template.

Single nucleotide polymorphisms (SNP) were determined by sequencing (2.2.1.17) with GATC-biotech. Additionally, a restriction digest of a 651 bp PCR fragment of *dhfr* was established revealing the S108N point mutation. The restriction enzymes cuts the parasite sensitive (3D7) *dhfr* sequence AGCT resulting in two fragments of 323 base pairs and 328 base pairs which were distinguished on agarose gelelectrophoresis from the uncut PCR fragment of 651 base pairs.

2.2.3.6 Competitive fitness assay

The relative fitness of the resistant parasite lines was assessed in a competitive fitness assay. 3D7 wild type parasites were mixed in a 1:10 dilution with the 3D7 resistant strains. Both lines were in synchronous cultures in the ring stage. Changes in the *dhfr* gene copy number served as indicator for the two lines. DNA was isolated after the first, the second and the third cycle and then again after 3 weeks.

2.2.4 Clinical methods

2.2.4.1 Study site Pingilikani

We conducted both studies at the Pingilikani study site, which is operated jointly by the Kenya Medical Research Institute (KEMRI) and the local Ministry of Health (Sasi et al, 2009). Malaria transmission in the area is perennial but with peaks trailing typically two annual rainy seasons (O'Meara et al, 2008). Coinciding with previously described reductions in severe malaria admissions to Kilifi District Hospital (O'Meara et al, 2008) we observed a reduction of the average annual proportion of malaria cases among non-immune infants between 6 and 12 months presenting with febrile disease at the Pingilikani health care facility from 62% in 2003 to 26% in 2005 and 13% in 2008. Between the introduction of AM-LM as first-line treatment in Kilifi District in December 2006 and the end of the study, 2,585 malaria episodes in 3,271 passively followed-up patients in Pingilikani received ACTs. Both studies were approved by the National KEMRI Ethical Review Committee, Kenya; the Oxford Tropical Research Ethics Committee, UK; and the Ethics Committee of the Heidelberg University School of Medicine, Germany.

2.2.4.2 Study design of amodiaquin study (Sasi et al, 2009)

The study was designed as a prospective observation of pediatric outpatients attending the Pingilikani Dispensary. Eligible patients received a supervised oral course of amodiaquine targeting a dose of 10 mg/kg/day for 3 days and were subsequently followed up for 28 days. The study was conducted from March through July 2006. Detailed describtion of the study is found in (Sasi et al, 2009).

2.2.4.3 Study design of artemisinin combination therapy (ACT) study

We enrolled paediatric outpatients aged 6-59 months with uncomplicated *P. falciparum* malaria who met the following selection criteria: reported or documented fever ≥37.5ºC, *P. falciparum* mono-infection, microscopically determined peripheral asexual parasite density of 2,000-200,000/µL, body weight >5 kg and signed informed consent by parent or legal guardian. We excluded patients with known allergies, severe malaria or danger signs, participation in an investigational drug study within previous 30 days, ECG abnormalities requiring urgent management, other relevant clinical conditions or severe malnutrition (defined as weight for height <70% of the median NCHS/WHO reference).

Study drugs were administered orally with food or drinks under direct supervision by study nurses. DHA-PPQ was given 24-hourly for 3 days at single target doses of 2.25

mg of DHA/kg body weight and 18 mg of PPQ/kg (formulated as paediatric or adult strength fixed dose combinations of 20/160 mg and 40/320 mg, respectively; Eurartesim™, SigmaTau, Italy). AM-LM was administered according to the manufacturer's instructions in 6 doses over 3 days at single target doses of 2 mg of AM/kg and 12 mg of LM/kg (Coartem™, Novartis, Switzerland). Participants who vomited or rejected the study drug within 30 min received a second full dose, and those who vomited or rejected the study drug after 30 min but within 1 h received a second half dose. Vomiting or rejecting the second dose led to withdrawal from the study and administration of rescue medication (3-day oral regimen of atovaquone-proguanil). Stability tests conducted in 2009, >10 months after completion of the study, on study drug batches used in the trial demonstrated that the titre and the degradation products of DHA/PPQ and AM/LM were within stringent specifications as submitted to the regulatory authorities (Swissmedic and EMEA, respectively; data not shown).

During the 3-day treatment phase patients were admitted to the KEMRI research ward in Pingilikani to ensure strict adhesion to dosing intervals. Patients were seen by a study clinician for baseline assessment before administration of the first dose of study medication on days 0, 1, 2 and 3 and then for weekly follow-up visits until day 63 and finally on day 84 (or whenever clinically indicated). Patients who failed to return for scheduled appointments were actively followed up in the community. On each visit during the treatment and follow-up phase, a medical history was obtained, vital signs were checked, axillary temperature was measured, thick and thin blood smears were prepared from a fingerprick blood sample, and adverse events were documented. To distinguish recrudescences from new infections, aliquots of EDTA–treated blood samples obtained on day 0 and on the day of reappearing asexual parasitaemia were stored at -80°C for PCR-based genotyping analysis. In addition, blood samples were collected in Vacutainer tubes (BD) containing acid citrate dextrose and transport medium for adaptation of *P. falciparum* in culture on day 0 and the day of parasite reappearance for *in vitro* drug-sensitivity assays.

2.2.4.4 Day 7

During clinical visit on day 7, one ml of venous blood was directly given into 10 ml of *RNA/DNA Stabilization reagent for blood (Roche)* and stored at 4°C until transport to KEMRI site in Kilifi town where the samples were stored at -80°C until purification. I analysed in total 156 samples from children who were either enrolled in the amodiaquine study (2.2.4.2) or the ACT study (2.2.4.3).

I isolated mRNA with *mRNA Isolation Kit for blood and bone marrow* (Roche) and re-suspended the mRNA in 12 µl of double distilled water. The samples from the ACT study were treated with DNase before cDNA synthesis.

From both sample sets 1 µl of isolated mRNA was used in a one step reverse transcription reaction with the *SuperScript III one-step RT-PCR System* (Invitrogen) and the remaining 10 µl were transcribed into cDNA with oligo dT primers and the *RETROscript* (Ambion). For the one step system the *Pfresa* specific primers a) and d) were used to amplify a ring stage-specific transcript and to distinguish PCR products originating from transcripts or genomic DNA. The designed oligonucleotides were intron spanning and thus allowed such differentiation and specific detection of viable asexual parasites circulating in the peripheral blood. To increase the sensitivity of the assay a second nested PCR was run using the first product as template. The primers used for this reaction were also resa specific (b and c) Table 2-2.

The cDNA synthesised with oligo dT primers and the RETROscript (Ambion) was also analysed with a nested PCR protocoll and the Pfresa specific primer a) and d) in the first round and the primer pair b) and c) in the second round. The reaction was repeated at least three times for each sample.

The sensitivity of the assay was determined with *in vitro* parasite culture. A dilution series was performed and parasite were detected down to 10 parasites /ml blood. This corresponds to 10^4 parasites in the total body and thus increases the sensitivity of 10^3 compared to a microscope.

2.2.4.5 Merozoite surface protein 2 (*msp2*) genotyping

Msp2 genotyping is a commonly used method to differentiate parasite lines *in vivo*. Recrudescent infections are distinguished from new infections after treatment. In the course of the Day 7 project the *msp2* genotyping was used for the *in vivo* differentiation. But *msp2* genotyping was also used to distinguish parasite populations *in vitro* after culture adaption of the isolated from the patients.

The underlying mechanism is the restriction fragment length polymorphism of a highly polymorphic region of the genome: *msp2*. The alleles of *msp2* fall into two allelic families (Smythe et al, 1990): 3D7 and FC27 with conserved regions and polymorphic repeat regions.

A primary and a nested PCR were performed with specific oligonucleotides in a conserved region of the locus, as described by Felger and Beck (Felger & Beck, 2002). Both reactions were performed with the same protocol and PCR program.

Protocol:

1 x Reaction buffer with KCL	Fermentas
200 µM d'NTP's Mix	Fermentas
1,5 mM $MgCl_2$	Fermentas
0,5 µM Oligonucleotide each	MWG or Invitrogen
2,5u/50µl Taq Polymerase	Fermentas,

Table 2-8 Cycling conditions for *msp2* genotyping. 30 cycles (Step2 – Step4)

Initial denaturation of the template DNA	4:00 min	94°C
Denaturation of the DNA (Step 2)	0:30 min	94°C
Annealing of the oligonucleotides (Step 3)	2:00 min	55°C
Extension of the fragments by the *Taq polymerase* (Step 4)	2:00 min	70°C
Final Extension to ensure complete amplification	7:00 min	72°C
Pause		4°C

The amplified fragment was incubated over night at 37°C with *HinfI* to ensure complete digest. This specific pattern of fragments was analysed on an agarose gel. Both families are clearly distinguishable: in FC27 the restriction digest generates two conserved fragments (137bp at the 5' end and 115 bp at the 3' end). Between these, the two variable repeats are located (36bp and 96bp) The repeats themselves are conserved in size but vary in copy number. One 96bp repeat is present in all members of this family. If a second is present the fragment will appear on the gel with increasing intensity. The 36bp repeat is responsible for the variable and countable fragments on the gel. One 36bp repeat results in a 162bp fragment, two repeats give a fragment of 234 and three of 270bp. Exceptions to this rules are described, one of them being a partial deletion reducing the size of the 162bp fragment to 126bp (Felger & Beck, 2002).

3D7 the representative of the second family is also characterized by two conserved fragments (70 and 108bp), both originating from the 3' end of the *msp2* PCR product. One, further variable fragment is generated by the restriction digest but the variable region of 3D7 is not as clearly definably as in the FC27 family since the repeats not only vary in copy numbers but also in size. If the two conserved fragments are subtracted, a variable fragment of approximately 250 to approximately 550bp results.

3. Results

3.1 Drug parasite interaction *in vivo*

Malaria control relies mainly on prompt and effective case management of uncomplicated disease episodes. The efficacy of the chemotherapeutic regimens is commonly determined by the *in vivo* test in which parasite persistence or reappearance is monitored for up to 8 weeks through microscopic analysis of blood smears.

Here, the attempt was made to replace this long lasting and rather insensitive test by a more sensitive method at an earlier time point, i.e. 7 days after initiation of treatment of infection. Particularly the discrepancy between prolonged parasite clearance time *in vivo* and the absence of an increased 50 % growth inhibition concentration *in vitro*, show the importance of new tools to detect arising drug failure. The results are presented in the following paragraph.

The project was embedded in two clinical studies: an *in vivo* efficacy trial of amodiaquine and a comparative study of two artemisinin combination therapies (ACTs): artemether-lumefantrine (AM-LM) and dihydroartemisinin-piperaquine (DHA-PPQ). Both were conducted at the Pingilikani Clinical Trial facility as acollaborative peoject between the Dep. Of Infectious Disease, Heidelberg University School of Medicine (PI Dr. Steffen Borrmann) and the Kenya Medical Research Institute (KEMRI), Centre for Geographic Medicine Research-Coast (CGMR-C) (Directors Prof. Kevin Marsh and Dr. Norbert Peshu), which is located 20 km south of the town of Kilifi, on the Kenyan coast.

3.1.1 Artemether – lumefantrine and dihydroartemisin – piperaquine

The project was embedded in a comparative study in which patients received either AM-LM or DHA-PPQ. Samples were collected on day 7 after start of treatment and processed and analysed as described in 2.2.4.4.

In 48/105 (45.7%) samples we detected metabolically active persistent asexual parasites 7 days after start of treatment (i.e., 4 days after last dose) (Figure). This high proportion contrasts with a three-fold lower Kaplan-Meier estimated failure rate of 15% by day 84 across both treatment groups. Persistence of infection on day 7, however, poorly agreed with subsequent recrudescence at the individual level. Twenty-nine children with detectable parasite populations surviving in their blood on day 7 either cleared the parasites in the following 77 days or were re-infected, as

determined by *msp2* genotyping. And 18 patients with undetectable parasite population presented with recrudescent parasites in the following 21 days. This discrepancy did not depend on treatment. In the patient group treated with DHA-PPQ 45.83 % had cleared the parasites by day 7 and 45.61% in the AM-LM group.

Therefore I studied the relationship between potential confounding factors such as age as the best-established clinical correlate of acquired immunity, baseline parasite density, during-treatment parmacodynamic parameter (24-hour parasite reduction ratio) and 7 plasma concentrations of the long half-life companion drugs LM-PPQ. LM and PPQ are expected to remove residual and potential resistant parasite populations, which may have survived the potent but short acting doses of AM or DHA, respectively. Because transmission intensity decreased over the last years in Kilifi (O'Meara et al., 2008), we decided to split the analysis in two periods (2005-2006 and 2007-2008).

In Figure 3-1 a box graph depicts the median baseline parasite densities in patients with or without subpatent parasitaemia on day 7. Panel A shows the results obtained from the first phase of the study, panel B from the second phase of the study. We found that baseline parasite density correlated with prevalence of subpatent parasitaemia on day 7 in the second ($p<0.03$), but not the first, phase of the study suggesting that predicted decline in immunity over the same time period exposed the expected relationship between initial parasite biomass and persistence (Figure 3) and thus, indirectly also supported the validity of my sensitive RT-PCR approach.

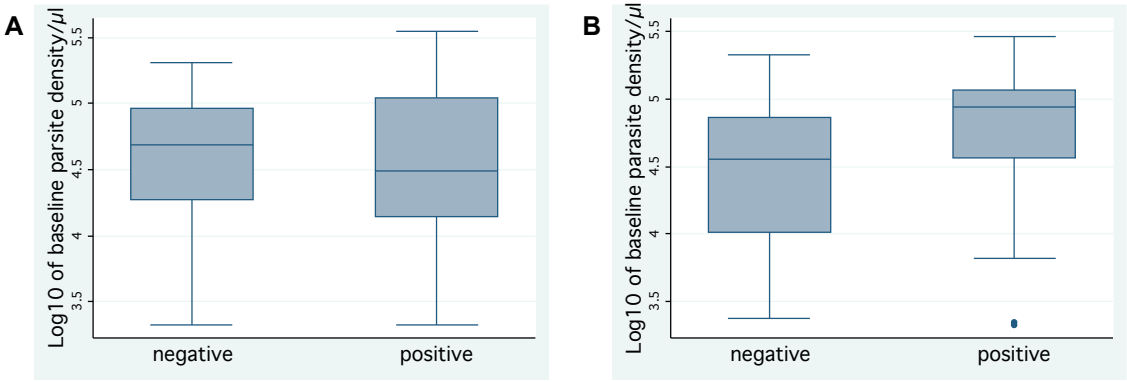

Figure 3 Box plots of baseline parasite density over PCR results on day 7. A) Phase one (2005 – 2006) B) Phase two (2007 – 2008) The parasite density at baseline did not significantly differ between patients who had cleared parasites by day 7 and those carrying subpatent parasitaemia during the first period of the study (A). In the second period of the study (B) the parasite density at baseline showed a significant increase in patients with subpatent parasitaemia on day 7 ($p<0,03$)

Figure 3-1 shows that prevalence of subpatent parasitaemia on day 7 is independent of the parasite reduction ratio within the first 24 hours after treatment. Again panel A) shows the results obtained from the first phase of the study, panel B) from the second phase of the study. We found that the 24 hours parasite clearance ration (the best available *in vivo* correlate of drug potency in an infection at peak plasma concentration) was not associated with persistence of parasite until day 7 after treatment. This was surprising since I had postulated that parasite persistence by day 7 would primarily be related to drug effects.

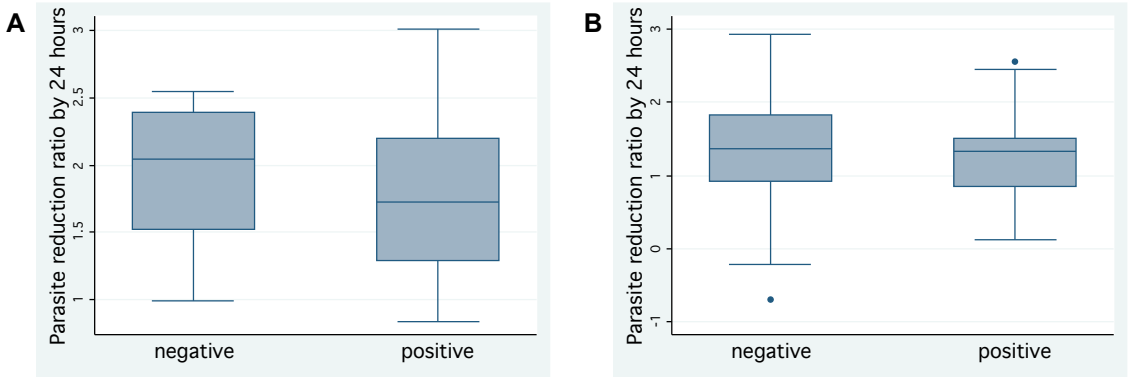

Figure 3-1 Box plot of parasite reduction ratio by 24 hours and subpatent parasitaemia on day 7. A) Phase one (2005 – 2006) B) Phase two (2007 – 2008). No difference in the parasite elimination rate was found in the two groups with subpatent and cleared parasite by day 7 in the two periods of the study.

Figure 3-2 demonstrates that the observed prevalence of subpatent parasitaemia on day 7 cannot be explained by differences in PPQ or LM plasma concentration of individual patients. During the entire period of the study, no difference in plasma concentration of PPQ or LM was observed between patients presenting with subpatent parasitaemia and patients, who had cleared parasites on day 7.

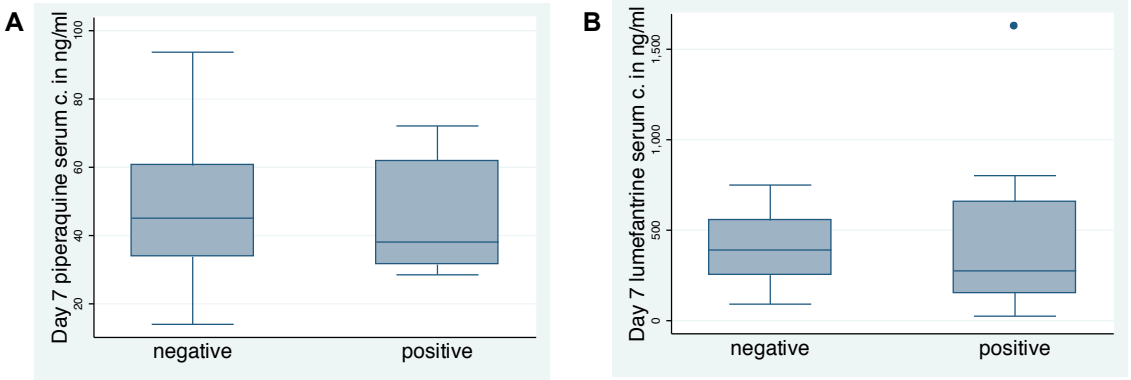

Figure 3-2 Box plot of Day 7 piperaquine (A) and lumefantrine (B) concentration over PCR results on day 7. Piperaquine and lumefantrine serum concentration on day 7 showed no clear relationship over the both phases of the study and between the two groups.

Intriguingly, I found a strong correlation of platelet counts on day 0 with the prevalence of subpatent parasitaemia on day 7 (Figure 3-3). Patients were categorised according to baseline platelet counts (<125,00/µl or >125,00/µl). The y-axis represents the proportion of subpatend infections by day 7. Interestingly the platelet counts on day 0 were inversely correlated with clearance of parasites by day 7 (Figure 3-3) suggesting either a direct killing effect (McMorran et al, 2009) and/or perhaps, progressive depletion of platelets.

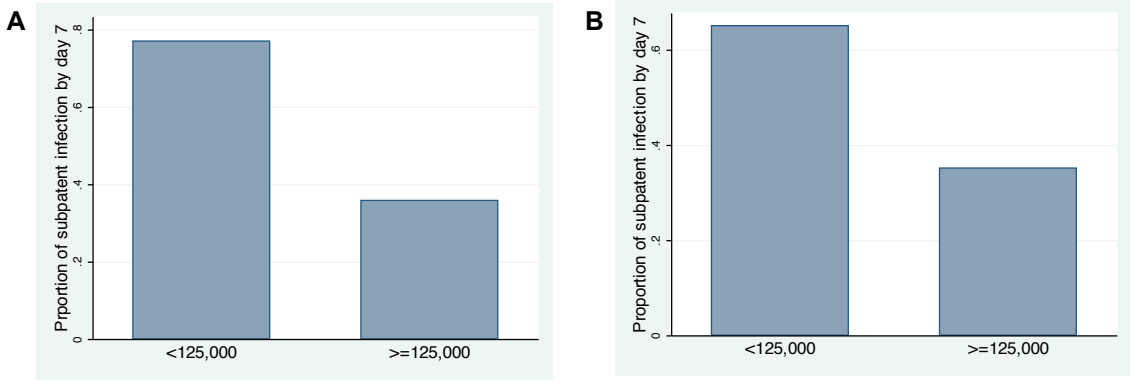

Figure 3-3 Bar charts showing the relationship between subpatent *P. falciparum* infections and platelet counts on day 0. A) Phase one (2005 – 2006) B) Phase two (2007 – 2008) In both periods of the study a significant correlation was found for the two parameters. Higher baseline platelets counts were associated with a negative PCR result on day 7 ($p < 0.014$ Phase 1, $p < 0.03$ Phase 2)

Finally, I studied the effect of patient age as clinical correlate of acquired immunity on the day 7 prevalence of subpatent infections. Figure 3-4 shows that patient age was not associated with the prevalence of parasitaemia on day 7 in the first phase of the study. I detected a weak association with age and prevalence of parasites in day 7 (p=0.13) the first phase of the study.

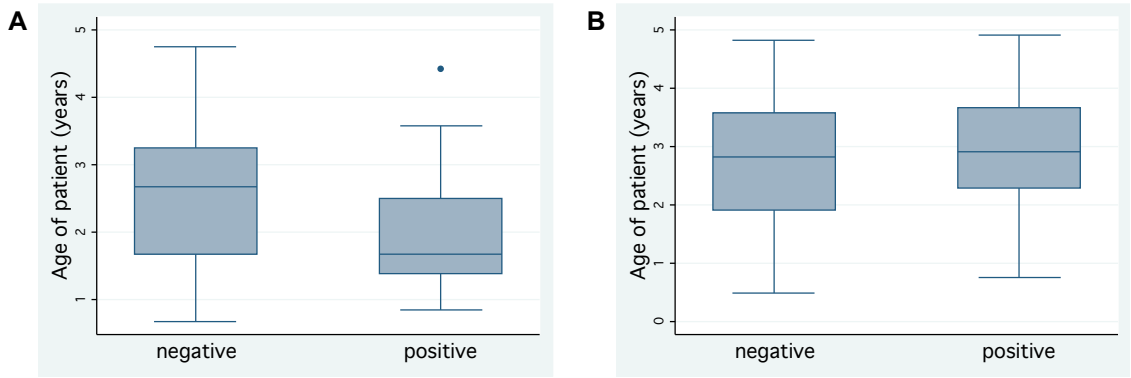

Figure 3-4 Correlation of age with persistence of subpatent parasitaemia until day 7 A) Phase one (2005 – 2006) B) Phase two (2007 – 2008) In the first phase of the study, older patients were more likely to clear the parasites until day 7. In the second phase of the study no difference in age was found in the two groups.

In summary, I found a poor correlation between presence of asexual parasites on day 7 as a marker of incompletely eliminated persistent blood stage infections and subsequent risk of recrudescence. Vice versa, we failed to detect asexual blood stage infections in children who later experienced recrudescence of their primary infection according to *msp2* genotyping, likely reflecting the difficulty of capturing very low biomass infections due to daily fluctuations in sequestered vs. circulating blood stage forms.

Interestingly, I observed that baseline parasite density correlated with prevalence of subpatent parasitaemia on day 7 in the second, but not the first, phase of the study (Figure 3-1) correlating with a predicted decline in adaptive immunity over the same time period, which may have exposed an expected relationship between initial parasite biomass and persistence. The weak association with age in the first phase of the study (Figure 3-4) supports this interpretation. Platelets, an important component of the innate immune defence against microbial pathogens, were strongly associated with clearance of infections by day 7 (Figure 3-3).

3.1.2 Amodiaquine

The results presented in this paragraph were obtained from patients, enrolled in an *in vivo* efficacy trial of amodiaquine (Sasi et al, 2009) in the years 2005 and 2006 at the same time as the first period of the previously presented data on ACT 3.1.1.

In 16/51 (31%) samples we detected metabolically active persistent asexual parasites 7 days after start of treatment (i.e., 4 days after last dose). Persistence of infection on day 7, however, poorly agreed with subsequent recrudescence at the individual level. Age as a reliable indicator of acquired immunity did not correlate with our results obtained on day 7. Likewise, children with or without positive samples on day 7 differed only marginally in the initial parasite load Figure 3-5

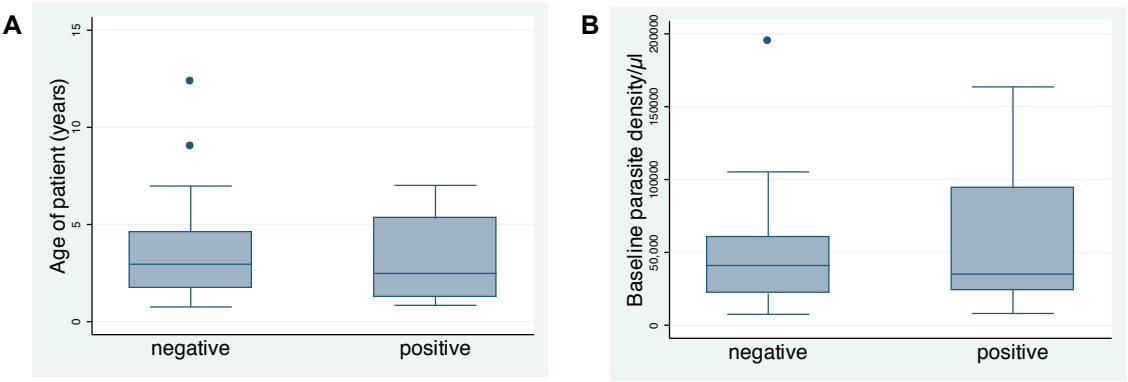

Figure 3-5 A) Correlation of age with persistence of subpatent parasitaemia until day 7, B) Box plots of baseline parasite density over PCR results on day 7.

3.2 *In vitro* characterisation of phenotypic and genotypic signatures of naturally acquired drug resistance in *P. falciparum*

The focus of the analysis was the folate pathway involving the anti-folates pyrimethamine, cycloguanil (one active metabolite of proguanile) and trimethoprim to assess *in vitro* sensitivity.

In the following paragraphs I will describe the genotypic analysis of parasite isolates collected from children with uncomplicated *P. falciparum* malaria in Kilifi, Kenya. I will correlate these results with *in vitro* drug response rates of culture-adapted parasites.

3.2.1 Culture adaption of parasites and *msp2* genotyping

Paediatric patients presenting with uncomplicated *P. falciparum* malaria at the Pingilikani clinic in coastal District of Kilifi often carry multiple infections determined by *msp2* genotyping on the day of admission and the day of recurrence (Sasi et al, 2009). Parasites were culture adapted from the same blood and thus the starting material for culture adaptation was not necessarily a homogenous parasite population but consisted of up to 6 clones as shown below in Table 3-1. The procedure of adapting parasites to culture can take several weeks and only when the parasites showed a constant replication rate at standard culture conditions, genomic DNA was isolated and their *in vitro* response to drugs were analysed. The adapted parasites were compared to the initial parasites population in the patient. This analysis gave insights in diversity and survival rate when adapting parasites from *in vivo* to *in vitro* culture.

Figure 3-6 A) shows the electrophoretic mobility of PCR-amplified *msp2* fragments after *HinfI* restriction on 4% agarose gel (2% tiny agaorse, 2 % standard agarose). Pairs of lanes are labelled with isolates IDs.

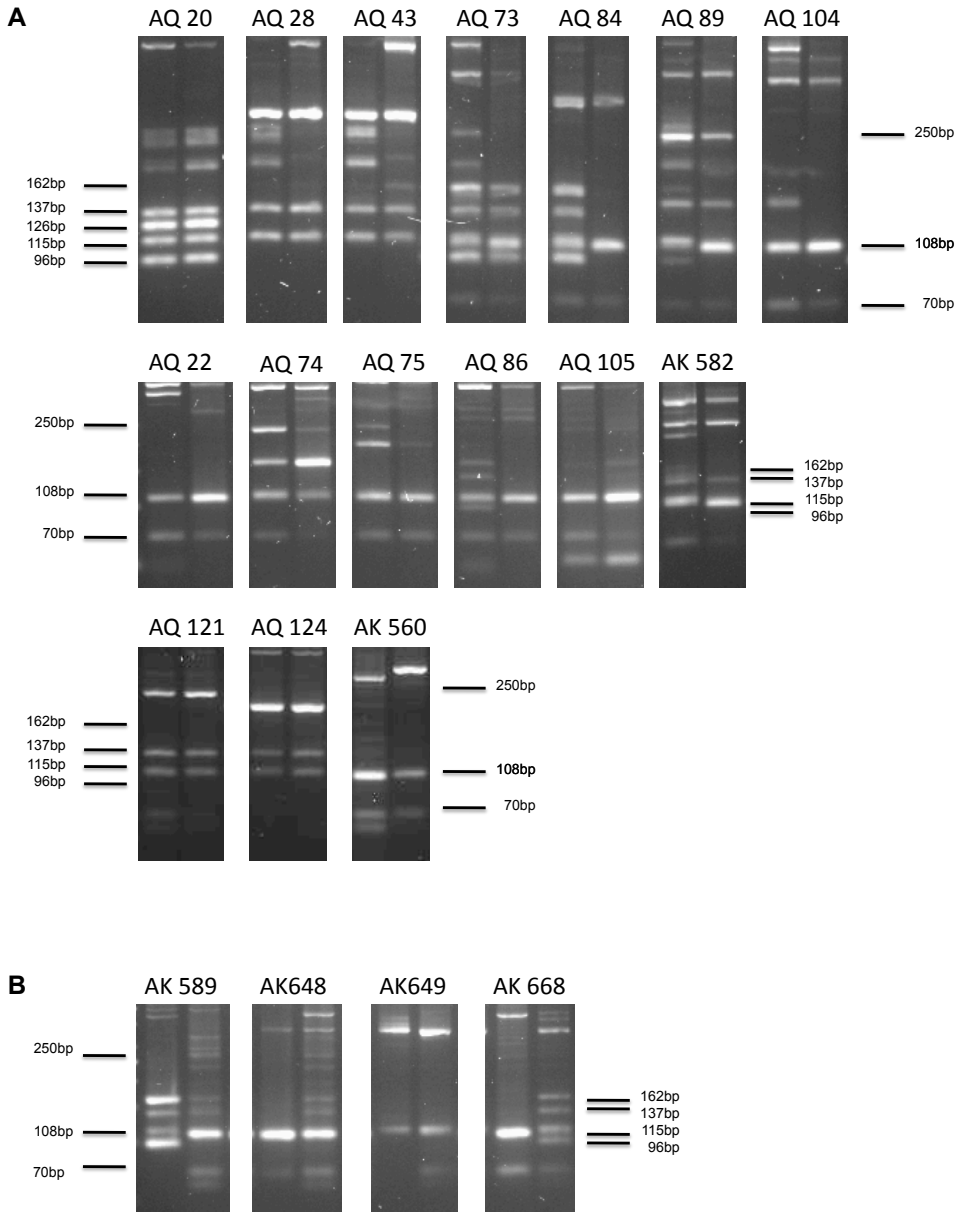

Figure 3-6 *Hinf I* restriction digest of *msp2* locus on agarose gel. The first lane of each pair shows the analysis of parasite population directly isolated from the patient. The second lane the results obtained from the parasites population surviving the adaption to culture for four weeks and more. In **B)** the picture is inversed. The first lane shows the analysis of culture adapted parasite population and the second lane the initial parasite population directly isolated from the patient. Above the panel the letters indicate from which study the samples were isolated. AK : ACT study, AQ: amodiaquine study and the numbering indicates the patient number. Black bars with size indication (kilobases) at either side mark the conserved fragments 2.2.4.5 of the 3D7 and the FC27 families generated by a *Hinf I* restriction.

Table 3-1 the results obtained from the *Hinf I* restriction digest of the *msp2* locus in Figure 3-6 are analysed and represented in a tabular format. Clones were counted by three independent persons and assigned to the 3D7 and FC27 two families at admission and after culture adaption.

Most of the isolates appear to consist of multiple clones (multiple infection). Out of the 20 isolates analysed with this method only AK 649 showed a single infection. The remaining 19 isolates were multiple infections consisting of two to six clones. In summary, we detected an average of 3.4 clones / patient.

During the procedure of cell culture adaption 4 isolates lost all their clones except one (AQ 84, AK 560, AK 648, and AK 668). They can therefore be regarded as clonal parasite populations in the following work. In these cases the predominant clone from the infection is not always identical with the predominant parasite clone in the adapted culture. In the two isolates AQ 84 and AK 648 the different clones at admission contribute in comparable size to the total parasite biomass and one of these equally represented clones survived the adaption to culture.

Table 3-1 Analysis of the *Hinf I* restriction digest of the MSP 2 locus. Number of clones of each family was counted before and after cell culture adaption. (I) one clone, (-) no clone.

	Parasites isolated directly from patient		Parasites isolated from adapted cell culture	
Isolate Nr.	Nr. clones FC 27	Nr. Clones 3D7	Nr. clones FC 27	Nr. Clones 3D7
AQ 20	IIII	-	IIII	-
AQ 22	-	II	-	II
AQ 28	IIII	-	II	-
AQ 43	IIII	-	IIII	-
AQ 73	III	II	I	I
AQ 74	I	II	I	II
AQ 75	-	III	-	II
AQ 84	I	I	-	I
AQ 86	I	III	-	III
AQ 89	III	III	II	I
AQ 104	I	III	-	II
AQ 105	I	II	I	II
AQ 121	I	I	I	I
AQ 124	II	-	II	-
Art 560	III	I	-	I
Art 582	II	I	I	I
Art 589	II	I	II	-
Art 648	III	II	-	I
Art 649	-	I	-	I
Art 668	I	III	-	I

In the two isolates AK 560 and AK 668 one minor clone, which was initially represented by a very week band became the predominant clone in culture. From the 16 remaining isolates a variable number of parasites survived the procedure of culture adaption. These cultures are non-clonal parasite population in culture.

In summary, we detected an average of 2.15 clones/culture and a loss of 1.25 (36.8%) clones per culture adaption procedure. Figure 3-7 shows the loss of clones through culture adaption.

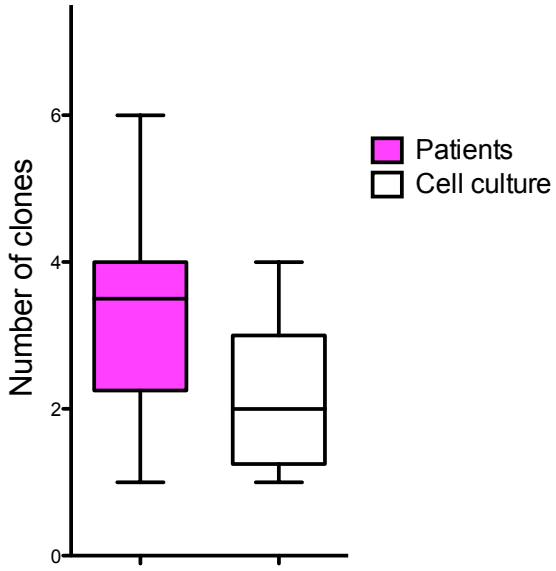

Figure 3-7 Multiplicity of infection before and after culture adaptation. The magenta box shows the mean number of clones carried by the patients. The white box indicated the mean number of clones surviving in a culture adaption of each infection ($p < 0.0009$)

3.2.2 Analysis of *P. falciparum* isolates after natural exposure

The culture-adapted parasites were analysed for single nucleotide polymorphisms (SNP) and copy number variation (CNV). The phenotypic analysis was performed in an assay with chloroquine, trimethoprim, cycloguanil and pyrimethamine.

The genetic analysis was only performed with the five enzymes directly involved in the folate pathway. These are: GTP cyclohydrolase (*Pfgch*, *PFL1155w*), 6-pyruvoyltetrahydropterin synthase (*Pfptps*, *PFF1360w*), dihydropteroate synthetase (*Pfdhps,* PF08_0095), dihydrofolate synthase / folylpolyglutamate synthase (*Pfdhfs* PF13_0140) and bifunctional dihydrofolate reductase-thymidylate synthase (*Pfdhfr* PFD0830w). I analysed for SNP's by sequencing and for CNV's by a real time PCR assay.

3.2.2.1 Single nucleotide polymorphisms in enzymes of the folate pathway

A genotypic analysis of the folate pathway was performed in the set of field isolates described above. The five enzyme of the pathway were sequenced with the primer pairs listed in the methods parts (Table 2-2 and 2.2.1.11) and the sequencing reaction was performed and analysed as described.

***Pfgch* (PFL1155w)**

Two single nucleotide polymorphisms (SNPs) are annotated on PlasmoDB (www.plasmodb.org Version 6.2, 13 Nov 09) at nucleotide position 262 and 689. One of our isolates (AQ 89) showed an adenine instead of a guanine at position 689. This exchange results in an amino acid substitution (230) replacing arginine by lysine. When aligning the protein sequence from *E. coli* in which the active sites of the enzymes are well characterised (Nar et al, 1995), the result shows that this exchange is right next to one of the key amino acids of the active site Figure 3-8.

```
                                        65  68
EcGCH 39   IAGHMTEIMQLLNLDLADDSLMETPHRIAK--MYVDEIFSGLDYANFPKITLIENKMKVD  96
           I+ H+ +I+ +  L   D  L  T  R A+  +Y+   ++ LD     K +L +   K +
PfGCH 206  ISKHIYKILNISKLPKCD-ILKRTNRRYAETFLYLTNGYN-LDIEQIIKRSLYKRMYKNN  263
                             AQ 89  K

                      110 112/3                 132 135/6 138          151/2
EcGCH 97   EMVTVRDITLTSTCEHHFVTIDGKATVAYIPKDSVIGLSKINRIVQFFAQRPQVQERLTQ  156
            ++ V  I + S C+HH +  +G   + YIP   +IGLSK +RIV  F++R Q+QE LT
PfGCH 264  SIIKVTGIHIYSLCKHHLLPFEGTCDIEYIPNKYIIGLSKFSRIVDVFSRRLQLQEDLTN  323

                                  179 181  185
EcGCH 157  QILIALQTLLGTNNVAVSIDAVHYCVKARGIROATSATTT  196
            I  AL+  L    + VSI A H C+  RG++   + T T
PfGCH 324  DICNALKKYLKPLYIKVSIVAKHLCINMRGVKEHDAKTIT  363
```

Figure 3-8 Amino acid alignment of active site of GTP cyclohydrolase *E. coli* and of *Plasmodium falciparum*. In yellow the active residues for *E. coli* (Nar et al, 1995) are shown in cyan the position in the protein. The red mark shows the amino acid exchange in isolate AQ 89, right next to an active site residue.

The amino acids defining the active site are highlighted in yellow. The position at which I found a nucleic acid substitution is marked in red. Whether this amino acid substitution has consequences for the activity and efficiency of the enzyme or whether it is involved in development of resistance further downstream the pathway remains to be solved.
In addition, I found two previously unidentified synonymous point mutations at nucleotide position 327 and 564 in isolates AQ 121 and AK 560 respectively.

***Pfptps* (PFF1360w)**

No SNP is currently annotated on PlasmoDB for *ptps* (www.plasmodb.org Version 6.2, 13 Nov 09). In the isolates I only found one SNP at the nucleotide position 5. Thymine is replaced by a guanine resulting in an amino acid exchange from methionine to arginine. The sequence published on PlasmoDB starts with ATGATG, I found that one of our isolates showed the sequence ATGAGG, indication of a potential different transcription start site.

***Pfdhps* (PF08_0095)**

Pearce et al, identified five major haplotypes, when analysing samples from 50 locations across Africa from 1997 until 2007 at nucleic acid position S436A/F, A437G and K540E of *Pfdhps* (Pearce et al, 2009). Three resistant haplotypes SGE, SGK and AGK were previously identified. SAK is regarded as the ancestral haplotype and AAK as an alternative wild type haplotype. In our samples, collected on the Kenyan cost, I found two isolates (AQ 20 and AQ 105) carrying the ancestral SAK haplotype. All the remaining isolates harboured the SGE haplotype, dominant in East Africa (Pearce et al, 2009).
The mutation at nucleotide position 581 described to emerge in northern Tanzania (Gesase et al, 2009) was not found in our set of samples from Kilifi, Kenya.

***Pfdhfs* (PF13_0140)**

Two nucleotide polymorphisms are known at codon positions 1 and 75. No mutation was found within the first 520 nucleotides of this gene.

***Pfdhfr* (PFD0830w)**

It has been shown that several specific nucleotides substitutions in *Pfdhfr* result in an amino acid changes and thereby confer a stepwise increase of resistance to anti-folates (Sirawaraporn et al, 1997). The genomic sequence of *dhfr* was fully sequenced in the isolates presented here.

All the isolates (21/21, 100%) harboured the codon-changing mutations from Ser to Asn at codon position 108 (S108N) and 19 out of 21 (90,5%) also harbour the substitution of Asn by Ile at codon position 51 (N51I). The mutation from Cys to Arg at the codon position 59 (C59R) was detected in 14 out of 21 (66,6%). No mutations were found at the codon positions 16, 164 and 184 (0/21, 0%).
The two major haplotypes, AIRNIT (14/21, 66,6%) and AICNIT (5/21, 23,8%) were found in the parasite population from Kilifi. One parasite was found with the rare haplotype ANRNIT (AQ 74, same as Dd2) and another parasite with haplotype ANCNIT (AQ 86). AQ 86 was the only isolate with only one point mutation at all six known polymorphic positions. However I found an additional previously unidentified synonymous mutation at position 533. Because the SNP is located at the binding site of the real time probe for *dhfr* I was unable to generate *dhfr* gene copy data for this isolate.

In summary, I found 12 isolates harbouring the triple-mutant *dhfr* (N51I, C59R and S108N) and the double-mutant *dhps* (A437G and K540E), associated with highly resistant phenotypes for pyrimethamine and sulfadoxine, respectively. Six isolates were double mutant *dhfr* (one with C59R and S108N instead of N51I and S108N) and double mutant *dhps*. Two isolates were triple-mutant *dhfr* but wild type or sensitive at the *dhps* locus. And one isolate harboured only the S108N at the *dhfr* locus but double mutation at *dhps*.
In addition to the commonly found SNPs, we found one previously unidentified SNP in the *dhfr* gene and one amino acid substitution adjacent to the predictive active site of *gch*.

3.2.2.2 Copy number variations (CNV) in enzymes of the folate pathway

I analysed copy number variations (CNV) in the folate pathway genes with a real time PCR based assay described in chapter 2.2.1.13. The field isolates were analysed in reference to the *P. falciparum* laboratory strains: 3D7, FCR3, Dd2 and D10. Genomic DNA (2.2.1.1) for the assay was isolated from regular adapted parasite culture (chapter 2.2.3.1). To control the amount of DNA used in each reaction, I used the gene coding for β-tubulin (PF10_0084) as internal control.
The methodology allows a robust relative quantification of copy numbers. To facilitate the interpretation, the copy number from the reference genome is always set at one.

Pfgch copy number variation in field isolates

First the available laboratory strains (3D7, FCR3, Dd2, D10, 7G8, HB3 and NF54) were analysed for copy number variation (CNV) with the established assay. In Figure 3-9 the graph displays the relative gene copy numbers of the individual laboratory strains in reference to D10. The parasite lines Dd2 and D10 were found to give the lowest value for *GCH* copy numbers and were therefore used as reference genome for the analysis of the field isolates.

3D7, FCR3 and NF 54 show significantly more genomic copies of *gch* compared to D10, Dd2 and HB3. The bigger error bar in 3D7 may indicate heterogeneity in the parasite population, i.e. there are genomes with 3 and some maybe 4 copies of the gene. The genotype seems to be stable, as no reduction in the signal was observed over the culturing period.

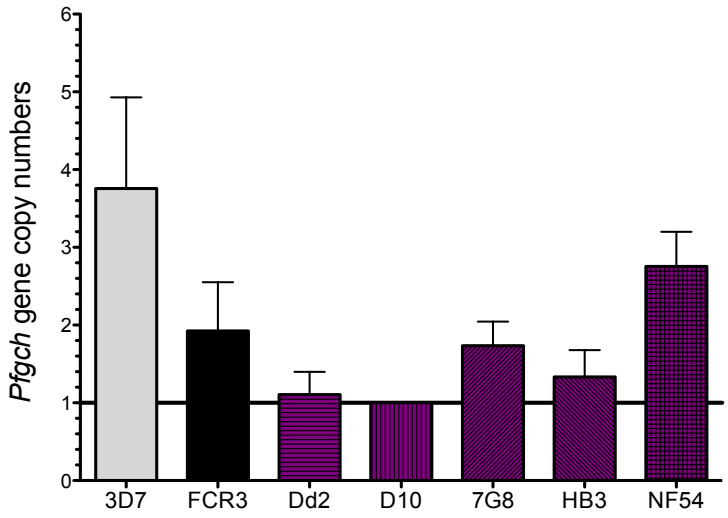

Figure 3-9 *P. falciparum* GTP cyclohydrolase gene copy numbers in laboratory strains. Gene copy numbers were analysed in a real time PCR assay, in which β-tubulin served as internal control. Means with standard deviation are plotted in the graphic, each bar representing the result from at least independent experiments. D10 served as reference genome since this strain gave the lowest value.

The field isolates were then measured in reference to Dd2 and the results are shown in Figure 3-10 on the x-axis the 21 different field isolates are plotted with their initials and on the y-axis the relative copy numbers are indicated. One isolate was measured in at least 3 independent assays.

While no significant variation in *gch* copy numbers was found within the field isolates and in comparison with the two reference genomes Dd2 and D10, 3D7 and FCR3

had significantly more ($p<0.001$) genetic copies compared to Dd2 and compared to the field isolates.

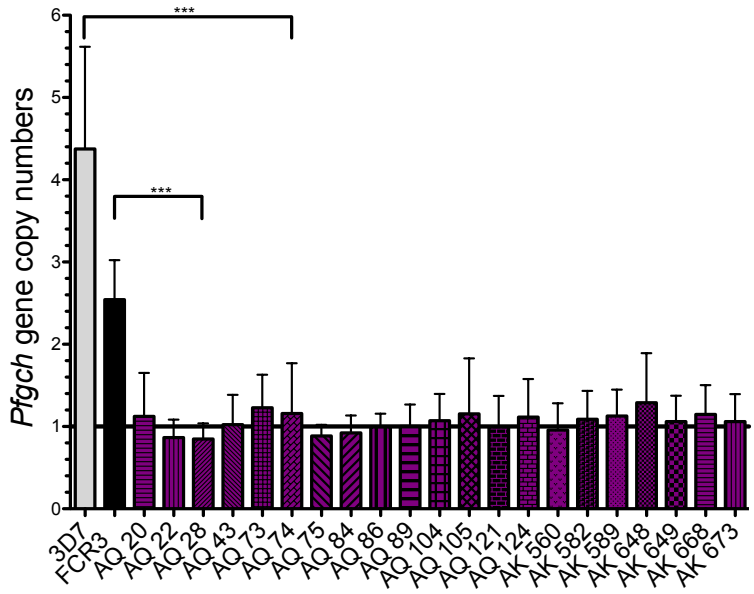

Figure 3-10 *P.falciparum* GTP cyclohydrolase gene copy numbers in field isolates from Kilifi (purple), Kenya. Gene copy numbers were analysed in a real time PCR assay, in which β-tubulin served as internal control. Means with standard deviation are plotted in the graphic, each bar representing the result from at least independent experiments. Dd2 served as reference genome. 3D7 (grey) and FCR3 (black) are also shown on the graph as control AQ: samples from amodiaquine study, AK: samples from ACT study.

Pfdhfr copy number variation in field isolates

The 20 isolates of this study were analysed for copy number variances at the *dhfr* locus. First the available laboratory strains (3D7, FCR3, Dd2, D10 and 7G8) were analysed for copy number variation (CNV) with the established assay. The results show no significant variation within the laboratory strains Figure 3-11.

The results for the field isolates are shown in Figure 3-12. On the x-axis the 21 different field isolates are plotted with their initials and on the y-axis the relative gene copy numbers are indicated. One isolate was measured in at least 3 independent assays and the means with standard deviations are plotted in the graphic, each bar representing the results for one parasite isolate.

No significant variation in *Pfdhfr* copy numbers was found in the field isolates from Kilifi and in comparison with the two reference genomes 3D7 and FCR3.

The isolate AQ 86 gives no signal at the locus under investigation as the isolate carries a rare point mutation (3.2.2.1) in the sequence were the real time probe binds to the DNA. I confirmed the presence of the *dhfr* gene using conventional PCR.

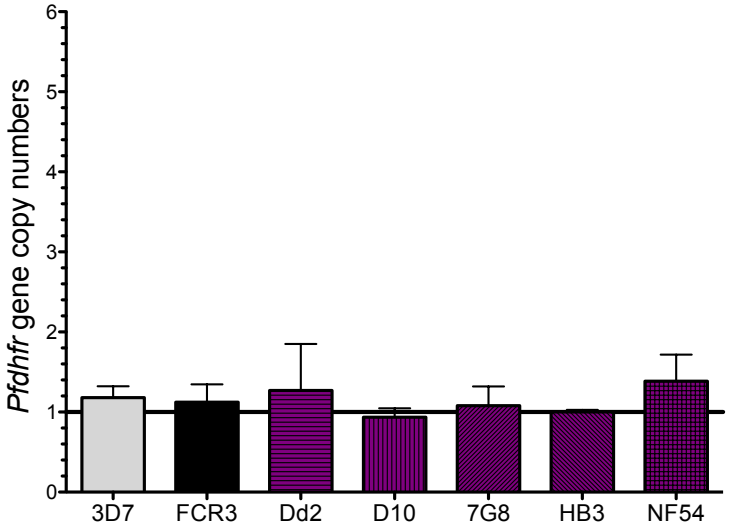

Figure 3-11 *P. falciparum dhfr* gene copy numbers in laboratory strains. Gene copy numbers were analysed in a real time PCR assay, in which β-tubulin served as internal control. Means with standard deviation are plotted in the graphic, each bar representing the result from at least independent experiments.

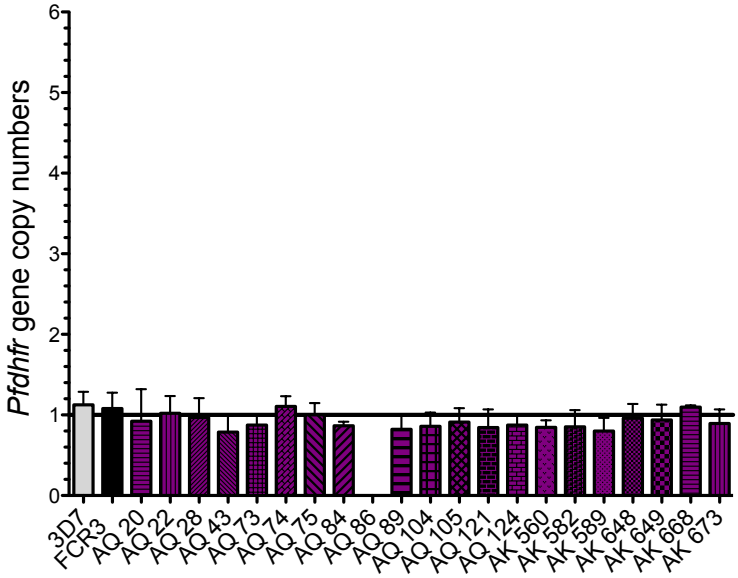

Figure 3-12 P.f. DHFR gene copy numbers in field isolates from Kilifi (purple), Kenya. Gene copy numbers were analysed in a real time PCR assay, in which β-tubulin served as internal control. Means with standard deviation are plotted in the graphic, each bar representing the result from at least independent experiments. Dd2 served as reference genome. 3D7 (grey) and FCR3 (black) are also shown on the graph as control AQ: samples from amodiaquine study, AK: samples from ACT study.

3.2.2.3 Phenotypic analysis of field isolates

The same *P. falciparum* isolates, which were adapted to culture and genotyped for SNPs and CNVs were subjected to a phenotypic analysis. The *in vitro* drug response rate for anti-folates was measured with a validated and well-established fluorescence-based assay described in chapter 2.2.3.4. I tested the activities of pyrimethamine (Figure 3-16), cycloguanil (Figure 3-15) and trimethoprim (Figure 3-14). Chloroquine (Figure 3-13) served as experimental control.

In Figure 3-13 the IC_{50} results for chloroquine are presented. The measured IC_{50} values vary between 10 nM and 350 nM. The results can be divided into two clearly distinct groups. 3D7 and 9 out of 21 parasites (42,9%) had an IC_{50} value smaller than 25 nM and are therefore considered sensitive to the drug. For Dd2, FCR3 and 12 isolates (57,1%) an IC_{50} value of greater than 100 nM was measured. These strains are therefore considered resistant to the drug. The responsiveness against chloroquine did not correlate with any SNP combination of *dhfr*.

The results are in accordance to the previously reported decline of chloroquine resistant phenotypes after its withdrawal in Kenya (Mwai et al, 2009).

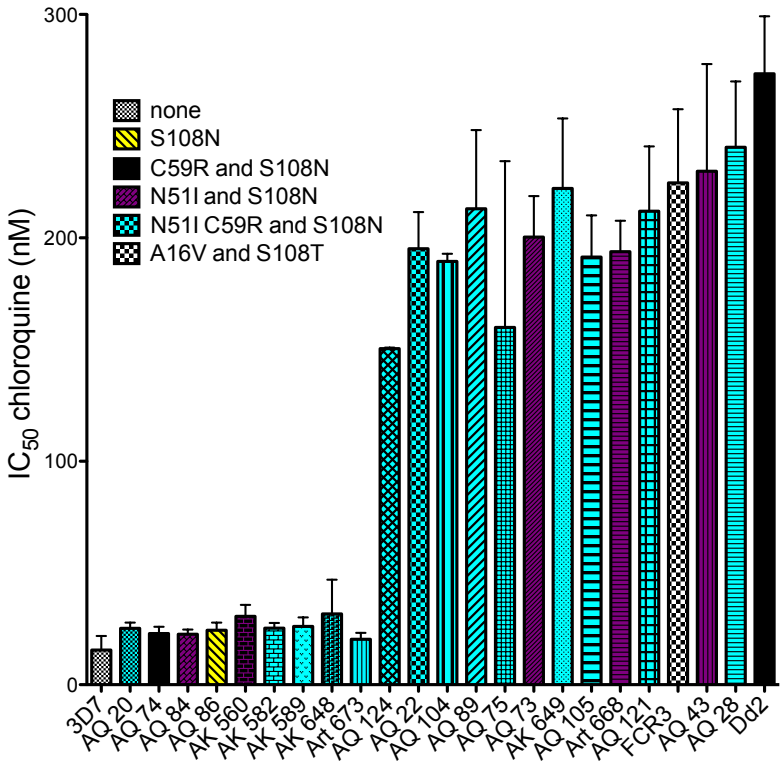

Figure 3-13 Chloroquine *in vitro* response rates in Kenyan *P.f.* isolates. (cyan) triple *dhfr* mutant, (purple) double *dhfr* mutant I, (yellow) single *dhfr* mutant, (black) double *dhfr* mutant II, (grey) 3D7 and FCR3. IC_{50}s were calculated for each isolate from at least three independent experiments and are plotted in nM on the y-axis. The isolates are sorted on the x-axis by IC_{50} values < 100nM and >100nM. AQ is the abbreviation for samples originating from the amodiaquine study and AK for samples originating from the ACT study. The numbers indicate

In Figure 3-14 the *in vitro* response rates for trimethoprim are shown. The measured values vary between 0,6 µM and 380 µM. The results cannot be divided into distinct groups but follow a steady increase. In 13 out of 21 isolates (61,9%) the determined IC_{50} was smaller than 200 µM. Only 8 out of 21 (38,1%) showed a value greater than 200 µM. 3D7 with 4 µM and FCR3 with 0,6 µM have to be considered as the most sensitive strains from the parasites measured in this work.

The responsiveness against trimethoprim did not correlate with any significant SNP combination of *Pfdhfr* (p=0.2238). Only FCR3 with a very particular haplotype (A16V and S108T) at the *dhfr* locus shows a significantly (p=0.0039) higher responsiveness against trimethoprim. The presumably wild type 3D7 with no mutations in *dhfr* was 10 fold less sensitive against trimethoprim. But since only one parasite strain with the combination of mutation A16V and S108T was available, no general conclusion can be drawn from this result.

AQ 86 with a single mutation at position S108N is the most sensitive one of the collected field isolates. AQ 74 could not be measured, as the responsiveness was so low that the values lay outside of the measurable range of the assay.

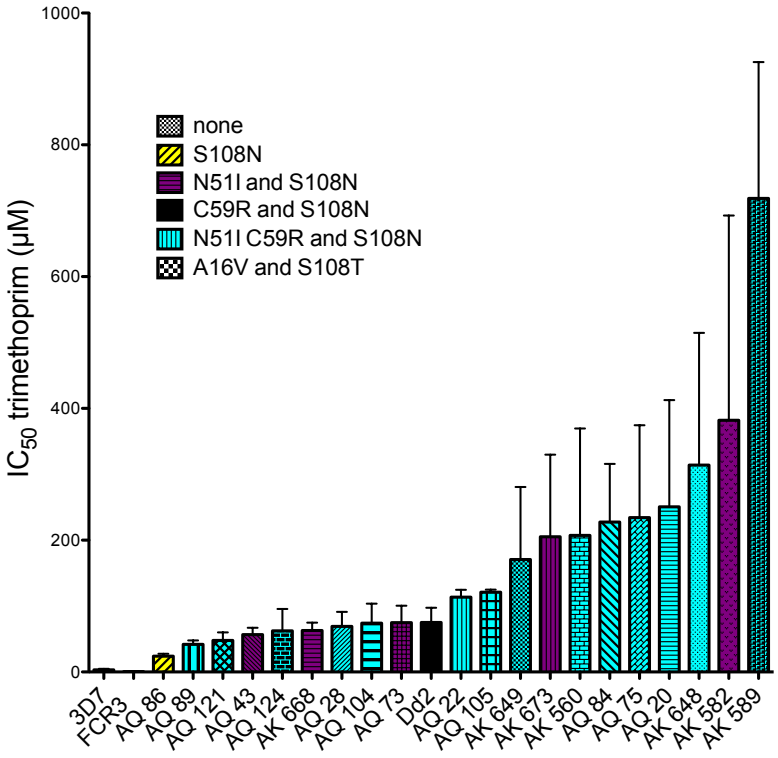

Figure 3-14 Trimethoprim *in vitro* response rates in Kenyan *P.f.* isolates. (cyan) triple *dhfr* mutant, (purple) double *dhfr* mutant I (yellow) single *dhfr* mutant, (black) double *dhfr* mutant II, (grey) 3D7 and FCR3. IC_{50} were calculated for each isolate from at least three independent experiments and are shown in µM on the y-axis with standard deviation. The isolates are sorted on the x-axis by increasing IC_{50} values. AQ is the abbreviation for samples originating from the amodiaquine study and AK for samples originating from the ACT study. The numbers indicate from which patient the isolate is adapted.

In Figure 3-15 the measured IC_{50} values for cycloguanil are given. The measured values vary between 160 nM and 3400 nM with no distinct groups of responses. 3D7 with a mean 14,35 ± 6.2 nM is the most sensitive strain and FCR3 with 3265 ± 1267 nM one of the most resistant ones. The IC_{50} values for cycloguanil correlated significantly (p=0.004) with *dhfr* haplotypes. AQ 86 (yellow bar), which harbours only a single SNP at codon position S108N, had the lowest mean IC_{50} in the studied field isolates (264,7 ± 26,03 nM). The five neighbouring parasite isolates were found to harbour two SNP's, at the codon position S108N and N51I (purple bars). The parasite isolates with a cyan coloured bar were found to be triple mutant. FCR3 with the particular haplotype (A16V and S108T) was highly resistant to cycloguanil. This finding points towards an inverse mechanism of resistance of cycloguanil and trimethoprim, to which FCR3 was highly sensitive (Figure 3-14).

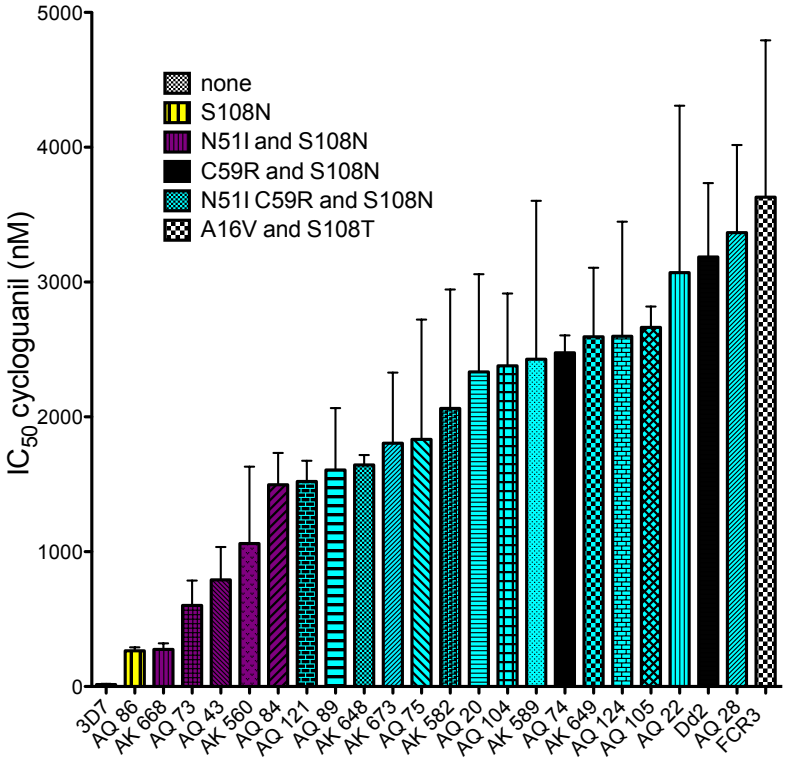

Figure 3-15 Cycloguanil *in vitro* response rates in Kenyan *P.f.* isolates. (cyan) triple *dhfr* mutant, (purple) double *dhfr* mutant I (yellow) single *dhfr* mutant, (black) double *dhfr* mutant II, (grey) 3D7 and FCR3. IC_{50} were calculated for each isolate from at least three independent experiments and are shown in nM on the y-axis. The isolates are sorted on the x-axis by increasing IC_{50} values. AQ is the abbreviation for samples originating from the amodiaquine study and AK for samples originating from the ACT study. The numbers indicate from which patient the isolate is adapted.

Interestingly the two less commonly found double mutant (C59R with S108N) in AQ 74 (black bar) and Dd2 (black bar) clustered with the triple mutant (cyan) and not with the commonly found double mutant (N51I S108N) in purple, suggesting that the mutation at position 59 is more important for the development of cycloguanil resistance.

Figure 3-16 shows the IC_{50} values for pyrimethamine. The mean values vary between 26 nM and 80 µM. 3D7 and FCR3 were the most sensitive strains with means of 26.84 nM ± 1.8 nM and 61.37 nM ± 31.3 nM respectively. The most sensitive Kilifi isolates was AQ 86 with a mean of 6.8 µM. There was a correlation between the number of mutated residues in *dhfr* and the *in vitro* responsiveness against pyrimethamine (p=0.041).

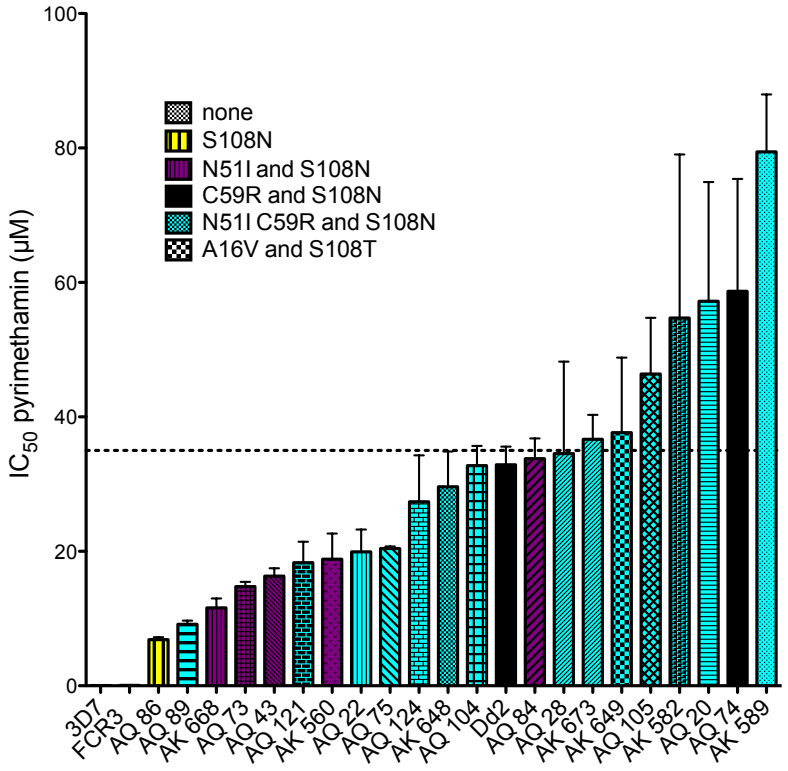

Figure 3-16 Pyrimethamin *in vitro* response rates in Kenyan *P.f.* isolates. (cyan) triple *dhfr* mutant, (purple) double *dhfr* mutant I (yellow) single *dhfr* mutant, (black) double *dhfr* mutant II, (grey) 3D7 and FCR3. IC_{50} values for each isolate were calculated from at least three independent experiments and are shown in µM on the y-axis. The isolates are sorted on the x-axis by increasing IC_{50} values. AQ is the abbreviation for samples originating from the amodiaquine study and AK for samples originating from the ACT study. The numbers indicate from which patient the isolate is adapted.The dashed black line indicates pyrimethamine peak plasma concentration, measured after a single dose of SP .

The maximum plasma concentration of pyrimethamine after a single dose of SP was estimated at 860 µg/L (35 µM) (Minzi et al, 2007). Seven out of 21 Kilifi isolates displayed IC_{50} values greater than the peak plasma concentration of pyrimethamine. Only fourteen isolates showed an IC_{50} value below that. Considering that IC_{50} values are well below the minimum inhibitory concentration (IC_{99}), it is obvious that parasites have developed high levels of resistance.

In summary, anti-folate resistance appears to be highly prevalent in Kilifi. Resistance is due to SNPs and not to CNV, which were not detected.

3.3 Induction of drug resistance *in vitro*

In the human host, parasites are exposed to a variety of factors determining the parasite's survival and, its propagation. The immune status and the genetic disposition, pharmacokinetic properties and potency of the drug are important determinants. The complex interactions between these factors make it difficult to assign causes and effect.

To directly study the impact of a drug on the parasite and its ability to adapt and escape drug pressure, I performed a drug pressure experiment as described in 2.2.3.5.

3.3.1 Drug pressure experiments *in vitro*

There are two well-described genetic mechanisms for the development of drug resistance in *Plasmodium falciparum*: amplification and single point mutations at gene loci coding for drug target or drug transporter proteins. Thus far, both mechanisms have been regarded as entirely independent outcomes of selection. In the present work I studied the relationship between these two mechanisms. The results presented in this chapter strongly suggest that gene amplification is an important intermediate step that accelerates the acquisition of single point mutations.

This question was addressed with the development of anti-folate resistance *in vitro* in the two parasite strains 3D7 and FCR3. I have confirmed that *gch*, the first enzyme of the folate pathway, is amplified in some lab strains (Figure 3-9). In contrast to data from Thailand I did not find evidence of amplification in our set of samples from Kilifi (Figure 3-10). Downstream of *gch*, the pyrimethamine drug target *dhfr* confers resistance to pyrimethamine by a series of three to four single point mutations in a step-wise manner (Sirawaraporn et al, 1997).

3D7 and FCR3 were subjected to increasing pyrimethamine pressure over a period of 10 months. Gene expression analysis was performed, parasite genomic DNA was analysed for gene amplification and emergence of single point mutations. Phenotypically the parasites were analysed in *in vitro* growth inhibition assays.

3.3.1.1 Phenotypic analysis *in vitro* drug response rate after adaption

Two laboratory strains 3D7 and FCR3 and three Kilifi isolates (AQ 84, AQ 86 and AQ 104) were subjected to sequentially increased pyrimethamine pressure over a period of 10 months. The experiment started with pyrimethamine concentration of 20 nM and was then stepwise increased up to 1600 nM. The protocol is described in detail in chapter 2.2.3.5.

Phenotypic characterisation was performed at baseline and whenever parasite replication rates had adapted to 200 nM ($3D7^{200nM}$, $FCR3^{200nM}$), 800 nM ($3D7^{800nM}$, $FCR3^{800nM}$) and 1600 nM ($3D7^{1600nM}$, $FCR3^{1600nM}$) of pyrimethamine in the medium. The IC_{50} values for chloroquine, pyrimethamine, cycloguanil and trimethoprim were determined (Figure 3-17, Figure 3-18, Figure 3-19 and Figure 3-20).

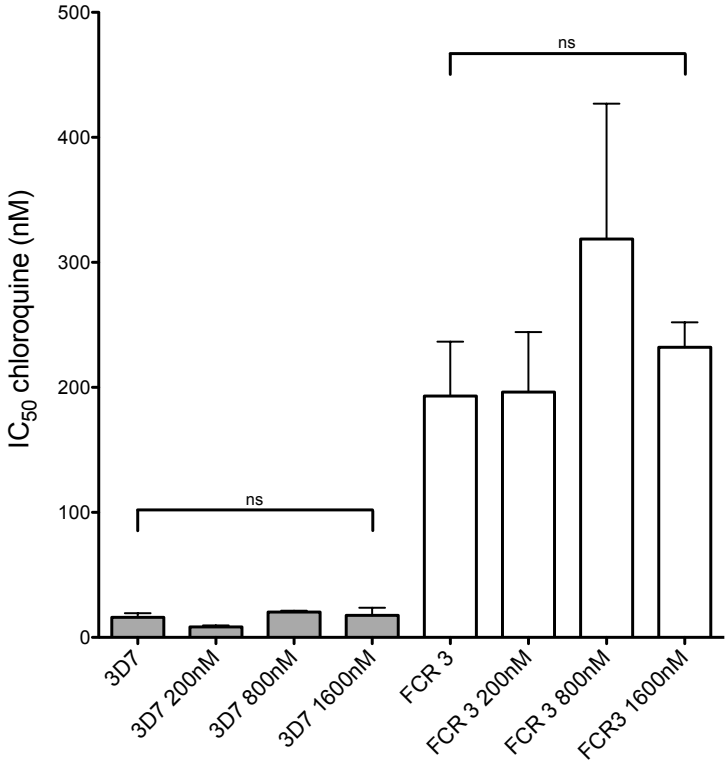

Figure 3-17 *In vitro* Chloroquine response rates during and after drug pressure experiment of 3D7 and FCR3. Both strains were adapted to 200 nM, 400 nM, 800 nM and 1600 nM (x-axis) of pyrimethamine in a step-wise manner. IC_{50} (y-axis) for chloroquine were measured at each pyrimethamine concentration. (grey) 3D7, (white) FCR3. Each bar represents the mean with standard deviation of at least three independent experiments.

As expected, pyrimethamine drug pressure did not affect the responsiveness against chloroquine (Figure 3-17 and Table 3-2) demonstrating that the resulting resistant phenotype was a specific response to selection with pyrimethamine.

IC_{50} values for the three anti-folates pyrimethamine, cycloguanil and trimethoprim correlated with rising drug pressure. 3D7 and FCR3 parasite strains not only lost their responsiveness against pyrimethamine to which they had been exposed but also to

trimethoprim (Figure 3-19 and Table 3-2). 3D7 also became resistant to cycloguanil (Figure 3-20 and Table 3-2). This points clearly towards a mechanism of cross-resistance, as none of the parasites have to the best of my knowledge ever been exposed to cycloguanil and trimethoprim.

The IC_{50} value for pyrimethamine dramatically increased during the drug pressure experiment, for both lines. The values are plotted in Figure 3-18 and listed with standard deviation in Table 3-2. In 3D7 a 10-fold increase of IC_{50} values was observed from baseline to $3D7^{200nM}$, a 250-fold increase from baseline to $3D7^{800nM}$ and a 330-fold increase from baseline to $3D7^{1600nM}$. In FCR3 a 4-fold increase of IC_{50} values was observed from baseline to $FCR3^{200nM}$, a 56-fold increase from baseline to $FCR3^{800nM}$ and a 86-fold increase from baseline to $FCR3^{1600nM}$.
From these results, I concluded that the relationship between drug pressure and decreased responsiveness was not linear and that it may be better characterised by an exponential dose-response equation.

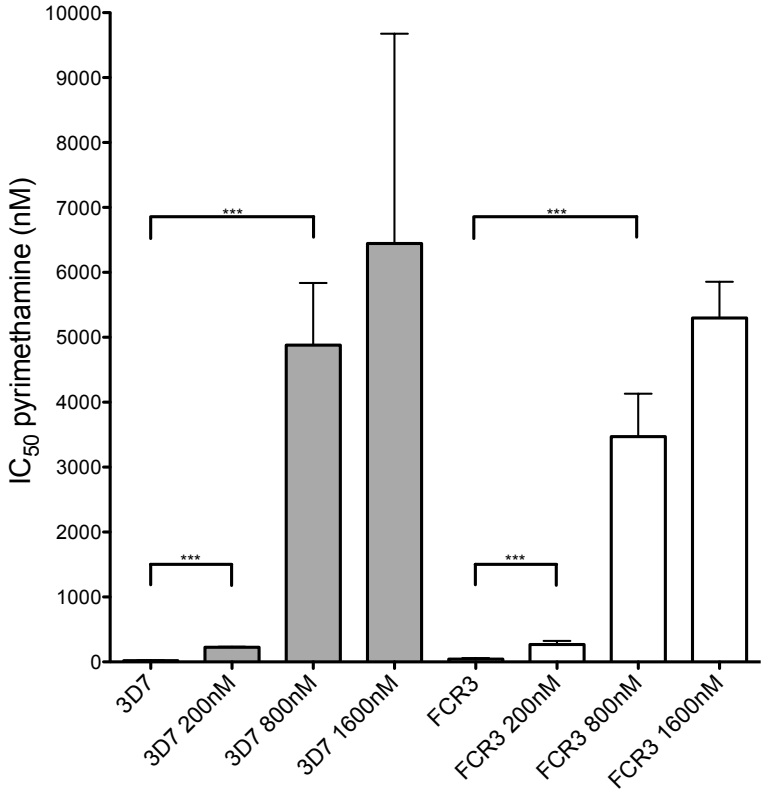

Figure 3-18 *In vitro* pyrimethamine response rates during and after drug pressure experiment of 3D7 and FCR3. Both strains were adapted to 200nM, to 400nM, to 800nM and to 1600nM (x-axis) of pyrimethamine in a step-wise manner. IC_{50}s (y-axis) for pyrimethamine were measured at each pyrimethamine concentration. (grey) 3D7, (white) FCR3.

In the following it is shown that a cross-resistance with the two anti-folates, cycloguanil and trimethoprim, was generated in the selection process. Not only the IC_{50} values for pyrimethamine, the drug the parasite have been exposed to increases significantly but also the sensitivity against the two anti-folates cycloguanil and trimethoprim, decreased significantly. This is demonstrated by the increased IC_{50} values for the two drugs.

The results for trimethoprim (Figure 3-19) are presented in this paragraph. Exact values are listed in Table 3-3. In 3D7 a 5-fold increase of IC_{50} values was observed from baseline to $3D7^{200nM}$, a 22-fold increase from baseline to $3D7^{800nM}$ and a 21-fold increase from baseline to $3D7^{1600nM}$. In FCR3 a 3-fold increase of IC_{50} values was observed from baseline to $FCR3^{200nM}$, a 35-fold increase from baseline to $FCR3^{800nM}$ and a 36-fold increase from baseline to $FCR3^{1600nM}$.

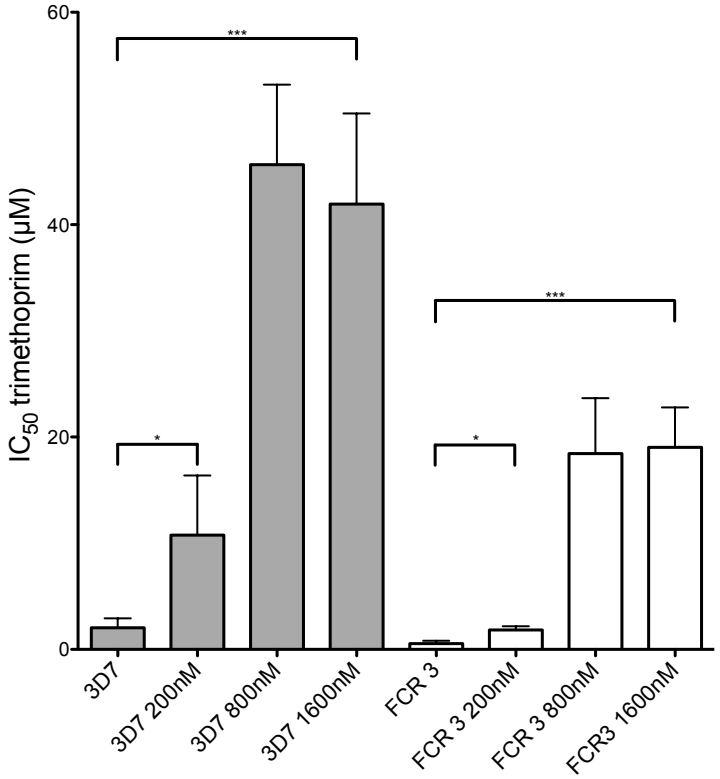

Figure 3-19 *In vitro* trimethoprim response rates during and after drug pressure experiment of 3D7 and FCR3. Both strains were adapted to 200nM, to 400nM, to 800nM and to 1600nM (x-axis) of pyrimethamine in a step-wise manner. IC_{50} (y-axis) for trimethoprim were measured at each pyrimethamine concentration. (grey) 3D7, (white) FCR3.

In Figure 3-20 IC_{50} values of cycloguanil for 3D7 are shown before and after the exposure to pyrimethamine. Exact values with standard deviation are listed in Table 3-2. In 3D7 a 9-fold increase of IC_{50} values was observed from baseline to $3D7^{200nM}$, a 28-fold increase from baseline to $3D7^{800nM}$ and a 3-fold increase from baseline to $3D7^{1600nM}$. The IC_{50} for cycloguanil could not be measured in FCR3 parasites, as the baseline parasite population was already highly resistant to this drug (Figure 3-15). The exposure to the anti-folate pyrimethamine for several months further increased the resistant phenotype until the value lied outside of the measurable range of the assay.

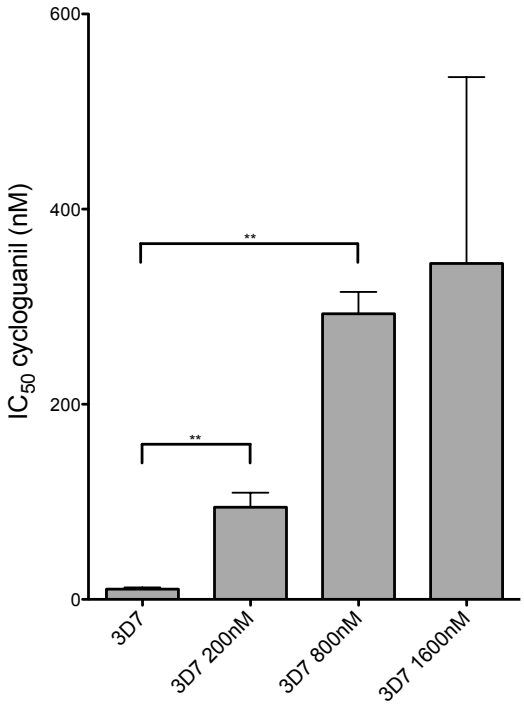

Figure 3-20 *In vitro* cycloguanil response rates during and after drug pressure experiment of 3D7. 3D7 was adapted to 200nM, to 400nM, to 800nM and to 1600nM (x-axis) of pyrimethamine in a step-wise manner. IC_{50} for cycloguanil (y-axis) were measured at each pyrimethamine concentration.

In summary the results show a high degree of cross-resistance for the 3 anti-folate drugs. The increase of the IC_{50} values for pyrimethamine is most impressive with a >300-fold increase in 3D7. The cross-resistance for cycloguanil and trimethoprim is less developed (20- to 36-fold).

Table 3-2 IC_{50} values for 3D7 and FCR3 before and during drug pressure experiment. Values were measured at baseline, 200nM, 800nM and 1600nM for chloroquine (CQ), pyrimethamine, cycloguanil and trimethoprim. (n.a.) not available.

	3D7			
	CQ (nM)	Pyrimethamine (nM)	Cycloguanil (nM)	Trimethoprim (nM)
Baseline	16.12 ± 3.30	19.3 ± 7.1	10.59 ± 1.73	2031 ± 890.1
200nM	8.45 ± 1.17	225.9 ± 9.1	94.4 ± 15.1	10759 ± 5628
800nM	20.25 ± 1.14	4880 ± 958	293 ± 22	45645 ± 7541
1600nM	17.64 ± 6.15	6446 ± 3230	344 ± 191	41934 ± 8541
	FCR3			
Baseline	193.1 ± 43.45	61.37 ± 31	3630 ± 1163	533 ± 265
200nM	196 ± 48	268 ± 55	n.a.	1831 ± 355
800nM	319 ± 153	3470 ± 663	n.a.	18436 ± 5233
1600nM	232 ± 40	5297 ± 560	n.a.	19032 ± 3758

In the following paragraphs the results obtained from the *in vitro* drug pressure experiment are compared with parasites isolates from Kilifi, Kenya with different *Pfdhfr* hapolytpes. For this purpose 3 isolates were chosen with a constant replication rate in cell culture and a consistent phenotype correlating to three different *Pfdhfr* haplotypes. AQ 84, AQ 86 and AQ 104 were found to be suitable for the analysis. The isolate AQ 84 represents the group with a triple mutant (N51I, C59R and S108N), the isolate AQ 86 is an example with a single mutant (S108N), and AQ 104 shows the phenotype of a double mutant (N51I and S108N). None of them showed any copy number variation in the *Pfdhfr* (Figure 3-12) and *pfgch* (Figure 3-10).

The IC_{50} values were plotted separately for each drug for better comparison (Figure 3-21). It can be seen that IC_{50} values of the drug-exposed parasites are comparable to IC_{50} values of AQ 86, which harbours only one *dhfr* SNP. The Kilifi isolates carrying two or more mutations exhibit higher resistant phenotypes for pyrimethamine, cycloguanil and trimethoprim than the isolate AQ86 and $3D7^{1600nM}$ and $FCR3^{1600nM}$.
Two explanations are conceivable. First, it could be that 3D7 and FCR3 were exposed to lower drug pressure during the *in vitro* (1.6µM) experiment compared to Kilifi isolates *in vivo*. The peak plasma concentration of pyrimethamine after a single dose of SP (Fansidar®) was estimated 35µM (Minzi et al, 2007). The observed discrepancy between the IC_{50} values of the Kilifi isolates and the resistance-induced

parasites could therefore be explained by the difference of applied drug concentration. Then 3D7^{1600nM} and FCR3^{1600nM} have to be regarded as intermediate phenotype before the acquisition of a highly resistant phenotype. Or secondly, differences in the genetic background between the Kilifi isolates and the laboratory strains (3D7 and FCR3) limit the development of high anti-folate resistance *in vitro*.

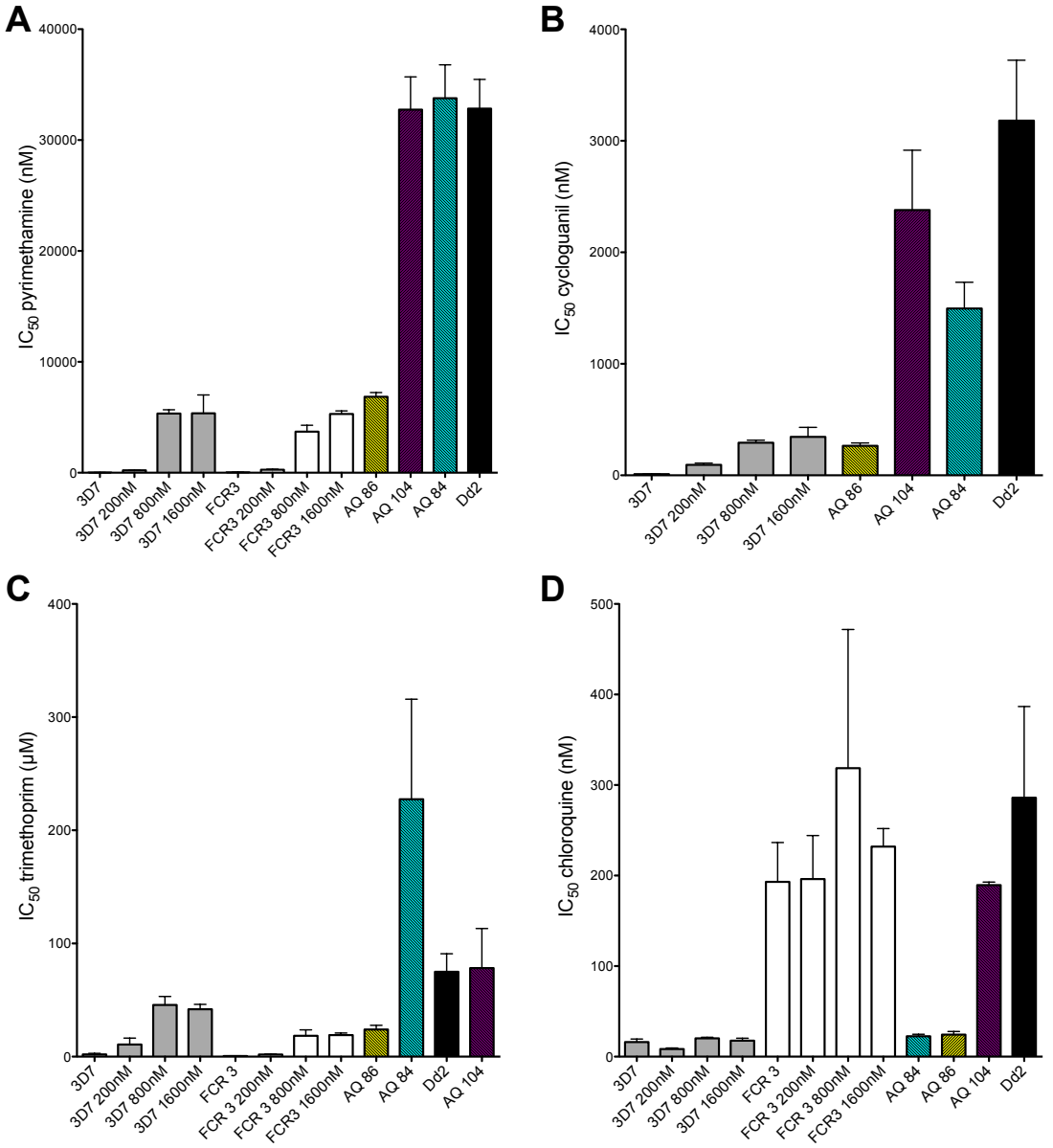

Figure 3-21 IC_{50} values in comparison to Kilifi isolates with four different *Pfdhfr* haplotypes. A) pyrimethamine B) cycloguanil C) Trimethoprim D) Chloroquine. (grey) 3D7 and (white) FCR3. The coloured bars show IC_{50} of field isolates without being exposed to drug pressure and with different SNP combinations. (cyan) triple mutant *dhfr*, AQ 84 (N51I, C59R, S108N), (pink) double mutant *dhfr*, AQ 104 (N51I, S108N), (yellow) single mutant AQ 86 (S108N), (black) rare double mutant Dd2 (C59R, S108N).

3.3.1.2 Expression analysis of folate enzyme in the resistant strains

Parasites adapted to pyrimethamine were subjected to an expression analysis of the five enzymes of the folate pathway. A real time PCR assay was used and the methodology is described in detail in chapter 2.2.1.13. Parasites (baseline and $3D7^{200nM}$/$FCR3^{200nM}$) were synchronised and then harvested at trophozoite stage with 10% parasitaemia. mRNA was isolated, treated with DNase and cDNA synthesised for a quantitative real time PCR assay. To exclude genomic DNA contamination, a negative control with only mRNA was always run in parallel and the results were only analysed if no signal was detected in these samples. *Ptps* was never detected in the expression analysis (Figure 3-22). This may have been due to very low to absent expression in the trophozoite stage. Technical problems can be excluded, as the designed *ptps* probe produces a strong signal on genomic DNA (data not shown) and the same cDNA successfully served as template for the expression analysis of the four other enzymes. *Gch* and *dhps* showed minor fluctuation in expression (Figure 3-22). *Dhfs*, the enzyme which catalyses the step in the folate pathway prior to *dhfr,* gave inconsistent results. Some, but not all runs indicated an elevated expression in lab and field strains (data not shown), when cultured in the presence of pyrimethamine (Figure 3-22). I therefore focused my investigations on *dhfr* as this enzyme displayed the most dramatic and consistent changes in the level of expression (Figure 3-22). In $3D7^{200nM}$ and $FCR3^{200nM}$ a twelve and thirteen fold increase of *dhfr* expression in comparison to baseline was observed.

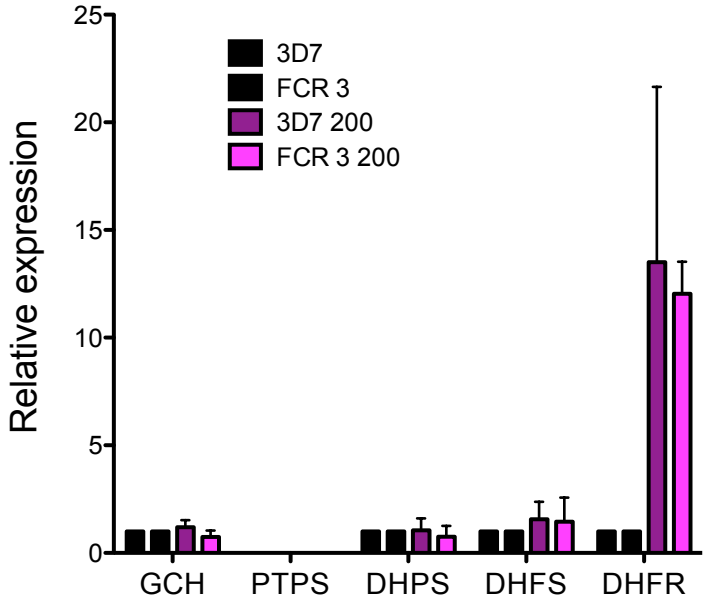

Figure 3-22 Expression analysis of folate enzymes in resistant and baseline parasites. (black) baseline parasite population 3D7 and FCR set one by definition, (purple) $3D7^{200nM}$, (magenta) $FCR3^{200nM}$. Values were determined with real time PCR in reference to baseline and with the internal control β-tubulin.

3.3.1.3 Copy number determination

As shown in the previous paragraph (3.3.1.2) *dhfr* displayed a dramatic increase of expression in pyrimethamine drug pressure-adapted parasites. I then asked whether this was due to heritable or simply transient transcriptional activation. Copy number variations (CNV) were studied for four of the five genes in the folate pathway. I could not measure genomic copies of *dhfs* since the Taqman probe was intron spanning and therefore unsuitable for genomic DNA analysis. The copy numbers were determined in reference to Dd2, D10 and to 3D7 and FCR3 baseline. Presented are the results obtained in reference to Dd2 (*gch*) and in reference to baseline (*dhfr*). As internal control served the gene PF10_0084 coding for β-tubulin.

I could not detect CNVs at *gch* (Figure 3-23), *ptps*, and *dhps* during the drug pressure experiment (data not shown). In addition to 3D7 and FCR3, the three Kilifi isolates, AQ 84, AQ 86 and AQ 104, grown in 400nM, 800nM and 1600nM of pyrimethamine, are also plotted on the graph. In none of the measured strains, the *gch* copy number varied in relation to drug pressure.

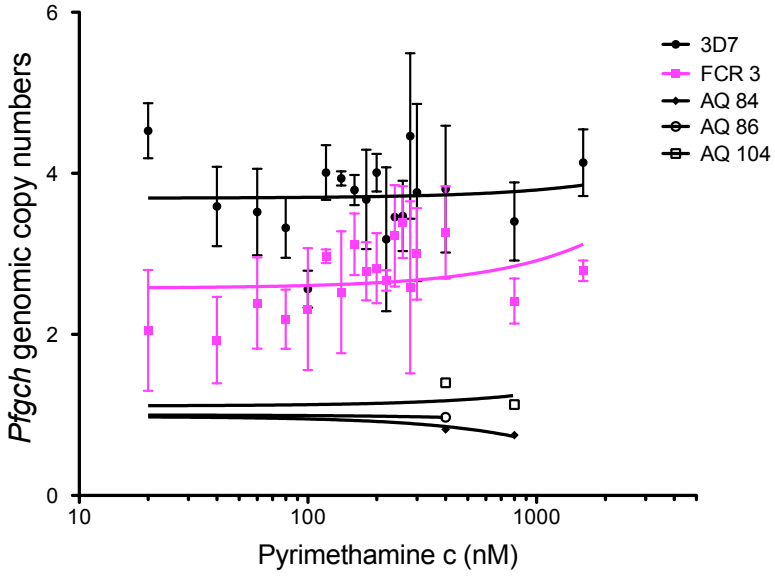

Figure 3-23 Variation of *Pfgch* copy numbers with increasing pyrimethamine concentration in the medium. Real time PCR results are shown from three independent experiments with standard deviation. (black circle) 3D7, (magenta square) FCR3, (diamond) AQ 84, (clear circle) AQ 86, (clear square) AQ 104.

In stark contrast copy numbers of *dhfr* increased significantly with increasing drug concentrations (Figure 3-24) indicating that elevated gene expression is mainly regulated by gene copy variation as opposed to differential transcriptional control. The results are shown for 3D7 and for FCR3 in Figure 3-24. In $3D7^{1600nM}$ the *dhfr* is amplified > 30 fold, in $FCR3^{1600nM}$ only 9 fold at the same pyrimethamine concentration. First evidence for amplification was detected at pyrimethamine concentration of 100 nM, i.e. after 10 weeks of drug pressure. This finding is consistent with existing literature (Thaithong et al, 2001). Once amplification was introduced in the population, additional copies were integrated within two weeks when the pyrimethamine concentration was further elevated. Various mechanisms for gene duplication have been proposed but all involve a step in which homologous sequence regions or repeats of all sorts play a major role.

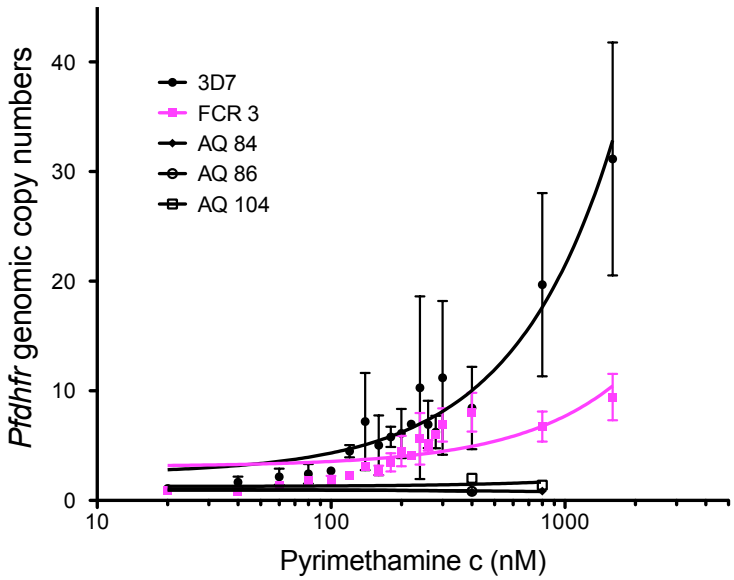

Figure 3-24 Variation of *Pfdhfr* copy numbers with increasing pyrimethamine concentration in the medium. Real time PCR results are shown from three independent experiments with standard deviation. Copy numbers were calculated in reference to baseline copy numbers of each strain, which is set at one. (black circle) 3D7, (magenta square) FCR3, (diamond) AQ 84, (clear circle) AQ 86, (clear square) AQ 104.

When comparing the relative expression (Figure 3-22) with genomic copy numbers, I found that on average each additional copy generated two and three surplus transcripts in 3D7 and FCR3 respectively. $3D7^{200nM}$ harbours 6.1 genomic *dhfr* copies and expresses 13.5 *dhfr* transcripts, whereas $FCR3^{200nM}$ carries 4.5 genomic copies

and expresses 12 transcripts, when baseline expression and copy numbers are set to one. The expression data are very preliminary and will have to be confirmed (also at different pyrimethamine concentrations), but if FCR3 requires fewer genomic copies to exhibits similar expression levels, this could explain the observed discrepancy in *dhfr* copy numbers between 3D7 and FCR3 (Figure 3-24).

Since I had determined *in vitro* growth inhibitory concentrations (3.3.1.1), the exact relationship between copy numbers and IC_{50} values could be investigated. As shown in Figure 3-25 there was evidence for a linear correlation in both strains. The slope in 3D7 (0.004) was steeper than in is FCR3 (0.001). Table 3-3 summarises these findings.

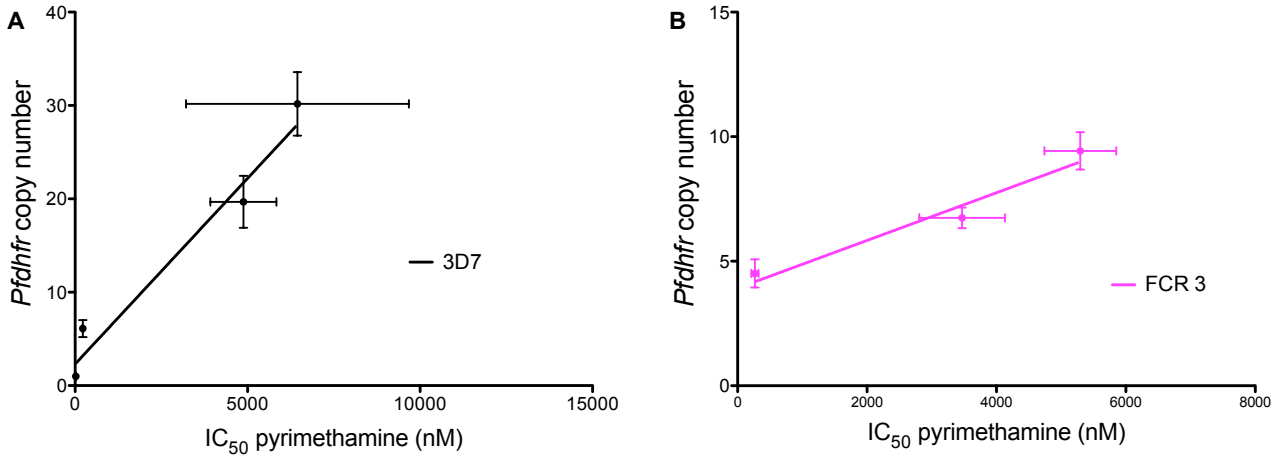

Figure 3-25 Correlation of copy numbers (*dhfr*) and pyrimethamine IC50 values. 3D7 and FCR3 copy numbers were plotted against the respective IC_{50} values determined at the same concentration.

Table 3-3 Relative increase of copy numbers and IC_{50} values compared to baseline. The values listed in this table are relative IC_{50} and copy number values.

	3D7		FCR3	
	IC50	*Pfdhfr* copies	IC50	*Pfdhfr* copies
Baseline	1	1	1	1
200nM	11 x	6.1 x	4 x	4.5 x
800nM	253 x	19.6 x	56 x	6.7 x
1600nM	335 x	31.15 x	86 x	9 x

3.3.1.4 Evidence for the emergence of resistant S108N mutation in amplified *Pfdhfr* locus

It has previously been shown that the appearance of serine to asparagine mutation at codon position 108 is the first step to the development of double and triple mutant *dhfr* (Cowman et al, 1988). I therefore analysed genomic DNA in regular intervals for the emergence of this point mutation. The emergence of S108N could easily be monitored with a restriction digest (*AluI*) over night of previously amplified region of the *DHFR* sequence. The methods are described in detail in chapter 2.2.1.14. *Alu I* recognises and cuts the double stranded DNA with the sequence AGCT. The wild type, pyrimethamine sensitive allele of *dhfr* carries a G at the nucleotide position 323 (codon position 108). If guanine is replaced by adenine, the amino acid serine (AGC) is also replaced by asparagine (AAC). In this case the DNA sequence remains uncut by the restriction enzyme *Alu I*. This undigested fragment is seen in a week band, framed by a red box, in the four restriction digests represented in Figure 3-26.

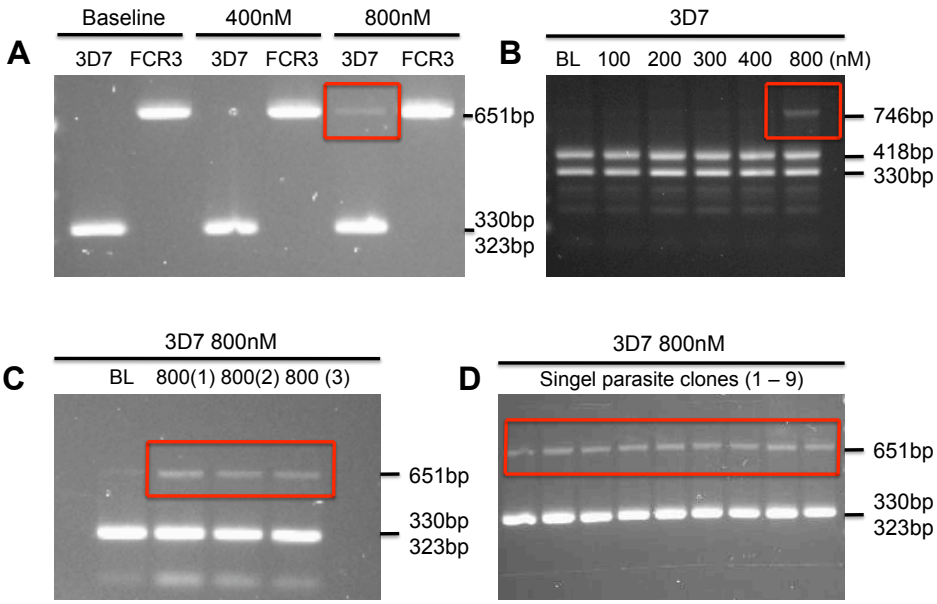

Figure 3-26 *AluI* restriction analysis of previously PCR amplified *dhfr* fragment. *Pfdhfr* SNP forward and *Pfdhfr* SNP reverse were used in the PCR reaction and the restriction digest was performed with *Alu I* over night to ensure complete digest. A) 3D7 and FCR3 at baseline and to 400nM and to 800nM pyrimethamine adapted parasites. B) 3D7 at baseline (BL) and at concentrations from 100 to 800nM of pyrimethamine. Primer pairs: *dhfr* 5' UTR for and *dhfr* SNP rev were used in this analysis creating two fragment with different sizes, when cut with *Alu I*. C) 3D7 baseline (BL) and three 800nM parasite population. D) 3D7, nine parasite clones adapted to 800nM were analysed. Undigested *dhfr* fragments, indicating a mutation at position 323 in *dhfr*, are framed in red.

In panel **A)** it is demonstrated that *Alu I* never cuts the *dhfr* locus of FCR3 (alternative wild type sequence ACCT, S108T) and that the *dhfr* of 3D7 and $3D7^{400nM}$ (wild type sequence AGCT) is completely cut by *AluI*. Only in $3D7^{800nM}$ parasites a small, undigested fraction remains (red frame). In panel **B)** the frame shows that the mutation only appeared when the parasites were exposed to 800nM of pyrimethamine in the medium. In panel **C)** the equally faint band in the three frames shows that the number of parasites carrying the mutation does not increase over time. The genomic DNA isolated from the culture was taken, once the parasites had adapted to 800nM of pyrimethamine in the culture and showed a constant replication rate (1), 48 hours later (2) and 120 hours later (3) than the first appearance of the mutation. No significant increase is observed. The thickness of the undigested product does not change over time. To investigate whether only a small subpopulation carried the newly acquired mutation, the parasite population was cloned out via serial dilution. All the nine recovered clones shown in panel **D)** harbour the newly arisen mutation at the codon position 108, conferring higher pyrimethamine resistance.

To rule out the possibility of undigested fragments due to loss of enzyme activity over time, the band was excised from the gel, purified, amplified with PCR and sequenced by standard Sanger method. This was done for the baseline parasite population 3D7, $3D7^{200nM}$, $3D7^{400nM}$, $3D7^{800nM}$ and $3D7^{1600nM}$.

The sequencing reaction proved that a nucleotide exchange from adenine to guanine at position 323 in the *dhfr* gene had indeed occurred. It also confirmed that the mutation first appeared in the 800nM adapted parasites and persisted in the 1600nM adapted parasite population (Figure 3-27**)**. Electropherograms of sequences obtained from 3D7, $3D7^{200nM}$, $3D7^{300nM}$, $3D7^{400nM}$, $3D7^{800nM}$ and $3D7^{1600nM}$ clearly demonstrated that the nucleotide was replaced in $3D7^{800nM}$ and $3D7^{1600nM}$. The still detectable adenine originates from the undigested wild type allele. Sequencing of the *dhfr* locus of parasites adapted to 300nM and 400nM (data not shown) of pyrimethamine showed the same results as wild type 3D7 and $3D7^{200nM}$ (Figure 3-26).

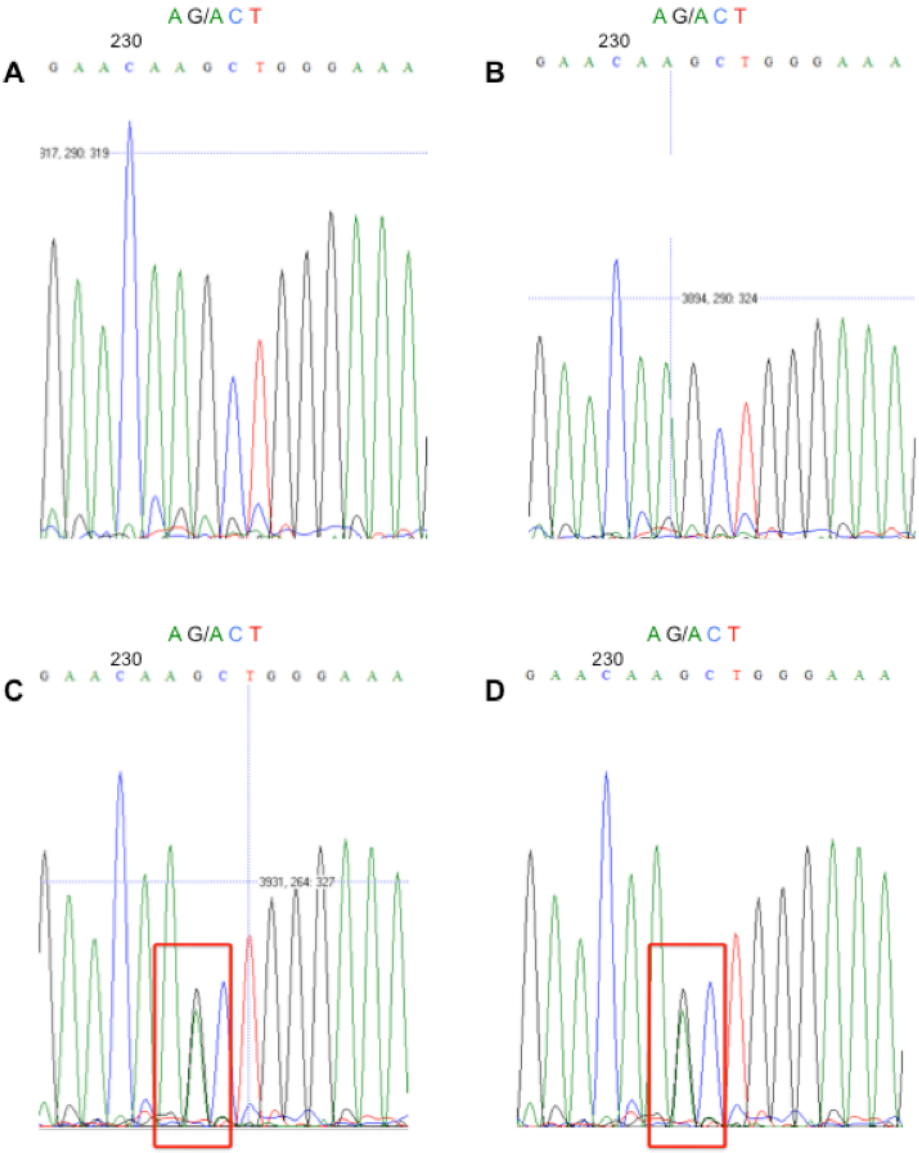

Figure 3-27 Electropherogram of sequencing reaction of *dhfr* (nucleotides 227 – 241). A) 3D7 baseline parasites B) 3D7 200nM adapted C) 3D7 800nM adapted D) 3D7 1600nM adapted. Baseline 3D7 parasites (A) and 200nM (B) adapted show a single clear green peak at position 323. In panel C) and D) a double peak consisting of a green and a black peak indicate that a guanine replaced the adenine at position 323 (framed in red).

I then attempted to quantify the number of mutated *dhfr* copies in the parasites population and in individual parasites. The *dhfr* locus was first amplified in $3D7^{800nM}$ and cloned-out-$3D7^{800nM}$ parasites with a PCR reaction and cloned in the TOPO vector (methods described in detail in chapter 2.2.2). After colony screening for integration of the insert, the PCR product of single colonies were subjected to *AluI* restriction digest. An example is shown in Figure 3-28.

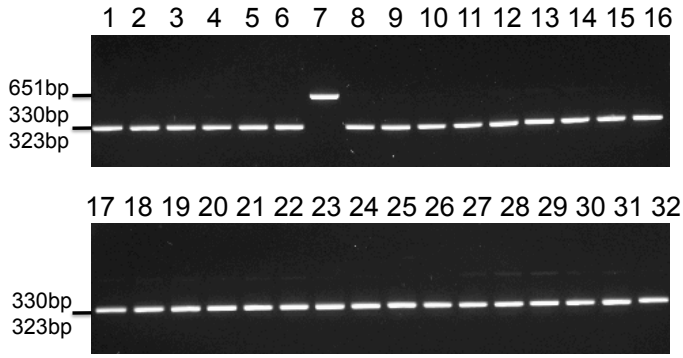

Figure 3-28 Restriction analysis of colony screening of *dhfr* cloned in the TOPO vector. 32 bacterial colonies were screened with PCR and analysed with *AluI* restriction enzyme.

It was possible to detect colonies, which remained uncut and thus confirmed again the mutation at nucleotide position 323. However, the quantification gave inconsistent results and was therefore abandoned. Possibly too many PCR steps biased the outcome. A plasmid preparation was performed but *Alu I* cuts the TOPO vector at multiple sites and therefore, a direct analysis of purified plasmids without additional PCR amplification or excision of the insert from the gel was not feasible. Excision from gels is not a suitable method for large-scale analysis, which would be needed for quantification.

In summary, it was shown that mutation S108N was introduced in the population once the gene copy number of *dhfr* had increased significantly. Recently it has been reviewed and hypothesised that gene amplification might accelerate the rate of acquisition of antibiotic resistance in bacteria (Sandegren, 2009). Here, I presented first evidence that a similar mechanism operates in *P. falciparum*. It also highlights the remarkable plasticity of adaptive genetic mechanism in *Plasmodium*.

3.3.1.5 Amplicon size determination and characterization

In the process of gene amplification, surrounding sequences and potentially whole genes will be co-amplified. To address this question, the amplified locus containing the *Pfdhfr* gene of the anti-folate resistant 3D7 and FCR3 strains was further analysed during the whole selection experiment. Two different methods were used. Genomic DNA surrounding the *dhfr* gene of resistant parasite lines was first analysed by real time PCR assay. Secondly after treatment with restriction enzymes, I analysed by southern blot (2.2.1.15). To reveal possible double strand break points in the genomic DNA I used standard PCR and sequencing methods.

Genomic DNA was isolated from parasite cultures at different time points and pyrimethamine concentrations. Real time PCR assay was performed with DNA isolated from the baseline parasite population and from parasites adapted to 200 nM, 300 nM, 400 nM, 800 nM and 1600 nM of pyrimethamine from both 3D7 and FCR3.

Quantitative real time PCR (sybr green based) assay to determine amplicon size

Genes adjacent to *dhfr* (Table 3-4 and Figure 3-29) were analysed for evidence of co-amplification with methods described in chapter 2.2.1.13. Figure 3-32 illustrate the genomic context of *dhfr*.

Table 3-4 Open reading frames with accession number and annotation from PlasmoDB surrounding the *dhfr* locus. For each of the genes at least one primer pair was designed to determine amplification in a sybr green-based real time PCR assay.

Accession Nr.	Annotation on plasmoDB
PFD0780w	glutamyl-tRNA(Gln) amidotransferase subunit A, putative
PFD0795w	conserved plasmodium protein, unknown function
PFD0810w	small GTP-binding protein sar1
PFD0815c	Conserved protein, unknown function
PFD0820w	Conserved protein, unknown function
PFD0825w	RNA-binding protein of pumilio/mpt5 family, putative
PFD0830w	bifunctional dihydrofolate reductase-thymidylate synthase
PFD0835c	LETM-like protein, putative
PFD0840w	conserved Plasmodium protein, unkown function
PFD0865c	cdc2-realted protein

As the specific primer for the genes only cover a small sequence region of the gene under investigation, the results cannot provide information on whether amplicons contain complete, i.e. functional additional gene copies.

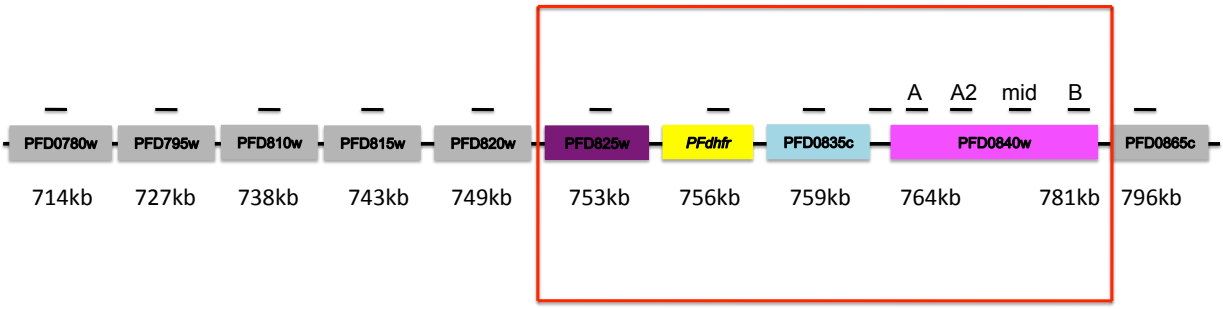

Figure 3-29 Schematic of the *dhfr* locus (plasmoDB). The boxes illustrate single genes with their accession number from PlasmoDB. (black lines) primer pair for sybr green based real time PCR assay. The values below the gene boxes indicate approximate position of the genes on the chromosomes 4 (PlasmoDB). The red box is magnified in Figure 3-30.

Figure 3-30 shows a graphic representation of the co-amplification surrounding the *dhfr* locus in 3D7, obtained in the pyrimethamine drug pressure experiment. In Figure 3-31 the graphic for FCR3 is shown. The distance on the x-axis does not represent the actual distance in kilobases on the chromosome. Distance information's are given in Figure 3-29. It is important to note, that the results obtained with this experiment are not comparable with the copy number determination in 3.3.1.3 in which a probe was used. The sybr green assay is less accurate to determine the exact copy number but identifies amplification or loss of copy.

Amplicon size determination for 3D7

Upstream of *dhfr* (PFD0830w), only the probe for the directly adjacent PFD0825w revealed co-amplification at all stages of the drug pressure experiment. Downstream of *dhfr,* the adjacent PFD0835c did not reveal gene amplification compared with baseline parasite population. Further downstream, PFD0840w A and PFD0840w A2 showed in the 5' region of the open reading frame gene amplification in reference to the baseline parasite population and at the same level as *dhfr.* PFD0840w A2 was measured only for $3D7^{800nM}$ and $3D7^{1600nM}$, which explains the straight connecting line between PFD0840w A and PFD0840w A2 for $3D7^{200nM}$, $3D7^{300nM}$ and $3D7^{400nM}$. PFD0840w A2 and PFD0840w mid are separated by a large 7980 bp fragment, the likely location of the amplicon breakpoint.

To confirm the loss of PFD0835c in the amplicon, an additional primer pair was designed in the intergenic region of PFD0835c and PFD0840w (PFD0835c – 840).

This sequence revealed also no co-amplification, suggesting an intact wild type locus. The distance between the two missing primer pairs was of 3564 bp and the distance between the next two present primers (*dhfr* and PFD0840 A) was of 7767 base pairs.

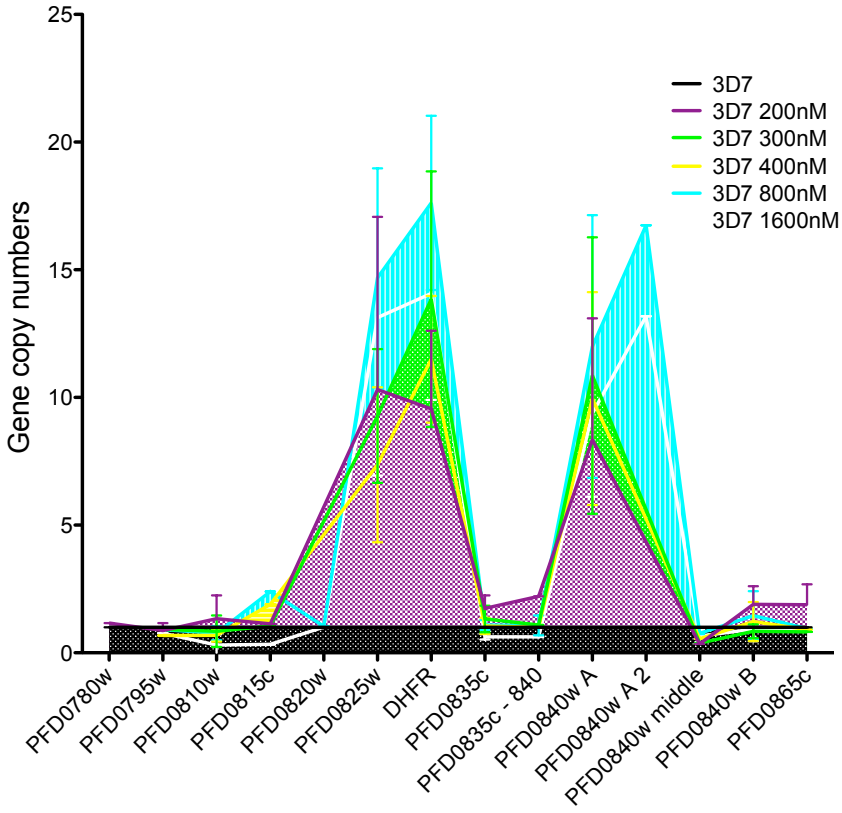

Figure 3-30 Co–amplification of genes surrounding *dhfr* locus in 3D7. On the x –axis genes adjacent to *dhfr* are ordered without representing actual genetic distances. The y –axis gives copy numbers. Values are means with standard deviations determined in at least three independent real time PCR assays. The size of the amplicon was determined for each pyrimethamine concentration, represented by different colours. The areas under the curves are filled out to illustrate the amplification. The exact breakpoints of the amplicon at the edged and in the middle for 3D7 are not shown in this figure.

Further upstream (PFD0820w, PFD0815w PFD0810w, PFD0795w, PFD0780w) and downstream (3' end of PFD0840w and PFD0865c) no evidence for gene amplifications was found. PFD0820w was only measured for $3D7^{800nM}$ and $3D7^{1600nM}$, which explains the straight connecting line between PFD0815w and PFD0825w for $3D7^{200nM}$, $3D7^{300nM}$ and $3D7^{400nM}$. The primer pairs of PFD0820w and PFD0825w are separated by 1685 base pairs in which the breakpoint most likely is situated.

Amplicon size determination in FCR3

Upstream of *dhfr* (PFD0830w), the adjacent PFD0825w and PFD0810w revealed co-amplification at all stages of the drug pressure experiment and downstream of *dhfr,* the adjacent PFD0835c showed co-amplification compared with the baseline parasite population.

Further upstream (PFD0795w and PFD0780w) and downstream (PFD0840w and PFD0865c) no evidence for gene amplification was found. These genes were found in a single copy in the genome.

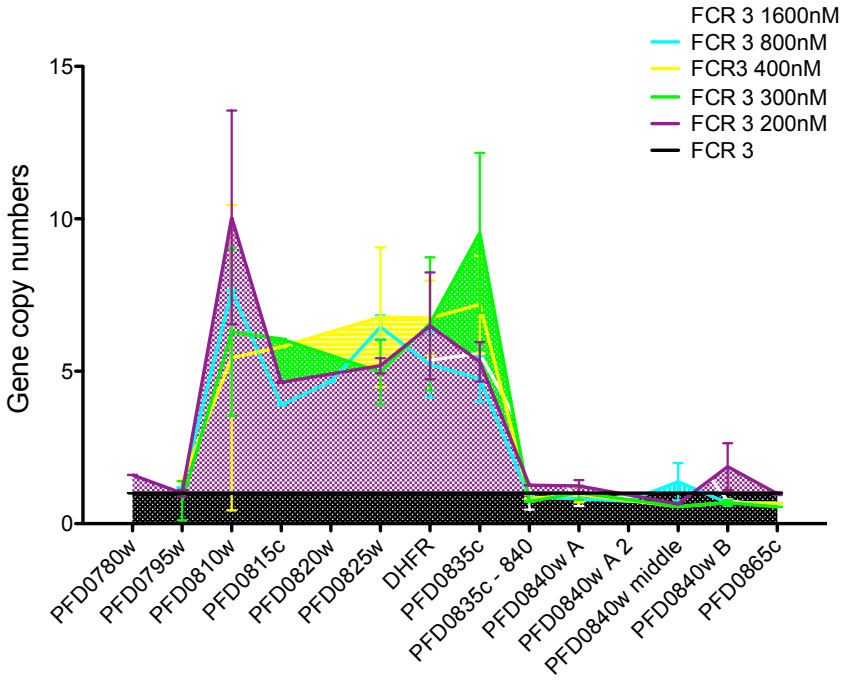

Figure 3-31 Co–amplification of genes surrounding the *dhfr* locus in FCR3. On the x – axis the neighbouring genes of *dhfr* are listed without considering the actual distance between them. On the y – axis the copy numbers of each gene in reference to its baseline are plotted. The values are means with standard deviations determined in at least three independent sybr green – based real time PCR assays. The size of the amplicon was determined for each pyrimethamine concentration, represented with the different colours. The areas under the curves are filled out to illustrate the amplification. The exact breakpoints of the amplicon at the edged are not shown in this figure.

Southern blot analysis of gDNA of 3D7 and FCR3 with amplified *dhfr* locus

A southern blot was performed to confirm the amplification of the *dhfr* locus and to further characterise the amplicon and its size in the two strains $3D7^{800nM}$ and $FCR3^{800nM}$. Figure 3-32 show a scheme of the *dhfr* locus. A small horizontal line on top of the genes represents primer pairs used to determine amplification. The two primer pairs highlighted in the red box are the ones, which did not reveal amplification in 3D7 (Figure 3-30). As a consequence restriction sites, represented with vertical coloured lines, within this region are also missing in the amplicon. For PFD0840w four primer pairs were designed (A, A2, mid and B).

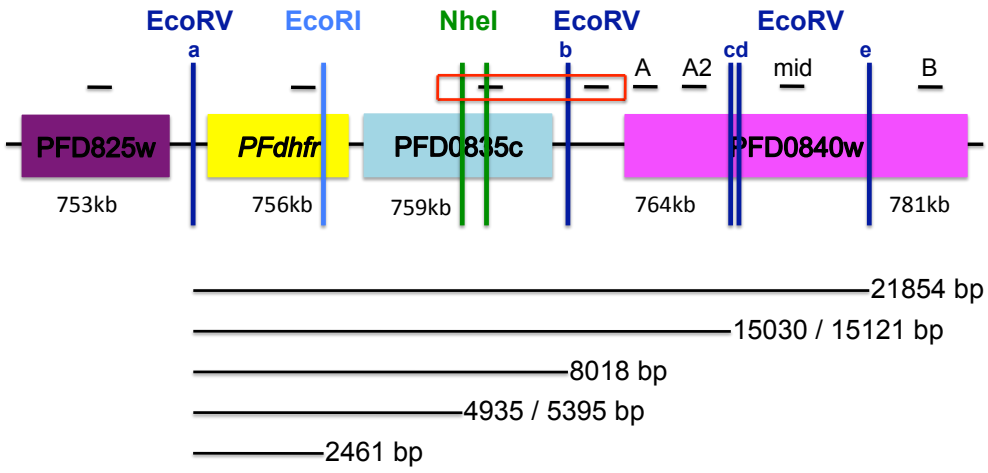

Figure 3-32 Schematic representation of *dhfr* locus. Each coloured box represents a gene with the accession number of PlasmoDB marked on it. On top of the boxes the short black lines illustrate the primer pair, which was used to determine amplification. Restriction sites of *EcoRV* (dark blue line), *EcoRI* (light blue line) and *NheI* (green line) are shown in the scheme and the black lines underneath illustrate the resulting fragment with size indication.

The southern blot was performed as described in detail in 2.2.1.15. The aim was not to detect a shift in size of the chromosomal region, but to confirm the results obtained with the sybr green based real time PCR assay. Therefore enzymes were chosen to cut within the amplicon (Figure 3-32) and thus, to produce an increase in hybridisation signal as opposed to a shift. The same amount of DNA was loaded in each lane and additionally a probe against actin (PFL2215w) was designed and synthesised to serve as loading control. Unfortunately the signal of actin was to weak (data not shown) to be detected in the conditions, used here.

Figure 3-33 shows the southern blot. The last panel confirms the amplification of the *dhfr* locus in 3D7^{800nM} and FCR3^{800nM} compared to the baseline parasite lines, untreated (-).

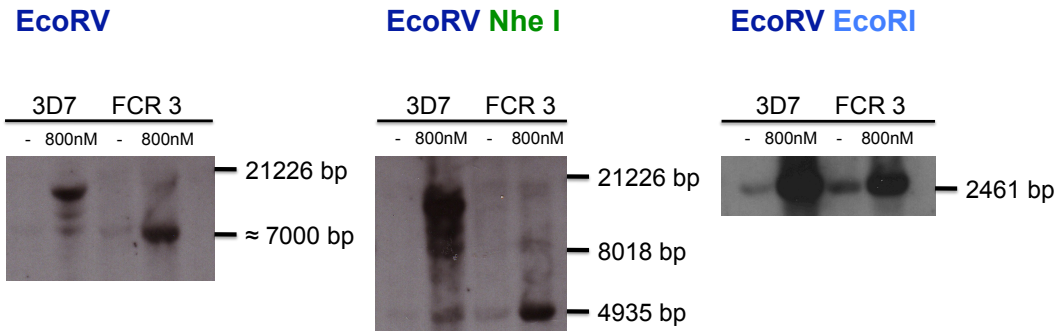

Figure 3-33 Southern blot of genomic DNA of 3D7 baseline (-) and 3D7^{800nM} and FCR3 (-) and FCR3^{800nM} digested with *EcoRV*, *EcoRV* + *NheI* and *EcoRV* + *EcoRI*. Sizes are indicated on the right hand side of each picture. The same amount (3µg) of genomic DNA was loaded in each lane, the loading control actin was not detectable (not shown).

Eco RV and Eco RI cut very close upstream of *dhfr* and at the 3' end of its open reading frame generating in both lines a fragment of 2461 bp (Figure 3-32). Fragments from parasite lines subjected to pyrimethamine pressure showed a much stronger hybridisation signal compared to unexposed parasites, thus confirming the amplification of the locus in both strains.

As the amplicons of 3D7 and FCR3 are of different sizes and composition, the analysis of the *EcoRV* and the double digest (*EcoRV* and *NheI*) will be presented in detail in the following paragraph, separately for 3D7 and FCR3, starting with FCR3.

The double digest (*EcoRV* and *NheI*) generates in FCR3 and FCR3^{800nM} a fragment of expected size (4935bp), which confirms the results obtained by real time PCR. The part of gene PFD0835c where the restriction site is located and where the real time primers were designed to bind is co-amplified in FCR3^{800nM}. The restriction analysis of *EcoRV* alone shows similar results but needs to be interpreted in consideration with the results presented in paragraph "breakpoint identification of FCR3" (see below). In this paragraph it is shown that the amplicons in FCR3 are arranged head to tail and the breakpoints were identified down to 200 base pairs. The restriction site of *EcoRV***b** between PFD0835c and PFD0840w (Figure 3-32) was found to be beyond the edges of the amplicon. Instead, another *EcoRV* restriction site (not shown) in the co–amplified PFD0810w at the 5' end of the amplicon (Figure 3-31) generates in combination with *EcoRV***a** an approximately 7200bp fragment.

This is an approximate value, generated and calculated from PCR analysis and sequencing information.
In conclusion, the southern blot experiments confirmed the real time PCR results regarding both size and composition of amplicon. However, they provide no further information on the exact genomic location of amplicons.

The amplicon arrangement in 3D7 is more intriguing. Two possible breakpoints and thus arrangements are conceivable. Assuming intact wild type locus, the amplicon could be one continuous fragment containing a gap (loss of PFD0835c), which positioned next to the wild type locus or anywhere in the genome. Alternatively, but also under the assumption of an intact wild type locus, two separate amplicons on either side of the wild type locus could generate the results obtained with the real time PCR (Figure 3-30). Three results suggest the existence of an intact wild type locus. First, the unamplified regions were detected at baseline level, proving their presence in the genome (Figure 3-30). Secondly two PCR reactions within and on one side probably beyond the unamplified region were successful proving the existence of a 6 kb segment exactly as the wild type locus (presented and discussed in detail below, Figure 3-36). Finally, the weak signal in 3D7 and 3D7^{800nM} in the southern blot at 4935 base pairs, resulting from the *EcoRV* and the *NheI* restriction analysis (Figure 3-33). The fact that this signal is one of the weaker signals in the lane of 3D7^{800nM} indicates that the wild type locus is present only once. The three upper bands of different sizes give an intense signal and are of the same size as the bands resulting from *EcoRV* restriction alone. This points toward the absence of both *NheI* restriction sites in the amplicon(s), in accordance with the real time data (Figure 3-30). As the two restriction sites are separated by only 460 base pairs, it is also very unlikely that one would be present and the other be missing.
An explanation for the three resulting bands from the *EcoRV* restriction and from the double restriction analysis of *EcoRV* and *NheI* remains to be found. The next restriction site *EcoRV* **b** is also missing in the amplified fragment (Figure 3-30 and Figure 3-32). *EcoRV* **c** and **d** are present and co – amplified and would produce a 15030 base pair long fragment. From this the lost sequence of at least 3564 bp (amplicon size determination of 3D7, see above) has to be subtracted, which would result in a fragment of 11466 bp. The size identification of the bigger fragments in the southern blot is under these conditions difficult to determine, but one of the three bands could thereby be explained. This implies that not only the wild type locus is intact, but also the existence of a single amplicon with a gap at PFD0835c and not two amplicons on either side of the wild type locus, but this is speculation and still

does not explain the remaining two fragments clearly apparent on the southern blot. Unfortunately even further PCR analysis of the breakpoints did not clarify the arrangement of this amplicon in 3D7 (shown below).

Identification of the amplicon breakpoint in FCR3

In the previous paragraph I demonstrated, that drug exposure led to amplification of *dhfr* and surrounding sequence fragments in 3D7 and FCR. However real time PCR and southern blotting only permitted an approximation of the amplicon's size. To further determine the exact location of amplicon breakpoints, I designed a set of PCR reactions (2.2.1.9) with different primer pair combinations (2.1.8.1). Sizes were estimated with the help of agarose gel electrophoresis and purified fragments were sequenced. The primers for sequencing reactions are listed in the paragraph 2.1.8.1.

Two possible arrangements of amplicons are conceivable: a head-to-tail or a tail-to-tail positioning on the chromosome. Both hypotheses were tested. Figure 3-34 illustrates a head-to-tail arrangement of two neighbouring amplicons. Coloured boxes represent genes (accession numbers) *dhfr* is highlighted in yellow. The black box shows the original chromosomal locus. If a gene amplification occurs and the newly synthesised DNA is arranged in a head-to-tail manner, the DNA fragment, shown underneath is produced. This results in a unique, newly generated sequence at the breakpoint, where a PCR reaction is possible (indicated by the red line) in the amplified but not in the wild type locus.

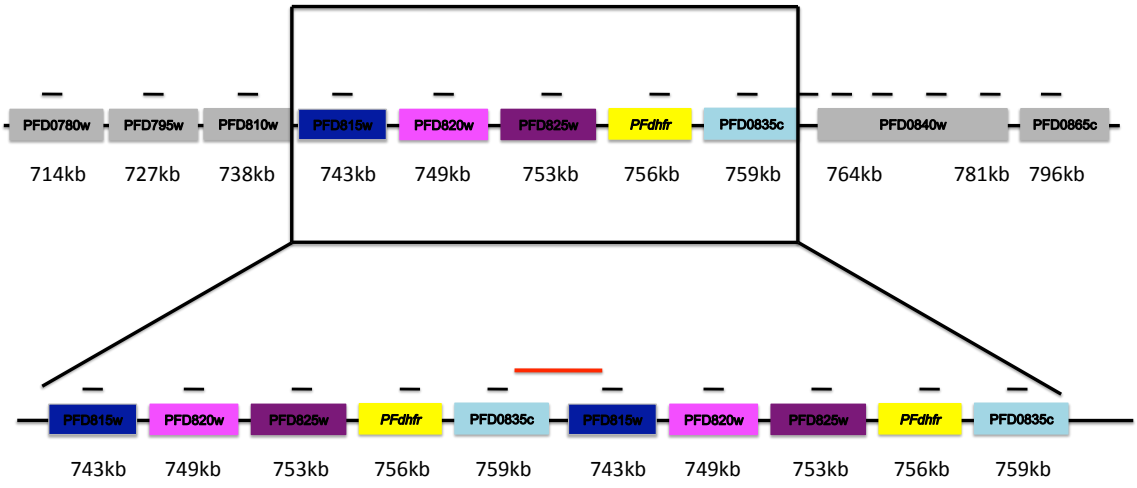

Figure 3-34 Model of amplicon arrangement in FCR3. Two FCR3 amplicons were positioned head-to-tail. The red line indicates a newly generated chromosomal sequence, which is absent in parasites with a wild type locus. A PCR reaction was successfully performed over this sequence part.

First real time PCR primers of two potentially adjacent genes were used in an attempt to amplify the breakpoint. PFD0835c is positioned on the (-) strand whereas PFD0815w is located on the (+) strand, so in both cases the reverse real time PCR primers were used. “Reverse” indicate reverse with respect to the open reading frame. Following successful amplification, I designed four additional primers to close in on the breakpoint.

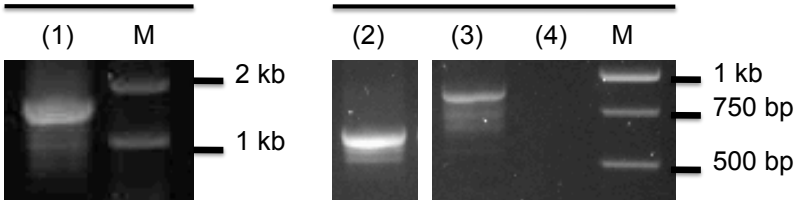

Figure 3-35 PCR analysis of FCR3^{1600nM} amplicon breakpoint.
(1) PFD0835crev and PFD0810wrev. (2) PFD0835crev/PFD0810w revnew1 (3) PFD0835c rev/PFD0810w rev new 2. (4) Negative control. The reaction was also performed for FCR3 baseline and no product was amplified (data not shown) confirming the head to tail arrangement.

The primer pairs from the real time PCR (PFD0835c and PFD0810w) amplified a product of approximately 1,5 kb (Figure 3-35 (1)), which was sequenced bidirectionally. The baseline parasite population gave no signal (data not shown). The success of amplifying a fragment with these primers supports the hypothesis of a head-to-tail conformation of the amplicon in FCR3^{1600nM}. The sequencing data showed that from PFD0835 rev on approximately 700 bp were readable and 300 bp from PFD0810w rev. Taken together these were 1000 base pairs and around 500 bp were still missing in between. In the PFD0810w a poly A stretch after 300 bp hinders the sequencing reaction and in PFD0835c the sequencing reaction reached with 700 bp already a maximum of achievable length. So the additionally designed primers were set right after the end of the already successfully identified sequences. In PFD0810w the two newly designed primer (PFD0810w rev new 1 and PFD0810w rev new 2) produced together with PFD0835c rev two products of approximately 680 bp and 850 bp (Figure 3-35 (2) and (3)). This confirms the existence of the sequence were the new primers were set. Unfortunately these products were never successfully sequenced, even though several attempts have been made. The breakpoint is probably not identical between all the amplicon or at least not as identical as a sequence reaction would require it to be. The degradation in the PCR analysis (Figure 3-35 (2) and (3)) could support this hypothesis, but this is pure

speculation. 228 base pairs separate the primer PFD0810w rev new 1 from the ATG of the gene (primer included). If the ATG is included in the amplicon and if these parasites thus carry an additional functional copy of PFD0810w is not possible to determine with these results.

In PFD0835c the two newly designed primers gave no amplification in the PCR reaction, indicating that this sequence is not part of the amplicon. Interestingly the breakpoint is approximately 300bp after the transcription start site of PFD0835c. So FCR3^{1600nM} has only amplified part of the gene but carries no additional functional copy. Interestingly 3D7 had built its amplicon around this gene (PFD0835c), suggesting that overexpression of PFD0835c might be toxic for *Plasmodium*.

As the last sequencing reaction did not succeed, the exact breakpoint could not be identified but it has to be located within these last 200 base pairs. No obvious repetitive sequences were identified within these 200 bp and an alignment of the relevant sequence part around the possible breakpoint did not reveal significant homology between the two sequences.

Identification of the amplicon breakpoint in 3D7

The results obtained from real time PCR and the southern blot for 3D7 were already more intriguing and not as conclusive as for FCR3. The identification of the breakpoint and the arrangement of the amplicon could also not be solved by standard PCR, even though numerous primer pairs were designed (2.1.8.1) and tested in various combinations (2.2.1.9).

At the edges, between PFD0820w and PFD0825w primers (named 5' in 2.1.8.1) were designed as well as between PFD0840 A2 and PFD0840w mid (named "z" in 2.1.8.1). Together with the real time primers, of which assured information of their presence or absence is available, a series of PCR reactions was performed without any positive result. A head to tail and a head to head conformation was considered. Both amplified regions on either side of PFD0835c were assumed to be independent or connected (as mentioned above) and no product was detected in the PCR reaction.

The arrangement and positioning of sequences around the unamplified region of PFD0835c remained similarly unsolved. The real time primer of *dhfr* and the PFD0840w A are separated by 8000 base pairs. Numerous primers were designed at either edge (named 3' of *dhfr* and 5' of LETM in 2.1.8.1) of the identified gap, which was found to be of at least 3500 base pairs. In case of a single amplicon, carrying *dhfr* and parts of PFD0840w, a PCR reaction over the gap should have been feasible as the fragment could only be of maximum 4500 base pairs. Specially, when primers

were designed to shorten the distance on either side, a PCR reaction was expected to work. Figure 3-36 shows the combination tested in a PCR reaction. The black lines underneath demonstrate the combinations tested without success, even when a special long range PCR Kit was used.

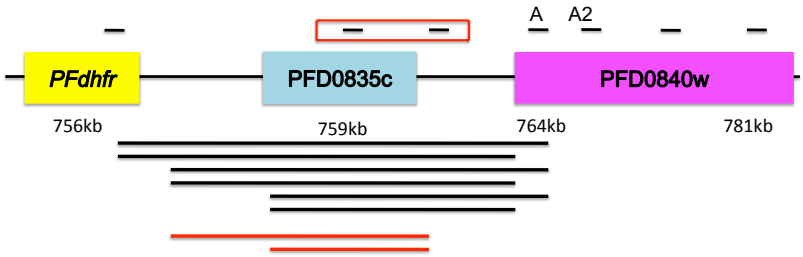

Figure 3-36 Enlarged model of *dhfr* and its downstream lying genes. (balck lines) unsuccessful PCR reactions (red lines) successful PCR reactions. (red box) unamplified region.

While these reactions never gave a signal, a reaction from a primer, designed in the gap (PFD0835c) and two others primers, 31 bp and 991 bp after the stop codon of *dhfr* were successful (Figure 3-36 red line and Figure 3-37) in 3D7 baseline (not shown) and 3D7^{800nM}. This proves that despite the amplification the wild type locus is present and intact at least once. As this is the only positive PCR result obtained, no further conclusion can be drawn from this series of analysis. From a negative PCR result, especially if it is a relatively long range PCR of over 3 kb, no assumption can be made. Various reasons are conceivable for the failing reaction, other than the simple non-existence of the sequence. Polymerases for example reach *in vitro* only a limited length before they fall of the template and the high A/T content in *Plasmodium falciparum,* particularly in intergenic regions, has to be considered, when analysing theses results. Nevertheless, it can be concluded that the wild type locus is present and intact in the strains with amplified *dhfr* and the amplicon in 3D7 seems to be arranged in a complex and unexpected way, especially when compared to FCR3. A possible explanation could be the potential toxicity of PFD0835c and its immediate proximity to *dhfr*, which renders a simple amplification of this gene with large surrounding sequence regions impossible.

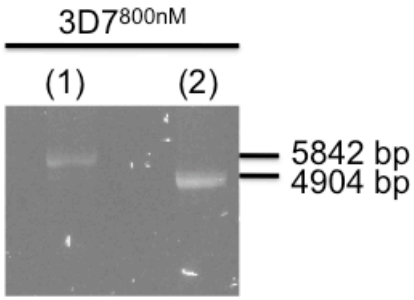

Figure 3-37 PCR analysis of 3D7^{800nM} over the gap (PFD0835c). (1) 3D7 3'for/1 LETM 5' rev (2) 3D7 3'for2/LETM 5'rev. Fragments of expected size for wild type locus

3.3.1.6 Competition

Parasites carrying mutations or chromosomal rearrangements might have to cope with a fitness cost compared to wild type parasites. To address this question wild type 3D7 cultured in a one to ten ratio in the presence of $3D7^{800nM}$ parasites for 8 weeks without drug pressure. As a control $3D7^{800nM}$ alone was also cultured without drug pressure.

In the initial phase, for up to one week after the start of the experiment $3D7^{800nM}$ parasites were dominant. However after 3 weeks the overall copy number in the co-culture was already reduced to 6. It was impossible to distinguish whether $3D7^{800nM}$ lost *DHFR* copies in the presence of wild type parasite or if they were overgrown by wild type 3D7 parasites.
In contrast $3D7^{800nM}$ cultured alone still carried all the amplified copies after 8 weeks suggesting stable integration of amplicons as opposed to episomal carriage of amplified DNA.

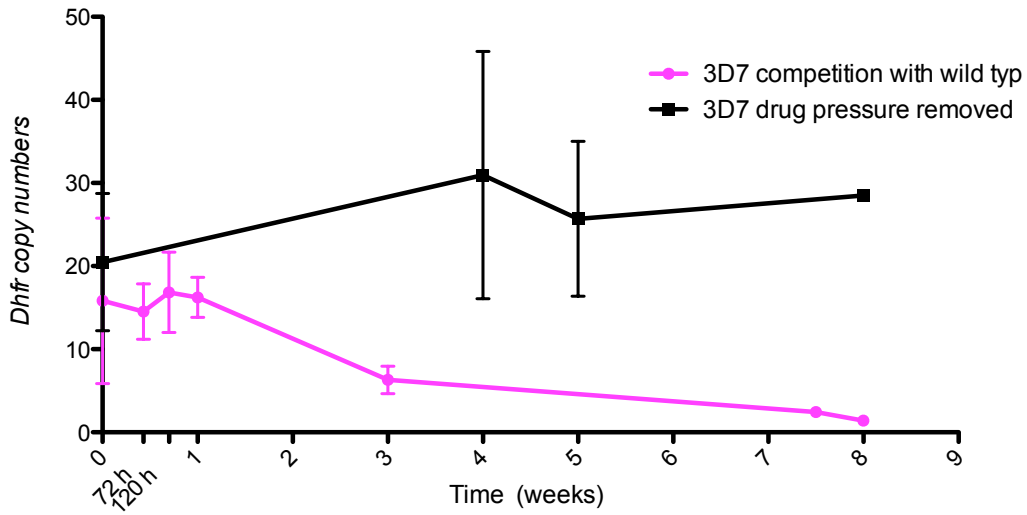

Figure 3-38 Competition and stability experiment. $3D7^{800nM}$ were cultured with 3D7 wild type starting with a 10:1 relation without pyrimethamine in the medium. Copy numbers were monitored over 8 weeks. As control $3D7^{800nM}$cultured alone also without pyrimethamine over the same period of 8 weeks.

4. Discussion

Malaria control and its elimination continue to rely on prompt and efficacious treatment of disease episodes.

The malaria parasite has evolved a remarkable capacity to adapt to new conditions, e.g. antimalarial drugs. Chloroquine was successfully employed for decades until resistance emerged first in South-East Asia and subsequently spread globally. Resistance against anti-folates developed in much shorter time and first signs of failures of newly and massively distributed artemisinin combination therapies (ACT) are already reported within 13 years of their introduction (Dondorp et al, 2009).

Because of the public health importance of drug-resistant *P. falciparum* malaria, the emergence and spread of resistance needs careful monitoring. Genetic composition and variation of parasite populations in different geographical regions is an important indication for existence and spread of resistance. However, *in vivo* and *in vitro* phenotypic analysis of parasite isolates are essential tools for confirming the emergence of drug-resistant infections.

Beside surveillance of the natural parasites population, it is equally important to understand molecular mechanism of resistance and its development. Mechanism of resistance itself can be due to various changes in the parasite. Transporters change their substrate specificity, drug targets alter their protein structure and/or increase in abundance to compensate for the effects of inhibition. All mechanisms of resistance share common features. Mutation and chromosomal rearrangements form the heritable basis of the parasite's ability to adapt. Whether these two mechanisms are independent or evolutionary related outcomes of adaptation is currently not known. A better understanding of the molecular events in the early phase of development of drug resistance is also of critical importance for improving the predictive accuracy of molecular surveillance tools in the field.

4.1 Drug parasite interaction *in vivo*

Drug sensitive parasite populations that are exposed to drugs need to ensure survival of a minimal parasite population in order to develop resistance.

In the first part of this work parasite survival and its determinants were investigated *in vivo*, i.e. in paediatric patients who received antimalarial treatment for uncomplicated *P. falciparum* malaria. Following recommendations by the World Health Organisation (WHO, 2008), drug efficacy is determined by the *in vivo* test. This tests monitors blood stage parasite recurrence by microscopic examinations of blood smears up to 84 days after start of treatment. Re-infections are distinguished from recrudescence by genotyping of highly polymorphic genomic regions, most commonly using the *msp2* locus. Sensitivity of this test remains very low and the classification of re-infection in high endemic areas is inaccurate. I attempted to study the potential for replacing long lasting and expensive follow up periods by applying a highly sensitive, *P. falciparum* asexual stage-specific reverse transcriptase PCR on a single sample taken seven days after start of treatment. Assuming a parasite reduction ratio of 10^2 to 10^5 parasites per 48 hours (White, 1997), I expected the parasite population to be detectable 7 days after start of treatment. The time point was also thought to be suitable for the analysis as it was also proposed for determination of drug plasma concentration (White et al, 2008) and sample collection could be minimized.

The rational was to detect viable asexual parasites seven days after treatment and the aim was successfully achieved with a very high sensitivity and specificity. Positive and negative results on day 7 were highly reproducible. Surprisingly, there was a poor correlation between detection of asexual parasites on day 7 as a marker of incompletely eliminated persistent blood stage infections and subsequent risk of recrudescence.

In the ACT study, in 48/105 (45.7%) samples metabolically active persistent asexual parasites were detected 7 days after start of treatment (i.e., 4 days after last dose). Persistence of infection on day 7, however, poorly agreed with subsequent recrudescence at the individual level. Twenty-nine with detectable parasite populations surviving in their blood on day 7 either cleared the parasites in the following 77 days or were re-infected, as determined by *msp2* genotyping. And 18 patients with undetectable parasite populations presented with recrudescent parasites in the following 77 days.

In the amodiaquine study arm, in 16/51 (31%) samples metabolically active persistent asexual parasites 7 days after start of treatment (i.e., 4 days after last

dose) were detected. Persistence of infection on day 7, however, also poorly agreed with subsequent recrudescence at the individual level.

There are three main possible explanations for the observed discrepancy between day 7 and subsequent recrudescence of primary infections. First, it is important to note, that no sensitive mRNA data are available for the period after day 7. Further monitoring of the parasitaemia was only performed by microscope and only if patients presented with fever in combination with a positive blood smear, DNA and RNA samples were taken, which were then analysed in my assay. Therefore, the possibility cannot be ruled out, that at least some of the healthy children carried undetectable, i.e. sub-patent parasitaemia until or beyond day 84.

Secondly, although the presented assay was shown to be up to 10^4 times more sensitive than standard light microscopy (corresponding to an estimated total parasite mass of 10^4-10^5 in a 3 year old) persistent infections could have escaped detection if the majority of the parasite population would have been sequestered in the deep vasculatures at the time of sampling.

Finally, another reason for the observed discrepancy between negative day 7 results and subsequent recrudescence could be found in the fact that the assay relies on correct genotyping. Even though the genotyping was performed with high accuracy, the possibility of misclassification cannot be ruled out and in endemic areas, children can be re-infected with the same parasites within a single household.

With additional clinical data being available for the ACT study arm, I attempted to correlate my results of the ACT study to initial parasite density, parasite reduction ratio within 24 hours, age of the children, drug plasma level and platelet counts. The results showed correlation of initial parasite density with persistence of parasites until day 7 in the second phase of the ACT study. Malaria incidences in Pingilikani (Kilifi, Kenya) are declining in all age groups since 2003, when the project was started. With reduced transmission and reduced parasite prevalence in the community, the immunity status of each individual is also declining (O'Meara et al, 2008). The observed association between initial parasite biomass and presence of subpatent infections on day 7 may therefore simply reflect a reduced impact of immunity on the clearance of parasites in peripheral blood compared to the first phase on the study.

It has been proposed that clearance time of a defined burden of 10^{12} parasite in the total body varies depending on the power of administered drugs (White, 1997). And the parasite reduction ratio is the essential parameter by which the power of the drug is measured *in vivo*. In this *in vivo* study presented here, two equally efficient drugs were used (Figure 4-1). The parasite reduction ratio is a constant, indicated by the

same slope in every infection, and thus, the prevalence of parasites on day 7 depends directly on the initial parasite load. However, when semi-immunity is fully established, its effect may mask the pharmacodynamic relationship between drug potency and parasite clearance. Figure 4-1 shows a model for this initial phase. My model also allows for a lack of correlation with subsequent recrudescence. Day 7 is probably not a suitable time point to address the question of recrudescence. An explanation could be that the time laps between day 7 and the day of recrudescence is too large and that other, yet undefined confounding factors exist, most likely adaptive immune responses.

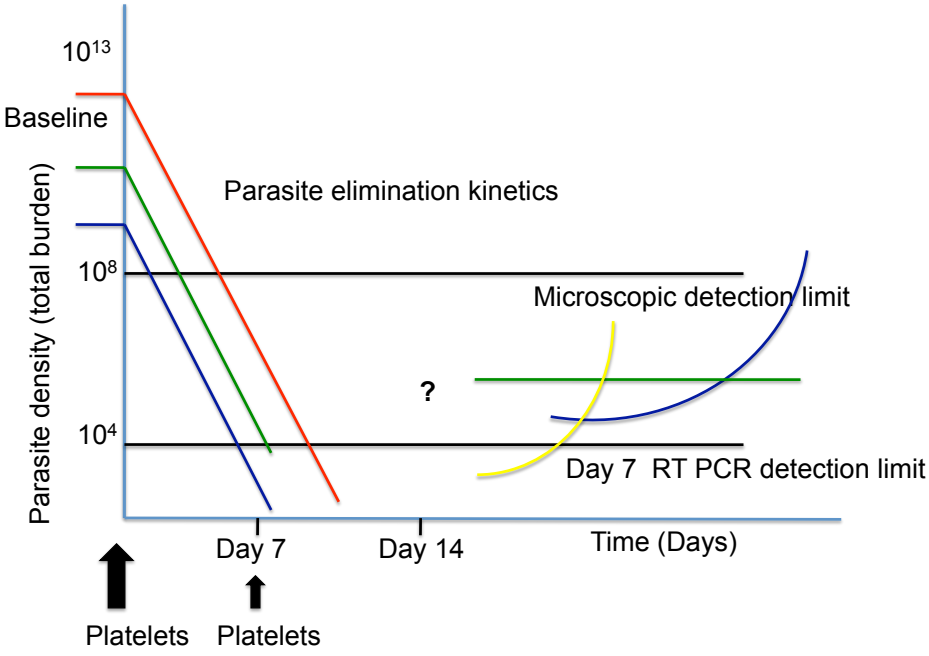

Figure 4-1 Parasite elimination, persistence and recovery below the microscopic threshold – a black box. (red) infection with high baseline parasitaemia, detectable on day 7. (green) infection with medium baseline parasite density, detectable on day 7 and subsequently remains subpatent below the microscopic detection limit. (blue) infection with low baseline parasite density, undetected on day 7 but develops to recurrence, either a true recrudescence or a re-infection by the same parasite within a single household. (yellow) unrelated re-infection can appear in at any time in any patient. (question mark) illustrate that no correlation between results on day 7 and individual outcome was found. Day 14 could be an alternative sampling time point to predict outcome.

Another interesting finding which merits further investigation in the future is related to the recent publication that low platelets counts during an infection are associated with poor outcome (Ladhani et al, 2002). *In vitro* studies have further confirmed their positive effect. Purified platelets were found to kill intraerythrocytic parasites *in vitro*

(McMorran et al, 2009). Here, the observation of a high correlation of elevated platelet counts at baseline and clearance of parasites by day 7 was also observed throughout the study. Innate immunity seems to play a fundamental role in parasite clearance. Importantly, this relationship remained significant even when controlling for initial parasite load.

In conclusion, parasite clearance time in our study is dependent on the potency of the drug (slope) and on the initial parasite load. Up until now, parasite clearance time has always been monitored by microscope, with a detection limit of 10^8 parasites in the total body. However, one to two days after start of treatment, the majority of patients carry an infection with a parasitaemia below this detection limit. With regard to the recent development of artemisinin resistance in western Cambodia (Dondorp et al, 2009) the observation that a high proportion of infections (up to 45%) persist after treatment with ACTs gains additional relevance. It may suggest that parasite populations frequently survive/escape the intense drug pressure exerted by the fast-acting artemisinin component of ACTs without subsequent removal by the intrinsically less potent long half-life companion drug. The new test methodology in this study may give further insights into the complex host-parasite interactions in subpatent infections after treatment or in the general population.

4.2 *In vitro* characterisation of phenotypic and genotypic signatures of naturally acquired drug resistance in *P. falciparum*

Parasite isolates obtained from patients with uncomplicated *P. falciparum* malaria were subjected to a phenotypic and a genotypic analysis with a particular focus on antifolate drug resistance. Before the introduction of artemether-lumefantrine (AM-LM), sulfadoxine-pyrimethamine (SP) was used as first-line treatment in Kenya including in the Pingilikani sub-location of Kilifi District. The massive historic exposure to SP has favoured the survival of stably antifolate-resistant parasites. My results show that even several years after the removal of SP as first line treatment, the parasites still exhibit a very high resistance against anti-folates. Pyrimethamine, the most prominent anti-folate drug was found to be almost completely ineffective to inhibit *in vitro* growth. The most sensitive parasite isolate (AQ 86) had an *in vitro* inhibitory concentration (IC_{50}) of 6.8 µM and the most resistant strain (AK 589) had an IC_{50} of almost 80 µM, which was about 2,000-fold higher than the value measured in sensitive reference strains (3D7 and FCR3). My data compare to previously published data (Sirawaraporn et al, 1997). Similarly, parasite isolates from Kilifi were also highly resistant to another DHFR inhibitor, cycloguanil. The IC_{50} of the most sensitive field isolates was 0.26 µM and of the most resistant one 3.3 µM. This is a 20 and 200-fold increase respectively compared to the sensitive laboratory strain 3D7 (14 nM). These values are also comparable to the literature (Sirawaraporn et al, 1997). Trimethoprim was the least potent drug in our assay and inhibits parasite growth only in higher µM range. Even 3D7, the usually sensitive laboratory strain shows a relative high 50 % inhibitory concentration (4 µM). FCR3 was the overall most sensitive parasite measured in this work (0.6 µM). The weak anti-malarial activity of trimethoprim has already been demonstrated (Iyer et al, 2001) and trimethoprim is only of interest in regard to its usage as chemoprophylaxis in HIV patients (Anglaret et al, 1999; Mermin et al, 2006; Wiktor et al, 1999).

Important for the evaluation of an assay is the repeatability and two distinct phenotypes. With the two laboratory strains 3D7 and FCR3 at least one sensitive control parasite line for each drug was available and measurable under the exact same conditions. Determining the anti-folate activity *in vitro* is critical and can be influenced and altered by addition or subtraction of pABA and folate to the medium, which demonstrates the parasite's ability to use exogenous folate (Chulay et al, 1984; Milhous et al, 1985). The folate salvage pathway (Krungkrai et al, 1989) was

shown to be functional in *P. falciparum* but to which extend it is able to recover anti-folate resistance has not yet been determined. The physiological concentration of folate was demonstrated to be 0.01 mg/L (Hoffbrand & Newcombe, 1967) and exactly the same concentration is contained in standard cultural RPMI medium (2.3 µM). The conditions of the *in vitro* assay were thus comparable to physiological conditions in a patient and the highly resistant phenotypes were thus directly of relevance for the *in vivo* situation.

The genetic mechanism underlying the anti-folate resistance was first described by Cowman (Cowman et al, 1988). Pyrimethamine and cycloguanil are inhibitors of DHFR (Bzik et al, 1987) and mutations in this gene confer resistance (Peterson et al, 1988). Cross-resistance between pyrimethamine, cycloguanil and trimethoprim is commonly found but often considered incomplete (Gregson & Plowe, 2005). Different combinations of mutated position in the *dhfr* gene confer differential resistance. The amino acid substitution at position 16 (A16V) co-exists with S108T and results in high cycloguanil resistance (1000 fold) (Sirawaraporn et al, 1997), without altering pyrimethamine sensitivity (Foote et al, 1990; Peterson et al, 1990). The laboratory strain FCR3 is a representative for this group of parasites and the results measured in this work confirm independently these data. In our field isolates the A16V mutation was not found and is generally not reported from field studies. Additionally I could demonstrate for the first time that the DHFR enzyme carrying the mutation A16V in combination with S108T (FCR3) is the only conformation of the enzyme, which exhibits sensitivity to trimethoprim (600 nM). According to these results the usage of trimethoprim as chemoprophylaxis in HIV patients would strongly select against this particular combination of mutation. These results suggest that counter selection by trimethoprim and the low catalytic activity of the enzyme carrying A16V alone and in combination with S108T (Sirawaraporn et al, 1997) are the reasons for its rareness.
Mutations at codon position 51, 59 and 108 conferred gradual resistance in the case of pyrimethamine and cycloguanil with one mutation exhibiting a relative sensitivity compared to parasites carrying three mutations. These findings are in accordance with previous reports (Cowman et al, 1988; Peterson et al, 1988; Sirawaraporn et al, 1997). Interestingly I did not find the mutation I164L, which is prevalent in south East Asia (Hyde, 2008) but has recently also been reported from western Kenya (Hamel et al, 2008; McCollum et al, 2006) and Kilifi (Kiara et al, 2009), where the samples from this study originated from.
Gene copy number variation (CNV) as a possible mechanism of resistance was ruled out as no gene amplification was found in the five genes encoding for enzymes of the

folate pathway in field isolates, suggesting that different SNP combination in the *dhfr* gene account for the observed resistant phenotype of the field isolates compared to the sensitive laboratory strain 3D7. However, the existence of the previously mentioned salvage pathway (Krungkrai et al, 1989) may provide the parasite with an alternative source of folate and it can not be excluded that an additional yet unknown mechanisms in the salvage pathway explains the discrepancy between the measurements of laboratory strains and field isolates in the order of two to three magnitudes. An altered folate transport activity in field isolates compared to 3D7 and FCR3 could also contribute to the overall observed anti-folate resistance.

Epidemiologically, the observed high prevalence of anti-folate resistance (67% triple mutant) even years after the withdrawal of SP from Kenya is intriguing. Parallel studies from Malawi and Tanzania confirm my data. The authors found triple mutant *dhfr* with a prevalence of 77-91% in southern and northern Malawi (Bridges et al, 2009) and a prevalence of 52% in southwest Tanzania (Schonfeld et al, 2007). The often-discussed fitness cost of parasites carrying mutations in the absence of drugs seems to be less pronounced for mutations targeting *dhfr*. All isolates still carry at least one mutation (S108N), 90.5 % of the isolates carried also the mutation at codon position N51I and 66% carry mutation C59R. The number of parasites measured in this work is limited but clearly shows 100% prevalence of mutated *dhfr*. This is remarkable years after the withdrawal of the drug and questions the relevance of previous findings of lowered *in vitro* activity of the enzyme (Sirawaraporn et al, 1997). My results seem to support more recent studies on the catalytic activity of wild type *vs.* mutant enzyme, which concluded the opposite. The authors of this study found actually higher catalytic activity of the mutant enzyme compared to wild type *dhfr* (Sandefur et al, 2007). This may explain the persistence of mutant *dhfr* in Africa (exemplified by my results from Kilifi), in Southeast Asia (Masimirembwa et al, 1999; Ngo et al, 2003; Wang et al, 1997; Zindrou et al, 1996), in Tanzania (Gesase et al, 2009) and in western, central and eastern Africa (Mita et al, 2009) even years after withdrawal of SP.

Chloroquine (CQ) was used in a control assay to demonstrate that mutated SNPs in the *dhfr* gene were only associated to the resistance of anti-folate and not generally to resistance against antimalarials. The drug was found suitable for the analysis for two reasons. First, CQ is a 4-aminoquinoline and is therefore structurally and functionally unrelated to anti-folates and secondly, CQ was used before the introduction of SP as first line treatment in the area and the question arose of how long the resistant phenotype would persist in the population after its withdrawal. Of

the measured isolates 57.1% still exhibited complete chloroquine resistance (CQR). This is a reduction of CQR prevalence in accordance to the previously reported studies in Kenya (Mwai et al, 2009) and in Malawi (Bridges et al, 2009). However, elimination of chloroquine resistant phenotypes seems to be slow in our study site compared to almost complete elimination (0-8% prevalence) of mutant *pfcrt* in Malawi (Bridges et al, 2009). A still remarkable number of resistant parasites were detected. This is even more astonishing as the withdrawal of chloroquine happened even before the withdrawal of SP. An explanation for the persistence of resistant phenotypes in our study site could be massive use of amodiaquine (AQ) as interim first line treatment after withdrawal of SP and before the introduction of ACT. AQ is also a 4-aminoquinoline and could therefore have co-selected for CQR during the years of its usage. In this case, AQ retarded the immediate decline of CQR and the prevalence of CQR has to be reassessed. Under these circumstance, prevalence is already remarkably reduced in the study area and expected to decline even more rapidly in the next year in analogy to Malawi (Bridges et al, 2009) and Tanzania.
In conclusion, it seems that CQR is accompanied by compromised fitness whereas mutant *dhfr* is not, even though the persistence of two different loci in the population is not comparable and both proteins are fundamentally different.

About adapting parasites to culture and in vitro vs. in vivo findings
The availability of standard culture protocols for *P. falciparum* blood stage parasites permits the convenient and reproducible characterisation of phenotypes *in vitro*. The adaptation of parasite isolates obtained from infected patients can last over several weeks and up until now partially conflicting information about parasite survival during this adaption procedure exists. My results highlight the importance of such an analysis. On average 36 % of initial clones were lost during adaption. The methodology of *msp2* genotyping has limitations (discussed above). With further development of affordable whole genome sequencing technologies in the future, this question could be addressed in more detail. Nonetheless, the high proportion of lost clones (36%) may help to explain an often-observed discrepancy between *in vitro* susceptibility measured in adapted parasite isolates and *in vivo* outcome (Sasi et al. JID 2008). The reasons for differential abilities to adapt to culture conditions are unknown. Survival of the parasites could be stochastic, i.e. due to chance alone or it is linked to genetic factors, which may confer differential survival chances *in vitro* and *in vivo*. The latter is a concern when interpreting results of *in vitro* drug susceptibility assays as a representative picture of naturally occurring parasites. Some *in vivo* phenotypes might not be compatible with *in vitro* culture conditions and will therefore

elude their identification. An example could be the recently observed *in vivo* resistance phenotype against artemisinins (Dondorp et al, 2009), which still lacks a corresponding, stable *in vitro* phenotype.

4.3 Induction of drug resistance *in vitro*

To investigate the emergence of anti-folate resistance *in vitro* and to better understand the molecular mechanism, parasites were grown *in vitro* under increasing pyrimethamine pressure. Two laboratory strains, 3D7 and FCR, were used for this experiment. Both strains are sensitive to pyrimethamine, but whereas FCR3 carries the mutation A16V and S108T, which confer a high cycloguanil resistance, 3D7 has wild type *dhfr* and is cycloguanil sensitive. Compared to field isolates, 3D7 (4 µM) and FCR3 (600 nM) exhibit sensitivity against trimethoprim, an overall weak antimalarial drug. But when exposing the parasites to pyrimethamine over a prolonged period, resistance developed not only against pyrimethamine (3D7 and FCR3) but also against cycloguanil in 3D7 (FCR being already highly resistant) and trimethoprim (3D7 and FCR3). The IC_{50} values for the three drugs increased significantly during the experiment, implying a mechanism of resistance, which confers cross-resistance to other anti-folates but not against unrelated anti-malarials. Responsiveness against chloroquine remained unchanged, except for $FCR3^{800nM}$. When I further increased the pyrimethamine concentration in the growth medium, the IC_{50} value of chloroquine dropped back again and since I could not find a plausible explanation for this phenomenon, it was not further investigated.

The increase of IC_{50} values did not follow a particular pattern, except for the first concentration measured. At 200 nM of pyrimethamine, both parasite lines had developed an IC_{50} of approximately 200 nM (3D7: 225 ± 9 nM; FCR3 268 ± 55 nM). The same parasites showed decreased cycloguanil sensitivity. The parasites had adapted to the concentration they were exposed to but multiplied with only half of their usual growth rate according to the measured IC_{50}. Therefore the status of the parasite at that time point of the experiment should not be defined resistant. Resistance would be defined as uninhibited growth in the presence of the drug. Interestingly this was a rather stable phenotype, as the parasites were kept over 2 month at 200 nM without noticeable change of their phenotype. When drug pressure was further increased a more complex pattern emerged. The concentrations of pyrimethamine necessary to inhibit 50% of maximal growth started to increasingly exceed the drug concentration in the medium. IC_{50} values of pyrimethamine were a multiple above the drug concentration in the medium: 4900 nM $3D7^{800nM}$, 3500 nM $FCR3^{800nM}$, 6400 nM $3D7^{1600nM}$ and 5300 nM in $FCR3^{1600nM}$ (pyrimethamine). Between 3 and 6 fold higher was the measured concentration, which inhibits 50 % of parasite growth. This pattern correlated with a recovery of normal growth rates in these parasite lineages. Cross-resistance to trimethoprim was equally strong developed.

3D7 showed approximately 5 fold increase and FCR3 a 10-fold increase between the development of anti-folate tolerance at 200 nM and resistance at 800 nM, suggesting a highly developed cross-resistance between pyrimethamine and trimethoprim. Cycloguanil in contrast remains the most potent drug (290 nM in $3D7^{800nM}$ and 340 nM in $3D7^{1600nM}$) and thus exhibits in these experiments less cross-resistance in accordance to results of previously reported studies (Ferone et al, 1969; Milhous et al, 1985; Nzila-Mounda et al, 1998). Interestingly, no change in IC_{50} values was observed when the drug pressure was elevated to 1600 nM in the growth medium. One explanation for this could be that selection pressure was not sufficiently strong as the parasites exhibited already an IC_{50} value greater than the drug pressure applied. The intriguing pattern in the rate of acquisition of stable resistance will be further discussed in the next paragraph.

In the parasites line 3D7 a single point mutation at position S108N was identified for the first time at a pyrimethamine concentration of 800nM in the medium. The mutation replaced the wild type amino acid serine (S) by asparagine (N) and confers thereby the above described highly and stable pyrimethamine resistance.
But before the introduction of the point mutation, an increased abundance of *dhfr* transcripts was found at 100nM of pyrimethamine, when an expression analysis was performed. Increased expression was due to amplification of the genomic locus containing the *dhfr* gene in both strains. The adapted laboratory strains developed resistance by increasing the abundance of the targeted enzyme to overcome inhibition. The malaria parasite's ability to amplify *dhfr in vitro* has previously been reported (Inselburg et al, 1987; Thaithong et al, 2001) but no detailed analysis of the number of amplification, of the amplified locus itself and of the occurrence of a SNP within the additional copies has been performed until now. In this study a continuous amplification of the *dhfr* locus in both strains was observed. Once the amplification was introduced in the parasite population at around 100nM of pyrimethamine, additional copies were added within 7 asexual parasite cycles (two weeks). In my experiment the number of *dhfr* copies increased up to 31 in 3D7, but only 9 fold in FCR3. Thaithong, et al. is the only group having carried out a similar experiment. First, they estimated a 44-fold increase at the *dhfr* locus in a clone carrying previously to the selection process mutation A16V and S108T. Secondly, they observed an increase of *dhfr* copies in parasites carrying a wild type *dhfr* allele but without quantification. And thirdly, no amplification was found in a clone carrying S16V (Thaithong et al, 2001). The authors argued that this clone (S16V) was already sufficiently resistant against pyrimethamine (Thaithong et al, 2001). This hypothesis

would ultimately lead to the consequence that their wild type clone should harbour even more than the partially resistant clone (A16V and S108T with 44 copies). Unfortunately no estimation about copy numbers of the wild type clone is given and the hypothesis can thus not be reconfirmed.

My results show a significant amplification in FCR3 parasites (carrier of A16V) but remarkably less pronounced compared to 3D7 (wild type) or to Thaithong's findings. Two possible reasons could explain this difference. Further amplification of the allele carrying the mutation A16V and S108T may be limited due to functional constraints on this particular haplotype or simply by higher intrinsic level of resistance. In support of the first explanation a parallel can be drawn from studies on the multidrug resistant transporter gene (*mdr*) coding for Pgh1, a homologue to the human P glycoprotein 1. This gene was found amplified in field isolates and amplification was correlated to the wild type allele (Price et al, 1999) suggesting a disadvantage of amplifying mutant alleles. An argument for the latter explanation is the elevated IC_{50} in $FCR3^{1600nM}$ and the relatively higher baseline IC_{50} of FCR3 (62nM) compared to 3D7 (20nM). The parasites are highly adapted at 1600nM (5300nM) and need no further amplification to encounter the drug in the medium, potentially due to their predisposition of A16V and S108T.

So why did 3D7 accumulate 10 additional copies (one third of its total copy number), when brought from 800nM to 1600nM of pyrimethamine even though no obvious phenotypic benefit is apparent, i.e. in the absence of further increased IC_{50} values? The hypothesis, that copy numbers depend strictly on the drug pressure applied and the parasite's need to escape the deteriorating effects of the drug, seems only partially be true. In the following paragraph an additional aspect is presented, which might give an indication for the above-described controversy.

Since gene amplification alone could not account for the highly resistant phenotype observed, I looked into the occurrence of mutations within *dhfr* gene copies. As mentioned above, in the parasites line 3D7, *dhfr* was not only amplified but at a pyrimethamine concentration of 800nM a single point mutation at position S108N was identified for the first time in a small number of copies, which replaced the wild type amino acid serine (S) by asparagine (N). It is the first time that gene amplification is shown to precede the emergence of a single point mutation in *Plasmodium falciparum* and that a functional link between amplification and SNP occurrence can be drawn. I propose in analogy to bacteria (Andersson et al, 1998) that gene amplification in *Plasmodium falciparum* facilitates the acquisition of single point mutations through increased copy numbers of the target gene (i.e. *dhfr*). Even when assuming no change in the per-nucleotide mutation rate this is expected to

result in higher probability of errors during DNA replication. The estimated mutation rate of 10^{-9} (Paget-McNicol & Saul, 2001) in the *DHFR* locus of *P. falciparum* was increased by at least one magnitude.

One single other study in *P. chabaudi* supports these findings. Selecting for pyrimethamine resistance in the rodent malaria parasite also showed *dhfr* amplification. Cowman and Lew found a 200kb region being amplified (Cowman & Lew, 1989) and later in a subsequent publication, a single point mutation at protein position 106 was identified within the amplified copies, which corresponds to 108 in *P.falciparum* (Cowman & Lew, 1990). Through amplification the emergence of a mutation in the amplified gene in *P. chabaudi* is facilitated. In *P. falciparum* though, no evidence for the existence of such mechanism was found until now. Thaithong et al found gene amplification as a mechanism of resistance in *dhfr* of *P. falciparum* and could also detect some mutations in the *dhfr* gene but not at position 108 and more importantly, they did not connect these two mechanisms as being functionally related (Thaithong et al, 2001). Other recent and past studies have only investigated the mutation rate of the *dhfr* gene in *Plasmodium falciparum* (Paget-McNicol & Saul, 2001) and the stepwise acquisition of single mutations (Lozovsky et al, 2009) without taking into account gene amplification. Cowman et al. even concluded that the molecular basis for pyrimethamine resistance in *P. falciparum* is only mutated *dhfr* and gene amplification did not play a role in conferring resistance (Cowman et al, 1988).

With the introduction of a point mutation in the amplified copies, some of the apparent conflicting results could be explained. Firstly the sudden and disproportional decline of responsiveness from $3D7^{200nM}$ to $3D7^{800nM}$ could be attributed to the mutation of S108N. This gatekeeper's substitution is known to be the first step in emergence of pyrimethamine resistance in *P. falciparum* field isolates (Peterson et al, 1991). Furthermore the responsiveness *in vitro* against pyrimethamine, cycloguanil and trimethoprim of AQ 86 (S108N only) is comparable to $3D7^{800nM}$ and $3D7^{1600nM}$ with amplified *dhfr* and S108N. The sudden establishment of resistance in 3D7 could therefore be explained by the mutation and gene amplification contributes at this stage of drug exposure less to the resistant phenotype than at lower pyrimethamine concentrations. It remains a mystery though, why the parasites, in a genetic background of S108N, acquired continuously further *dhfr* copies, when it was transferred from 800nM to 1600nM. Even more striking are these findings, when additional copies do not alter the resistant phenotype. Two possible explanations are conceivable. First, it could be that the mutation mainly determines the phenotype and the lack of significant drug pressure at 1600nM leaves the parasites enough

tolerance to add or loose copies at random. Or secondly, it is most likely that not all parasites carry the mutation and the measured phenotypes as well as the determined copy numbers are the results of a mixed population. However, when $3D7^{800nM}$ were cloned out, it became apparent, that all of the 8 recovered clones carried the mutation (confirmed only by restriction analysis) leading to the hypothesis that every single parasite carries the mutation in at least one *dhfr* copy. But to definitely resolve the further fate and prevalence of mutation and amplification in the selected parasites population, the drug pressure has to be increased at least at the level of the current IC_{50} or above. The continuous selection of the $3D7^{800nM}$ cloned parasites could also give further insights in the differential contribution of *dhfr* copy numbers and *dhfr* mutation for resistant phenotypes.
In summary, I conclude that both parasite strains have successfully amplified the *dhfr* gene in *Plasmodium falciparum* to overcome inhibition by pyrimethamine. I therefore suggest that amplification is a mechanism of resistance for the *dhfr* locus at low inhibitory concentration and that these amplifications facilitate introduction of a single point mutation to ultimately gain high pyrimethamine resistance. The high prevalence of CNVs in the *Plasmodium* genome (Cheeseman et al, 2009) further suggests that the relationship between copy number amplification and SNP acquisition rate may be a general, conserved mechanism that drives evolutionary adaptation in *Plasmodium*.

In the presented work, the first amplifications were introduced in the parasite populations at around 100nM of pyrimethamine. This is in accordance to previously presented work by Thaithong, et al. (Thaithong et al, 2001). Here for the first time, a detailed analysis of the amplicon was performed. Surrounding sequences and open reading frames were analysed. Surprisingly, amplicons in 3D7 and FRC3 strains were distinctively different, although a notable feature was the absence of co-amplification of PFD0835c, the immediately adjacent gene to *dhfr*. In 3D7 an amplicon was generated with a gap at PFD0835c and in FCR3 the amplicon contained only part of the gene without the transcription start site, i.e. non-functional copies. This suggested a strong selection pressure against co-amplification of PFD0835, as it is located in immediate proximity to *dhfr*. Both strains have undergone complex arrangements to avoid its co-amplification. By extension, this leads to the hypothesis, that PFD0835c might be toxic if over-expressed. PFD0835c is annotated as a LETM like protein. In yeast a protein with LETM1 domain is involved in K+/H+ exchange at the inner mitochondrial membrane (Froschauer et al, 2005) and in *Drosophila* a LETM1 protein, a homologue to the mammalian LETM1, has been identified as a Ca^{2+}/H^{+} antiporter (Jiang et al, 2009). In *Plasmodium*

falciparum no functional *in vitro* studies on the gene product of PFD0835c have yet been performed but a signalling sequence targeting the protein to the apicoplast was annotated for PFD0835c suggesting that PFD0835c is involved in K^+ and or Ca^+ homeostasis in the apicoplast of *P. falciparum*. Over expression could lead to breakdown of membrane potential and K^+ / H^+ / Ca^+ homeostasis. The channel seems to be essential, as no complete loss of the sequence had occurred. The relatively complex genesis of the *dhfr* amplicon may also explain the lack of *dhfr* amplification in field strains. In summary, these findings generated testable hypotheses that can be addressed experimentally.

The underlying mechanism of chromosomal rearrangement is not understood in *P. falciparum*. Various mechanisms described in model organisms and in human cancer have to be considered. Fundamentally two main mechanisms can be distinguished: chromosomal rearrangement and new DNA synthesis by copying sequence from other related or unrelated parts in the genome. From all current models, also presented in the introduction, I propose the FoSTeS (fork stalling and template switching) model (Lee et al, 2007) to be prim candidate for further studies. During DNA replication, the lagging strand disengages from its template and invades a neighbouring replication fork where it continues the replication but on the basis of a wrong template. The resultant sequence can be very diverse and randomly orientated since the strand switching can occur repeatedly at any place and in both direction for both longer and shorter sequences. No limitations are set for creation of newly copied and integrated sequences.

In *Plasmodium falciparum* it has been suggested that the majority of DNA replication starts in 28 to 31 hours post invasion of erythrocytes and increases during the following 8 to 10 hours during which the genome is replicated several times (Arnot & Gull, 1998; Graeser et al, 1996; Inselburg & Banyal, 1984). To accomplish massive multiplication within such a short time, it can be assumed that many replication forks are built at the same time and the abundance of repetitive sequences in *Plasmodium falciparum* (Wickstead et al, 2003) could then facilitate the annealing of a disengaged lagging strand into a neighbouring replication fork. The reasoning for such speculation is the fact that the amplicon of 3D7 is interrupted and the resulting sequence is difficult to explain by simple chromosomal crossing over and rearrangements, especially because the missing sequence in the amplicon is approximately 3 kb long and chromosomal rearrangement occur over much greater distances. Once a duplication of the genome has been created by FoSTeS, further amplification could then be generated by non-allelic homologous recombination

(NAHR) within chromatids and sister chromatids. The more copies are available the higher the homology within and between the two sister chromatids and this could then facilitate recombination. Further analysis of the sequences that result from amplification will have to be performed to conclude about the parasites favourite mechanism to amplify genes - if there is one.

The last aspect, which I will focus on, is fitness cost of parasites carrying amplification. Parasites carrying amplified *pfmdr* locus selected by mefloquine showed lower replication rates than parasites they were derived from (Preechapornkul et al, 2009). This is consistent with the results obtained in my experiment. *dhfr* amplification was stable in culture without drug pressure and when kept alone for at least 2 month but when grown in competition with wild type parasites amplification was lost or overgrown within two months. The stability of *dhfr* amplification is a small hint suggesting stable integration of amplicons as opposed to episomal carriage of amplified DNA. This question has not been addressed in more detail but will be part of future investigations.

The findings presented in this work provide compelling evidence that evolutionary function of gene amplification as an intermediate step for the acquisition of stably heritable genetic changes. This work also provides a range of testable hypotheses that can be addressed experimentally using established genetic tools.

5. References

Alker AP, Lim P, Sem R, Shah NK, Yi P, Bouth DM, Tsuyuoka R, Maguire JD, Fandeur T, Ariey F, Wongsrichanalai C, Meshnick SR (2007) Pfmdr1 and in vivo resistance to artesunate-mefloquine in falciparum malaria on the Cambodian-Thai border. *The American journal of tropical medicine and hygiene* **76:** 641-647

Aly AS, Matuschewski K (2005) A malarial cysteine protease is necessary for Plasmodium sporozoite egress from oocysts. *The Journal of experimental medicine* **202:** 225-230

Andersson DI, Slechta ES, Roth JR (1998) Evidence that gene amplification underlies adaptive mutability of the bacterial lac operon. *Science* **282:** 1133-1135

Anglaret X, Chene G, Attia A, Toure S, Lafont S, Combe P, Manlan K, N'Dri-Yoman T, Salamon R (1999) Early chemoprophylaxis with trimethoprim-sulphamethoxazole for HIV-1-infected adults in Abidjan, Cote d'Ivoire: a randomised trial. Cotrimo-CI Study Group. *Lancet* **353:** 1463-1468

Arnot DE, Gull K (1998) The Plasmodium cell-cycle: facts and questions. *Ann Trop Med Parasitol* **92:** 361-365

Babcock M, Pavlicek A, Spiteri E, Kashork CD, Ioshikhes I, Shaffer LG, Jurka J, Morrow BE (2003) Shuffling of genes within low-copy repeats on 22q11 (LCR22) by Alu-mediated recombination events during evolution. *Genome research* **13:** 2519-2532

Baer K, Klotz C, Kappe SH, Schnieder T, Frevert U (2007) Release of hepatic Plasmodium yoelii merozoites into the pulmonary microvasculature. *PLoS Pathog* **3:** e171

Bejon P, Berkley JA, Mwangi T, Ogada E, Mwangi I, Maitland K, Williams T, Scott JA, English M, Lowe BS, Peshu N, Newton CR, Marsh K (2007) Defining childhood severe falciparum malaria for intervention studies. *PLoS Med* **4:** e251

Bergthorsson U, Andersson DI, Roth JR (2007) Ohno's dilemma: evolution of new genes under continuous selection. *Proc Natl Acad Sci U S A* **104:** 17004-17009

Bhattarai A, Ali AS, Kachur SP, Martensson A, Abbas AK, Khatib R, Al-Mafazy AW, Ramsan M, Rotllant G, Gerstenmaier JF, Molteni F, Abdulla S, Montgomery SM, Kaneko A, Bjorkman A (2007) Impact of artemisinin-based combination therapy and insecticide-treated nets on malaria burden in Zanzibar. *PLoS Med* **4:** e309

Biswas S, Escalante A, Chaiyaroj S, Angkasekwinai P, Lal AA (2000) Prevalence of point mutations in the dihydrofolate reductase and dihydropteroate synthetase genes of Plasmodium falciparum isolates from India and Thailand: a molecular epidemiologic study. *Trop Med Int Health* **5:** 737-743

Borrmann S, Peto T, Snow RW, Gutteridge W, White NJ (2008) Revisiting the design of phase III clinical trials of antimalarial drugs for uncomplicated Plasmodium falciparum malaria. *PLoS Med* **5:** e227

Bridges DJ, Molyneux M, Nkhoma S (2009) Low level genotypic chloroquine resistance near Malawi's northern border with Tanzania. *Trop Med Int Health* **14:** 1093-1096

Brooks DR, Wang P, Read M, Watkins WM, Sims PF, Hyde JE (1994) Sequence variation of the hydroxymethyldihydropterin pyrophosphokinase: dihydropteroate synthase gene in lines of the human malaria parasite, Plasmodium falciparum, with differing resistance to sulfadoxine. *European journal of biochemistry / FEBS* **224:** 397-405

Brown DD, Dawid IB (1968) Specific gene amplification in oocytes. Oocyte nuclei contain extrachromosomal replicas of the genes for ribosomal RNA. *Science* **160:** 272-280

Bull PC, Marsh K (2002) The role of antibodies to Plasmodium falciparum-infected-erythrocyte surface antigens in naturally acquired immunity to malaria. *Trends Microbiol* **10:** 55-58

Bzik DJ, Li WB, Horii T, Inselburg J (1987) Molecular cloning and sequence analysis of the Plasmodium falciparum dihydrofolate reductase-thymidylate synthase gene. *Proceedings of the National Academy of Sciences of the United States of America* **84:** 8360-8364

Carman MD, Schornagel JH, Rivest RS, Srimatkandada S, Portlock CS, Duffy T, Bertino JR (1984) Resistance to methotrexate due to gene amplification in a patient with acute leukemia. *J Clin Oncol* **2:** 16-20

Carter R, Mendis KN (2002) Evolutionary and historical aspects of the burden of malaria. *Clin Microbiol Rev* **15:** 564-594

Ceesay SJ, Casals-Pascual C, Erskine J, Anya SE, Duah NO, Fulford AJ, Sesay SS, Abubakar I, Dunyo S, Sey O, Palmer A, Fofana M, Corrah T, Bojang KA, Whittle HC, Greenwood BM, Conway DJ (2008) Changes in malaria indices between 1999 and 2007 in The Gambia: a retrospective analysis. *Lancet* **372:** 1545-1554

Cheeseman IH, Gomez-Escobar N, Carret CK, Ivens A, Stewart LB, Tetteh KK, Conway DJ (2009) Gene copy number variation throughout the Plasmodium falciparum genome. *BMC Genomics* **10:** 353

Chulay JD, Watkins WM, Sixsmith DG (1984) Synergistic antimalarial activity of pyrimethamine and sulfadoxine against Plasmodium falciparum in vitro. *The American journal of tropical medicine and hygiene* **33:** 325-330

Claycomb JM, Benasutti M, Bosco G, Fenger DD, Orr-Weaver TL (2004) Gene amplification as a developmental strategy: isolation of two developmental amplicons in Drosophila. *Dev Cell* **6:** 145-155

Claycomb JM, Orr-Weaver TL (2005) Developmental gene amplification: insights into DNA replication and gene expression. *Trends Genet* **21:** 149-162

Coggeshall LT (1940) The Selective Action of Sulfanilamide on the Parasites of Experimental Malaria in Monkeys in Vivo and in Vitro. *The Journal of experimental medicine* **71:** 13-20

Cowman AF, Karcz S, Galatis D, Culvenor JG (1991) A P-glycoprotein homologue of Plasmodium falciparum is localized on the digestive vacuole. *J Cell Biol* **113:** 1033-1042

Cowman AF, Lew AM (1989) Antifolate drug selection results in duplication and rearrangement of chromosome 7 in Plasmodium chabaudi. *Mol Cell Biol* **9:** 5182-5188

Cowman AF, Lew AM (1990) Chromosomal rearrangements and point mutations in the DHFR-TS gene of Plasmodium chabaudi under antifolate selection. *Molecular and biochemical parasitology* **42:** 21-29

Cowman AF, Morry MJ, Biggs BA, Cross GA, Foote SJ (1988) Amino acid changes linked to pyrimethamine resistance in the dihydrofolate reductase-thymidylate synthase gene of Plasmodium falciparum. *Proc Natl Acad Sci U S A* **85:** 9109-9113

Delidakis C, Kafatos FC (1989) Amplification enhancers and replication origins in the autosomal chorion gene cluster of Drosophila. *EMBO J* **8:** 891-901

Denis MB, Tsuyuoka R, Lim P, Lindegardh N, Yi P, Top SN, Socheat D, Fandeur T, Annerberg A, Christophel EM, Ringwald P (2006a) Efficacy of artemether-lumefantrine for the treatment of uncomplicated falciparum malaria in northwest Cambodia. *Trop Med Int Health* **11:** 1800-1807

Denis MB, Tsuyuoka R, Poravuth Y, Narann TS, Seila S, Lim C, Incardona S, Lim P, Sem R, Socheat D, Christophel EM, Ringwald P (2006b) Surveillance of the efficacy of artesunate and mefloquine combination for the treatment of uncomplicated falciparum malaria in Cambodia. *Trop Med Int Health* **11:** 1360-1366

Dittrich S, Mitchell SL, Blagborough AM, Wang Q, Wang P, Sims PF, Hyde JE (2008) An atypical orthologue of 6-pyruvoyltetrahydropterin synthase can provide the missing link in the folate biosynthesis pathway of malaria parasites. *Molecular microbiology* **67:** 609-618

Dondorp AM, Nosten F, Yi P, Das D, Phyo AP, Tarning J, Lwin KM, Ariey F, Hanpithakpong W, Lee SJ, Ringwald P, Silamut K, Imwong M, Chotivanich K, Lim P, Herdman T, An SS, Yeung S, Singhasivanon P, Day NP, Lindegardh N, Socheat D, White NJ (2009) Artemisinin resistance in Plasmodium falciparum malaria. *N Engl J Med* **361:** 455-467

Drake JW, Charlesworth B, Charlesworth D, Crow JF (1998) Rates of spontaneous mutation. *Genetics* **148:** 1667-1686

Escalante AA, Ayala FJ (1994) Phylogeny of the malarial genus Plasmodium, derived from rRNA gene sequences. *Proceedings of the National Academy of Sciences of the United States of America* **91:** 11373-11377

Escalante AA, Ayala FJ (1995) Evolutionary origin of Plasmodium and other Apicomplexa based on rRNA genes. *Proceedings of the National Academy of Sciences of the United States of America* **92:** 5793-5797

Eskenazi B, Chevrier J, Rosas LG, Anderson HA, Bornman MS, Bouwman H, Chen A, Cohn BA, de Jager C, Henshel DS, Leipzig F, Leipzig JS, Lorenz EC, Snedeker SM, Stapleton D (2009) The Pine River statement: human health consequences of DDT use. *Environ Health Perspect* **117:** 1359-1367

Felger I, Beck HP (2002) Genotyping of Plasmodium falciparum. PCR-RFLP analysis. *Methods Mol Med* **72:** 117-129

Ferone R, Burchall JJ, Hitchings GH (1969) Plasmodium berghei dihydrofolate reductase. Isolation, properties, and inhibition by antifolates. *Mol Pharmacol* **5:** 49-59

Foote SJ, Galatis D, Cowman AF (1990) Amino acids in the dihydrofolate reductase-thymidylate synthase gene of Plasmodium falciparum involved in cycloguanil resistance differ from those involved in pyrimethamine resistance. *Proceedings of the National Academy of Sciences of the United States of America* **87:** 3014-3017

Force A, Lynch M, Pickett FB, Amores A, Yan YL, Postlethwait J (1999) Preservation of duplicate genes by complementary, degenerative mutations. *Genetics* **151:** 1531-1545

Fortna A, Kim Y, MacLaren E, Marshall K, Hahn G, Meltesen L, Brenton M, Hink R, Burgers S, Hernandez-Boussard T, Karimpour-Fard A, Glueck D, McGavran L, Berry R, Pollack J, Sikela JM (2004) Lineage-specific gene duplication and loss in human and great ape evolution. *PLoS biology* **2:** E207

Frevert U, Engelmann S, Zougbede S, Stange J, Ng B, Matuschewski K, Liebes L, Yee H (2005) Intravital observation of Plasmodium berghei sporozoite infection of the liver. *PLoS biology* **3:** e192

Froschauer E, Nowikovsky K, Schweyen RJ (2005) Electroneutral K+/H+ exchange in mitochondrial membrane vesicles involves Yol027/Letm1 proteins. *Biochim Biophys Acta* **1711:** 41-48

Gall JG (1968) Differential synthesis of the genes for ribosomal RNA during amphibian oogenesis. *Proceedings of the National Academy of Sciences of the United States of America* **60:** 553-560

Gesase S, Gosling RD, Hashim R, Ord R, Naidoo I, Madebe R, Mosha JF, Joho A, Mandia V, Mrema H, Mapunda E, Savael Z, Lemnge M, Mosha FW, Greenwood B, Roper C, Chandramohan D (2009) High resistance of Plasmodium falciparum to sulphadoxine/pyrimethamine in northern Tanzania and the emergence of dhps resistance mutation at Codon 581. *PloS one* **4:** e4569

Glover DM, Zaha A, Stocker AJ, Santelli RV, Pueyo MT, De Toledo SM, Lara FJ (1982) Gene amplification in Rhynchosciara salivary gland chromosomes. *Proceedings of the National Academy of Sciences of the United States of America* **79:** 2947-2951

Goodier JL, Kazazian HH, Jr. (2008) Retrotransposons revisited: the restraint and rehabilitation of parasites. *Cell* **135:** 23-35

Graeser R, Wernli B, Franklin RM, Kappes B (1996) Plasmodium falciparum protein kinase 5 and the malarial nuclear division cycles. *Mol Biochem Parasitol* **82:** 37-49

Gregson A, Plowe CV (2005) Mechanisms of resistance of malaria parasites to antifolates. *Pharmacol Rev* **57:** 117-145

Gu W, Zhang F, Lupski JR (2008) Mechanisms for human genomic rearrangements. *Pathogenetics* **1:** 4

Hamel MJ, Poe A, Bloland P, McCollum A, Zhou Z, Shi YP, Ouma P, Otieno K, Vulule J, Escalante A, Udhayakumar V, Slutsker L (2008) Dihydrofolate reductase I164L mutations in Plasmodium falciparum isolates: clinical outcome of 14 Kenyan adults infected with parasites harbouring the I164L mutation. *Trans R Soc Trop Med Hyg* **102:** 338-345

Han K, Lee J, Meyer TJ, Remedios P, Goodwin L, Batzer MA (2008) L1 recombination-associated deletions generate human genomic variation. *Proceedings of the National Academy of Sciences of the United States of America* **105:** 19366-19371

Hay SI, Guerra CA, Gething PW, Patil AP, Tatem AJ, Noor AM, Kabaria CW, Manh BH, Elyazar IR, Brooker S, Smith DL, Moyeed RA, Snow RW (2009) A world malaria map: Plasmodium falciparum endemicity in 2007. *PLoS Med* **6:** e1000048

Heck MM, Spradling AC (1990) Multiple replication origins are used during Drosophila chorion gene amplification. *J Cell Biol* **110:** 903-914

Hoffbrand AV, Newcombe BF (1967) Leucocyte folate in vitamin B 12 and folate deficiency and in leukaemia. *British journal of haematology* **13:** 954-966

Horns RC, Jr., Dower WJ, Schimke RT (1984) Gene amplification in a leukemic patient treated with methotrexate. *J Clin Oncol* **2:** 2-7

Hyde JE (2008) Antifolate resistance in Africa and the 164-dollar question. *Trans R Soc Trop Med Hyg* **102:** 301-303

Inoue K, Lupski JR (2002) Molecular mechanisms for genomic disorders. *Annu Rev Genomics Hum Genet* **3:** 199-242

Inselburg J, Banyal HS (1984) Synthesis of DNA during the asexual cycle of Plasmodium falciparum in culture. *Mol Biochem Parasitol* **10:** 79-87

Inselburg J, Bzik DJ, Horii T (1987) Pyrimethamine resistant Plasmodium falciparum: overproduction of dihydrofolate reductase by a gene duplication. *Molecular and biochemical parasitology* **26:** 121-134

Iyer JK, Milhous WK, Cortese JF, Kublin JG, Plowe CV (2001) Plasmodium falciparum cross-resistance between trimethoprim and pyrimethamine. *Lancet* **358:** 1066-1067

Jiang D, Zhao L, Clapham DE (2009) Genome-wide RNAi screen identifies Letm1 as a mitochondrial Ca2+/H+ antiporter. *Science* **326:** 144-147

Kaufman RJ, Bertino JR, Schimke RT (1978) Quantitation of dihydrofolate reductase in individual parental and methotrexate-resistant murine cells. Use of a fluorescence activated cell sorter. *The Journal of biological chemistry* **253:** 5852-5860

Kaufman RJ, Schimke RT (1981) Amplification and loss of dihydrofolate reductase genes in a Chinese hamster ovary cell line. *Mol Cell Biol* **1:** 1069-1076

Kazazian HH, Jr., Moran JV (1998) The impact of L1 retrotransposons on the human genome. *Nature genetics* **19:** 19-24

Khalil I, Ronn AM, Alifrangis M, Gabar HA, Satti GM, Bygbjerg IC (2003) Dihydrofolate reductase and dihydropteroate synthase genotypes associated with in vitro resistance of Plasmodium falciparum to pyrimethamine, trimethoprim, sulfadoxine, and sulfamethoxazole. *The American journal of tropical medicine and hygiene* **68:** 586-589

Kiara SM, Okombo J, Masseno V, Mwai L, Ochola I, Borrmann S, Nzila A (2009) In vitro activity of antifolate and polymorphism in dihydrofolate reductase of Plasmodium falciparum isolates from the Kenyan coast: emergence of parasites with Ile-164-Leu mutation. *Antimicrob Agents Chemother* **53:** 3793-3798

Kidgell C, Volkman SK, Daily J, Borevitz JO, Plouffe D, Zhou Y, Johnson JR, Le Roch K, Sarr O, Ndir O, Mboup S, Batalov S, Wirth DF, Winzeler EA (2006) A systematic map of genetic variation in Plasmodium falciparum. *PLoS pathogens* **2:** e57

Kim PM, Lam HY, Urban AE, Korbel JO, Affourtit J, Grubert F, Chen X, Weissman S, Snyder M, Gerstein MB (2008) Analysis of copy number variants and segmental duplications in the human genome: Evidence for a change in the process of formation in recent evolutionary history. *Genome research* **18:** 1865-1874

Kimura M (1968) Evolutionary rate at the molecular level. *Nature* **217:** 624-626

Krungkrai J, Webster HK, Yuthavong Y (1989) De novo and salvage biosynthesis of pteroylpentaglutamates in the human malaria parasite, Plasmodium falciparum. *Molecular and biochemical parasitology* **32:** 25-37

Krungkrai J, Yuthavong Y, Webster HK (1985) Guanosine triphosphate cyclohydrolase in Plasmodium falciparum and other Plasmodium species. *Molecular and biochemical parasitology* **17:** 265-276

Kublin JG, Dzinjalamala FK, Kamwendo DD, Malkin EM, Cortese JF, Martino LM, Mukadam RA, Rogerson SJ, Lescano AG, Molyneux ME, Winstanley PA, Chimpeni P, Taylor TE, Plowe CV (2002) Molecular markers for failure of sulfadoxine-pyrimethamine and chlorproguanil-dapsone treatment of Plasmodium falciparum malaria. *J Infect Dis* **185:** 380-388

Ladhani S, Lowe B, Cole AO, Kowuondo K, Newton CR (2002) Changes in white blood cells and platelets in children with falciparum malaria: relationship to disease outcome. *Br J Haematol* **119:** 839-847

Laicine EM, Alves MA, de Almeida JC, Rizzo E, Albernaz WC, Sauaia H (1984) Development of DNA puffs and patterns of polypeptide synthesis in the salivary glands of Bradysia hygida. *Chromosoma* **89:** 280-284

Langhorne J, Ndungu FM, Sponaas AM, Marsh K (2008) Immunity to malaria: more questions than answers. *Nat Immunol* **9:** 725-732

Lee CS, Salcedo E, Wang Q, Wang P, Sims PF, Hyde JE (2001) Characterization of three genes encoding enzymes of the folate biosynthetic pathway in Plasmodium falciparum. *Parasitology* **122 Pt 1:** 1-13

Lee JA, Carvalho CM, Lupski JR (2007) A DNA replication mechanism for generating nonrecurrent rearrangements associated with genomic disorders. *Cell* **131:** 1235-1247

Lee JA, Inoue K, Cheung SW, Shaw CA, Stankiewicz P, Lupski JR (2006) Role of genomic architecture in PLP1 duplication causing Pelizaeus-Merzbacher disease. *Human molecular genetics* **15:** 2250-2265

Leprohon P, Legare D, Raymond F, Madore E, Hardiman G, Corbeil J, Ouellette M (2009) Gene expression modulation is associated with gene amplification, supernumerary chromosomes and chromosome loss in antimony-resistant Leishmania infantum. *Nucleic Acids Res* **37:** 1387-1399

Liang C, Gerbi SA (1994) Analysis of an origin of DNA amplification in Sciara coprophila by a novel three-dimensional gel method. *Mol Cell Biol* **14:** 1520-1529

Liang C, Spitzer JD, Smith HS, Gerbi SA (1993) Replication initiates at a confined region during DNA amplification in Sciara DNA puff II/9A. *Genes Dev* **7:** 1072-1084

Lieber MR, Ma Y, Pannicke U, Schwarz K (2003) Mechanism and regulation of human non-homologous DNA end-joining. *Nat Rev Mol Cell Biol* **4:** 712-720

Lin YC, Hsu JY, Shu JH, Chi Y, Chiang SC, Lee ST (2008) Two distinct arsenite-resistant variants of Leishmania amazonensis take different routes to achieve resistance as revealed by comparative transcriptomics. *Molecular and biochemical parasitology* **162:** 16-31

Lozovsky ER, Chookajorn T, Brown KM, Imwong M, Shaw PJ, Kamchonwongpaisan S, Neafsey DE, Weinreich DM, Hartl DL (2009) Stepwise acquisition of pyrimethamine resistance in the malaria parasite. *Proceedings of the National Academy of Sciences of the United States of America* **106:** 12025-12030

Lupski JR (1998) Genomic disorders: structural features of the genome can lead to DNA rearrangements and human disease traits. *Trends Genet* **14:** 417-422

Lynch M, Force A (2000) The probability of duplicate gene preservation by subfunctionalization. *Genetics* **154:** 459-473

Lynch M, O'Hely M, Walsh B, Force A (2001) The probability of preservation of a newly arisen gene duplicate. *Genetics* **159:** 1789-1804

Marsh K, Forster D, Waruiru C, Mwangi I, Winstanley M, Marsh V, Newton C, Winstanley P, Warn P, Peshu N, et al. (1995) Indicators of life-threatening malaria in African children. *N Engl J Med* **332:** 1399-1404

Martin DC, Arnold JD (1968) The drug response of a normal and a multi-resistant strain of P. falciparum to sulphalene. *Trans R Soc Trop Med Hyg* **62:** 810-815

Masimirembwa CM, Phuong-dung N, Phuc BQ, Duc-Dao L, Sy ND, Skold O, Swedberg G (1999) Molecular epidemiology of Plasmodium falciparum antifolate resistance in Vietnam: genotyping for resistance variants of dihydropteroate synthase and dihydrofolate reductase. *Int J Antimicrob Agents* **12:** 203-211

Mbogo CM, Mwangangi JM, Nzovu J, Gu W, Yan G, Gunter JT, Swalm C, Keating J, Regens JL, Shililu JI, Githure JI, Beier JC (2003) Spatial and temporal heterogeneity of Anopheles mosquitoes and Plasmodium falciparum transmission along the Kenyan coast. *The American journal of tropical medicine and hygiene* **68:** 734-742

McCollum AM, Poe AC, Hamel M, Huber C, Zhou Z, Shi YP, Ouma P, Vulule J, Bloland P, Slutsker L, Barnwell JW, Udhayakumar V, Escalante AA (2006) Antifolate resistance in Plasmodium falciparum: multiple origins and identification of novel dhfr alleles. *J Infect Dis* **194:** 189-197

McGready R, Stepniewska K, Seaton E, Cho T, Cho D, Ginsberg A, Edstein MD, Ashley E, Looareesuwan S, White NJ, Nosten F (2003) Pregnancy and use of oral contraceptives reduces the biotransformation of proguanil to cycloguanil. *Eur J Clin Pharmacol* **59:** 553-557

McMorran BJ, Marshall VM, de Graaf C, Drysdale KE, Shabbar M, Smyth GK, Corbin JE, Alexander WS, Foote SJ (2009) Platelets kill intraerythrocytic malarial parasites and mediate survival to infection. *Science* **323:** 797-800

Menard R (2005) Medicine: knockout malaria vaccine? *Nature* **433:** 113-114

Mermin J, Ekwaru JP, Liechty CA, Were W, Downing R, Ransom R, Weidle P, Lule J, Coutinho A, Solberg P (2006) Effect of co-trimoxazole prophylaxis, antiretroviral therapy, and insecticide-treated bednets on the frequency of malaria in HIV-1-infected adults in Uganda: a prospective cohort study. *Lancet* **367:** 1256-1261

Milhous WK, Weatherly NF, Bowdre JH, Desjardins RE (1985) In vitro activities of and mechanisms of resistance to antifol antimalarial drugs. *Antimicrobial agents and chemotherapy* **27:** 525-530

Minzi OM, Gupta A, Haule AF, Kagashe GA, Massele AY, Gustafsson LL (2007) Lack of impact of artesunate on the disposition kinetics of sulfadoxine/pyrimethamine when the two drugs are concomitantly administered. *Eur J Clin Pharmacol* **63:** 457-462

Mita T, Tanabe K, Takahashi N, Culleton R, Ndounga M, Dzodzomenyo M, Akhwale WS, Kaneko A, Kobayakawa T (2009) Indigenous evolution of Plasmodium falciparum pyrimethamine resistance multiple times in Africa. *The Journal of antimicrobial chemotherapy* **63:** 252-255

Mwai L, Ochong E, Abdirahman A, Kiara SM, Ward S, Kokwaro G, Sasi P, Marsh K, Borrmann S, Mackinnon M, Nzila A (2009) Chloroquine resistance before and after its withdrawal in Kenya. *Malar J* **8:** 106

Mwangi TW, Ross A, Snow RW, Marsh K (2005) Case definitions of clinical malaria under different transmission conditions in Kilifi District, Kenya. *J Infect Dis* **191:** 1932-1939

Nair S, Miller B, Barends M, Jaidee A, Patel J, Mayxay M, Newton P, Nosten F, Ferdig MT, Anderson TJ (2008) Adaptive copy number evolution in malaria parasites. *PLoS Genet* **4:** e1000243

Nar H, Huber R, Auerbach G, Fischer M, Hosl C, Ritz H, Bracher A, Meining W, Eberhardt S, Bacher A (1995) Active site topology and reaction mechanism of GTP cyclohydrolase I. *Proc Natl Acad Sci U S A* **92:** 12120-12125

Ngo T, Duraisingh M, Reed M, Hipgrave D, Biggs B, Cowman AF (2003) Analysis of pfcrt, pfmdr1, dhfr, and dhps mutations and drug sensitivities in Plasmodium falciparum isolates from patients in Vietnam before and after treatment with artemisinin. *The American journal of tropical medicine and hygiene* **68:** 350-356

Noedl H, Se Y, Schaecher K, Smith BL, Socheat D, Fukuda MM (2008) Evidence of artemisinin-resistant malaria in western Cambodia. *N Engl J Med* **359:** 2619-2620

Normark S, Edlund T, Grundstrom T, Bergstrom S, Wolf-Watz H (1977) Escherichia coli K-12 mutants hyperproducing chromosomal beta-lactamase by gene repetitions. *Journal of bacteriology* **132:** 912-922

Nzila-Mounda A, Mberu EK, Sibley CH, Plowe CV, Winstanley PA, Watkins WM (1998) Kenyan Plasmodium falciparum field isolates: correlation between pyrimethamine and chlorcycloguanil activity in vitro and point mutations in the dihydrofolate reductase domain. *Antimicrobial agents and chemotherapy* **42:** 164-169

O'Meara WP, Bejon P, Mwangi TW, Okiro EA, Peshu N, Snow RW, Newton CR, Marsh K (2008) Effect of a fall in malaria transmission on morbidity and mortality in Kilifi, Kenya. *Lancet* **372:** 1555-1562

Omar SA, Adagu IS, Warhurst DC (2001) Can pretreatment screening for dhps and dhfr point mutations in Plasmodium falciparum infections be used to predict sulfadoxine-pyrimethamine treatment failure? *Trans R Soc Trop Med Hyg* **95:** 315-319

Osheim YN, Miller OL, Jr., Beyer AL (1988) Visualization of Drosophila melanogaster chorion genes undergoing amplification. *Mol Cell Biol* **8:** 2811-2821

Paget-McNicol S, Saul A (2001) Mutation rates in the dihydrofolate reductase gene of Plasmodium falciparum. *Parasitology* **122:** 497-505

Pearce RJ, Pota H, Evehe MS, Ba el H, Mombo-Ngoma G, Malisa AL, Ord R, Inojosa W, Matondo A, Diallo DA, Mbacham W, van den Broek IV, Swarthout TD, Getachew A, Dejene S, Grobusch MP, Njie F, Dunyo S, Kweku M, Owusu-Agyei S, Chandramohan D, Bonnet M, Guthmann JP, Clarke S, Barnes KI, Streat E, Katokele ST, Uusiku P, Agboghoroma CO, Elegba OY, Cisse B, IE AE, Giha HA, Kachur SP, Lynch C, Rwakimari JB, Chanda P, Hawela M, Sharp B, Naidoo I, Roper C (2009) Multiple origins and regional dispersal of resistant dhps in African Plasmodium falciparum malaria. *PLoS Med* **6:** e1000055

Peterson DS, Di Santi SM, Povoa M, Calvosa VS, Do Rosario VE, Wellems TE (1991) Prevalence of the dihydrofolate reductase Asn-108 mutation as the basis for pyrimethamine-resistant falciparum malaria in the Brazilian Amazon. *Am J Trop Med Hyg* **45:** 492-497

Peterson DS, Milhous WK, Wellems TE (1990) Molecular basis of differential resistance to cycloguanil and pyrimethamine in Plasmodium falciparum malaria. *Proceedings of the National Academy of Sciences of the United States of America* **87:** 3018-3022

Peterson DS, Walliker D, Wellems TE (1988) Evidence that a point mutation in dihydrofolate reductase-thymidylate synthase confers resistance to pyrimethamine in falciparum malaria. *Proceedings of the National Academy of Sciences of the United States of America* **85:** 9114-9118

Preechapornkul P, Imwong M, Chotivanich K, Pongtavornpinyo W, Dondorp AM, Day NP, White NJ, Pukrittayakamee S (2009) Plasmodium falciparum pfmdr1

amplification, mefloquine resistance, and parasite fitness. *Antimicrob Agents Chemother* **53:** 1509-1515

Pribat A, Jeanguenin L, Lara-Nunez A, Ziemak MJ, Hyde JE, de Crecy-Lagard V, Hanson AD (2009) 6-pyruvoyltetrahydropterin synthase paralogs replace the folate synthesis enzyme dihydroneopterin aldolase in diverse bacteria. *Journal of bacteriology* **191:** 4158-4165

Price RN, Cassar C, Brockman A, Duraisingh M, van Vugt M, White NJ, Nosten F, Krishna S (1999) The pfmdr1 gene is associated with a multidrug-resistant phenotype in Plasmodium falciparum from the western border of Thailand. *Antimicrobial agents and chemotherapy* **43:** 2943-2949

Reed MB, Saliba KJ, Caruana SR, Kirk K, Cowman AF (2000) Pgh1 modulates sensitivity and resistance to multiple antimalarials in Plasmodium falciparum. *Nature* **403:** 906-909

Reiter LT, Hastings PJ, Nelis E, De Jonghe P, Van Broeckhoven C, Lupski JR (1998) Human meiotic recombination products revealed by sequencing a hotspot for homologous strand exchange in multiple HNPP deletion patients. *Am J Hum Genet* **62:** 1023-1033

Rownd R, Kasamatsu H, Mickel S (1971) The molecular nature and replication of drug resistance factors of the Enterobacteriaceae. *Ann N Y Acad Sci* **182:** 188-206

Rownd R, Mickel S (1971) Dissociation and reassociation of RTF and r-determinants of the R-factor NR1 in Proteus mirabilis. *Nat New Biol* **234:** 40-43

Salcedo E, Cortese JF, Plowe CV, Sims PF, Hyde JE (2001) A bifunctional dihydrofolate synthetase--folylpolyglutamate synthetase in Plasmodium falciparum identified by functional complementation in yeast and bacteria. *Molecular and biochemical parasitology* **112:** 239-252

Sandefur CI, Wooden JM, Quaye IK, Sirawaraporn W, Sibley CH (2007) Pyrimethamine-resistant dihydrofolate reductase enzymes of Plasmodium falciparum are not enzymatically compromised in vitro. *Molecular and biochemical parasitology* **154:** 1-5

Santelli RV, Siviero F, Machado-Santelli GM, Lara FJ, Stocker AJ (2004) Molecular characterization of the B-2 DNA puff gene of Rhynchosciara americana. *Chromosoma* **113:** 167-176

Sasi P, Abdulrahaman A, Mwai L, Muriithi S, Straimer J, Schieck E, Rippert A, Bashraheil M, Salim A, Peshu J, Awuondo K, Lowe B, Pirmohamed M, Winstanley P, Ward S, Nzila A, Borrmann S (2009) In vivo and in vitro efficacy of amodiaquine against Plasmodium falciparum in an area of continued use of 4-aminoquinolines in East Africa. *J Infect Dis* **199:** 1575-1582

Schimke RT, Alt FW, Kellems RE, Kaufman RJ, Bertino JR (1978a) Amplification of dihydrofolate reductase genes in methotrexate-resistant cultured mouse cells. *Cold Spring Harb Symp Quant Biol* **42 Pt 2:** 649-657

Schimke RT, Kaufman RJ, Alt FW, Kellems RF (1978b) Gene amplification and drug resistance in cultured murine cells. *Science* **202:** 1051-1055

Schirch V, Strong WB (1989) Interaction of folylpolyglutamates with enzymes in one-carbon metabolism. *Arch Biochem Biophys* **269:** 371-380

Schonfeld M, Barreto Miranda I, Schunk M, Maduhu I, Maboko L, Hoelscher M, Berens-Riha N, Kitua A, Loscher T (2007) Molecular surveillance of drug-resistance associated mutations of Plasmodium falciparum in south-west Tanzania. *Malar J* **6:** 2

Shaw CJ, Lupski JR (2004) Implications of human genome architecture for rearrangement-based disorders: the genomic basis of disease. *Human molecular genetics* **13 Spec No 1:** R57-64

Singh B, Kim Sung L, Matusop A, Radhakrishnan A, Shamsul SS, Cox-Singh J, Thomas A, Conway DJ (2004) A large focus of naturally acquired Plasmodium knowlesi infections in human beings. *Lancet* **363:** 1017-1024

Sirawaraporn W, Sathitkul T, Sirawaraporn R, Yuthavong Y, Santi DV (1997) Antifolate-resistant mutants of Plasmodium falciparum dihydrofolate reductase. *Proceedings of the National Academy of Sciences of the United States of America* **94:** 1124-1129

Skold O (2001) Resistance to trimethoprim and sulfonamides. *Vet Res* **32:** 261-273

Smith T, Charlwood JD, Kihonda J, Mwankusye S, Billingsley P, Meuwissen J, Lyimo E, Takken W, Teuscher T, Tanner M (1993) Absence of seasonal variation in malaria parasitaemia in an area of intense seasonal transmission. *Acta Trop* **54:** 55-72

Smythe JA, Peterson MG, Coppel RL, Saul AJ, Kemp DJ, Anders RF (1990) Structural diversity in the 45-kilodalton merozoite surface antigen of Plasmodium falciparum. *Mol Biochem Parasitol* **39:** 227-234

Snow RW, Guerra CA, Noor AM, Myint HY, Hay SI (2005) The global distribution of clinical episodes of Plasmodium falciparum malaria. *Nature* **434:** 214-217

Spradling AC (1981) The organization and amplification of two chromosomal domains containing Drosophila chorion genes. *Cell* **27:** 193-201

Spradling AC, Digan ME, Mahowald AP, Scott M, Craig EA (1980) Two clusters of genes for major chorion proteins of Drosophila melanogaster. *Cell* **19:** 905-914

Staedke SG, Sendagire H, Lamola S, Kamya MR, Dorsey G, Rosenthal PJ (2004) Relationship between age, molecular markers, and response to sulphadoxine-pyrimethamine treatment in Kampala, Uganda. *Trop Med Int Health* **9:** 624-629

Stankiewicz P, Lupski JR (2002) Genome architecture, rearrangements and genomic disorders. *Trends Genet* **18:** 74-82

Sturm A, Amino R, van de Sand C, Regen T, Retzlaff S, Rennenberg A, Krueger A, Pollok JM, Menard R, Heussler VT (2006) Manipulation of host hepatocytes by the malaria parasite for delivery into liver sinusoids. *Science* **313:** 1287-1290

Thaithong S, Ranford-Cartwright LC, Siripoon N, Harnyuttanakorn P, Kanchanakhan NS, Seugorn A, Rungsihirunrat K, Cravo PV, Beale GH (2001) Plasmodium falciparum: gene mutations and amplification of dihydrofolate reductase genes in parasites grown in vitro in presence of pyrimethamine. *Exp Parasitol* **98:** 59-70

Thony B, Auerbach G, Blau N (2000) Tetrahydrobiopterin biosynthesis, regeneration and functions. *The Biochemical journal* **347 Pt 1:** 1-16

Toffolatti L, Cardazzo B, Nobile C, Danieli GA, Gualandi F, Muntoni F, Abbs S, Zanetti P, Angelini C, Ferlini A, Fanin M, Patarnello T (2002) Investigating the mechanism of chromosomal deletion: characterization of 39 deletion breakpoints in introns 47 and 48 of the human dystrophin gene. *Genomics* **80:** 523-530

Trent JM, Buick RN, Olson S, Horns RC, Jr., Schimke RT (1984) Cytologic evidence for gene amplification in methotrexate-resistant cells obtained from a patient with ovarian adenocarcinoma. *J Clin Oncol* **2:** 8-15

Triglia T, Cowman AF (1994) Primary structure and expression of the dihydropteroate synthetase gene of Plasmodium falciparum. *Proceedings of the National Academy of Sciences of the United States of America* **91:** 7149-7153

Triglia T, Menting JG, Wilson C, Cowman AF (1997) Mutations in dihydropteroate synthase are responsible for sulfone and sulfonamide resistance in Plasmodium falciparum. *Proceedings of the National Academy of Sciences of the United States of America* **94:** 13944-13949

Waldman AS, Liskay RM (1988) Dependence of intrachromosomal recombination in mammalian cells on uninterrupted homology. *Mol Cell Biol* **8:** 5350-5357

Wang P, Lee CS, Bayoumi R, Djimde A, Doumbo O, Swedberg G, Dao LD, Mshinda H, Tanner M, Watkins WM, Sims PF, Hyde JE (1997) Resistance to antifolates in Plasmodium falciparum monitored by sequence analysis of dihydropteroate synthetase and dihydrofolate reductase alleles in a large number of field samples of diverse origins. *Molecular and biochemical parasitology* **89:** 161-177

White NJ (1997) Assessment of the pharmacodynamic properties of antimalarial drugs in vivo. *Antimicrobial agents and chemotherapy* **41:** 1413-1422

White NJ, Stepniewska K, Barnes K, Price RN, Simpson J (2008) Simplified antimalarial therapeutic monitoring: using the day-7 drug level? *Trends Parasitol* **24:** 159-163

WHO (2008) Methods and techniques for clinical trials on antimalarial drug efficacy. Geneva.

Wickstead B, Ersfeld K, Gull K (2003) Repetitive elements in genomes of parasitic protozoa. *Microbiol Mol Biol Rev* **67:** 360-375, table of contents

Wiktor SZ, Sassan-Morokro M, Grant AD, Abouya L, Karon JM, Maurice C, Djomand G, Ackah A, Domoua K, Kadio A, Yapi A, Combe P, Tossou O, Roels TH, Lackritz EM, Coulibaly D, De Cock KM, Coulibaly IM, Greenberg AE (1999) Efficacy of trimethoprim-sulphamethoxazole prophylaxis to decrease morbidity and mortality in HIV-1-infected patients with tuberculosis in Abidjan, Cote d'Ivoire: a randomised controlled trial. *Lancet* **353:** 1469-1475

Wilson RJ, Williamson DH (1997) Extrachromosomal DNA in the Apicomplexa. *Microbiol Mol Biol Rev* **61:** 1-16

Wu N, Liang C, DiBartolomeis SM, Smith HS, Gerbi SA (1993) Developmental progression of DNA puffs in Sciara coprophila: amplification and transcription. *Dev Biol* **160:** 73-84

Yokosawa J, Soares MA, Dijkwel PA, Stocker AJ, Hamlin JL, Lara FJ (1999) DNA replication during amplification of the C3 puff of Rhynchosciara americana initiates at multiple sites in a 6 kb region. *Chromosoma* **108:** 291-301

Zindrou S, Nguyen PD, Nguyen DS, Skold O, Swedberg G (1996) Plasmodium falciparum: mutation pattern in the dihydrofolate reductase-thymidylate synthase genes of Vietnamese isolates, a novel mutation, and coexistence of two clones in a Thai patient. *Experimental parasitology* **84:** 56-64